Progress on *High Peak Current* Laser Wakefield Electron Acceleration

U. Schramm

Helmholtz-Zentrum Dresden-Rossendorf

HELMHOLTZ ZENTRUM DRESDEN ROSSENDORF

Progress on *High Peak Current* Laser Wakefield Electron Acceleration

(laser + accelerator) based light sources

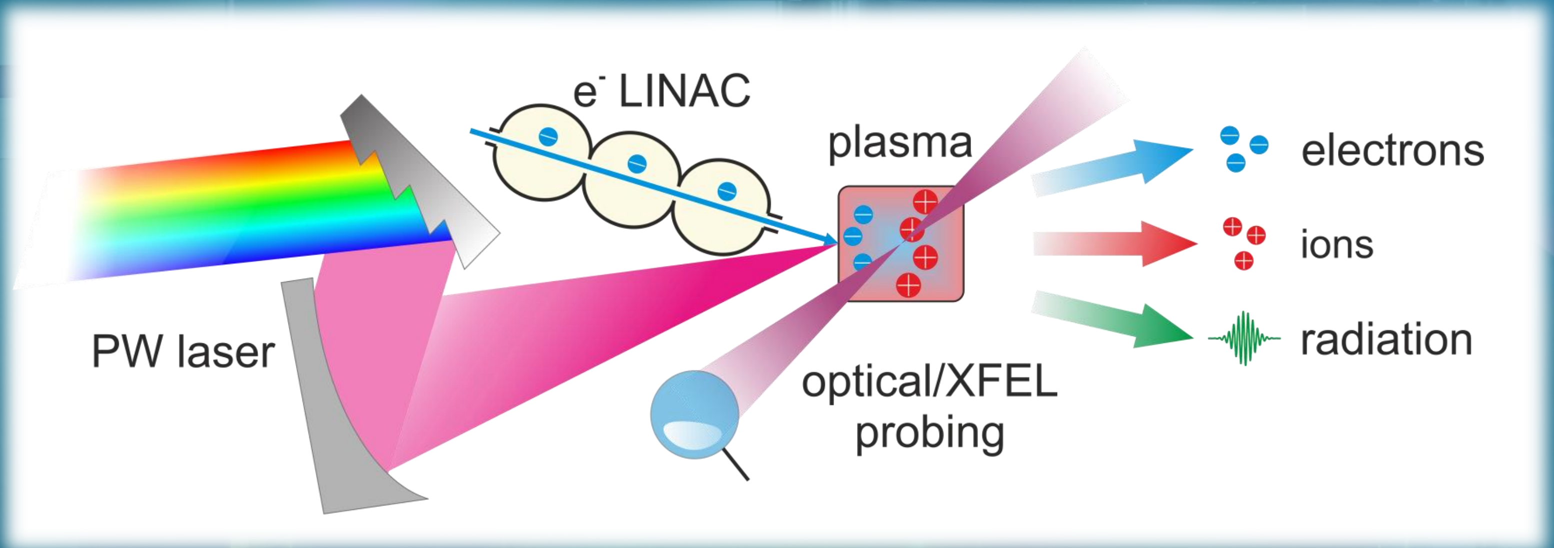

Advanced accelerator research embedded in independent national programs (Helmholtz Association)

MT ARD

Accelerator research and development
(**DESY, HZDR, GSI**, KIT, **HI-Jena**, HIB)

- *cw superconducting rf accelerators and radiation sources*
- *plasma accelerators (**from acceleration to accelerators**)*
- ***femtoscale diagnostics** matched with synthetic diagnostic*
- *for predictive simulation capability*

PIConGPU

Advanced accelerator research embedded in independent national programs (Helmholtz Association)

Accelerator research and development
(**DESY, HZDR, GSI**, KIT, **HI-Jena**, HIB)

- *cw superconducting rf accelerators and radiation sources*
- *plasma accelerators (**from acceleration to accelerators**)*
- ***femtoscale diagnostics** matched with synthetic diagnostic*
- *for predictive simulation capability*

PIConGPU

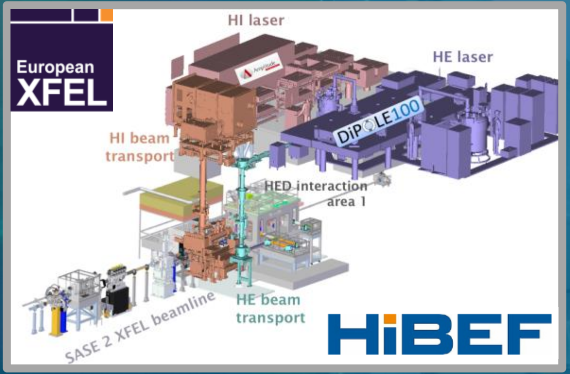

Advanced accelerator research embedded in independent national programs (Helmholtz Association)

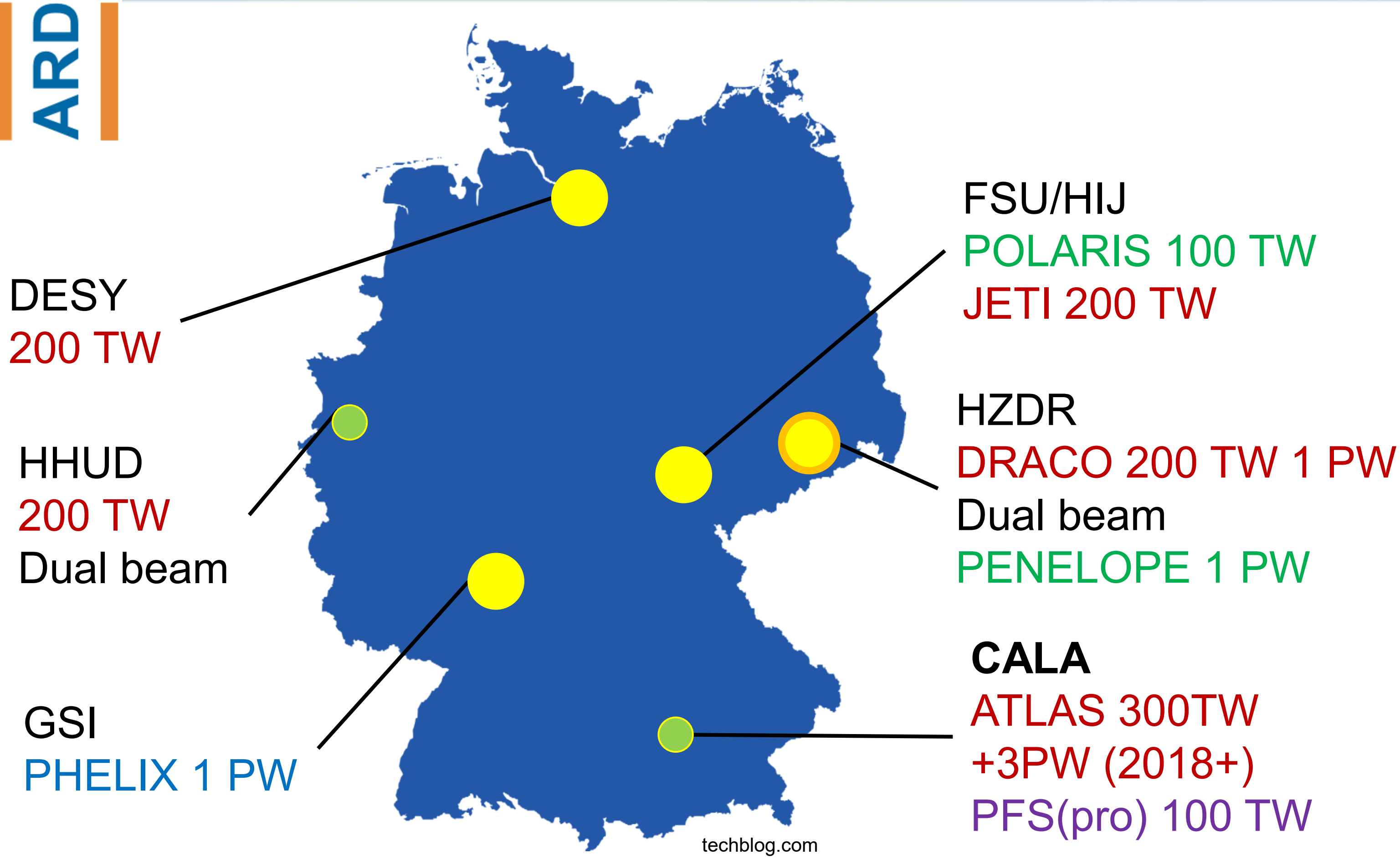

ELBE center for high power radiation sources

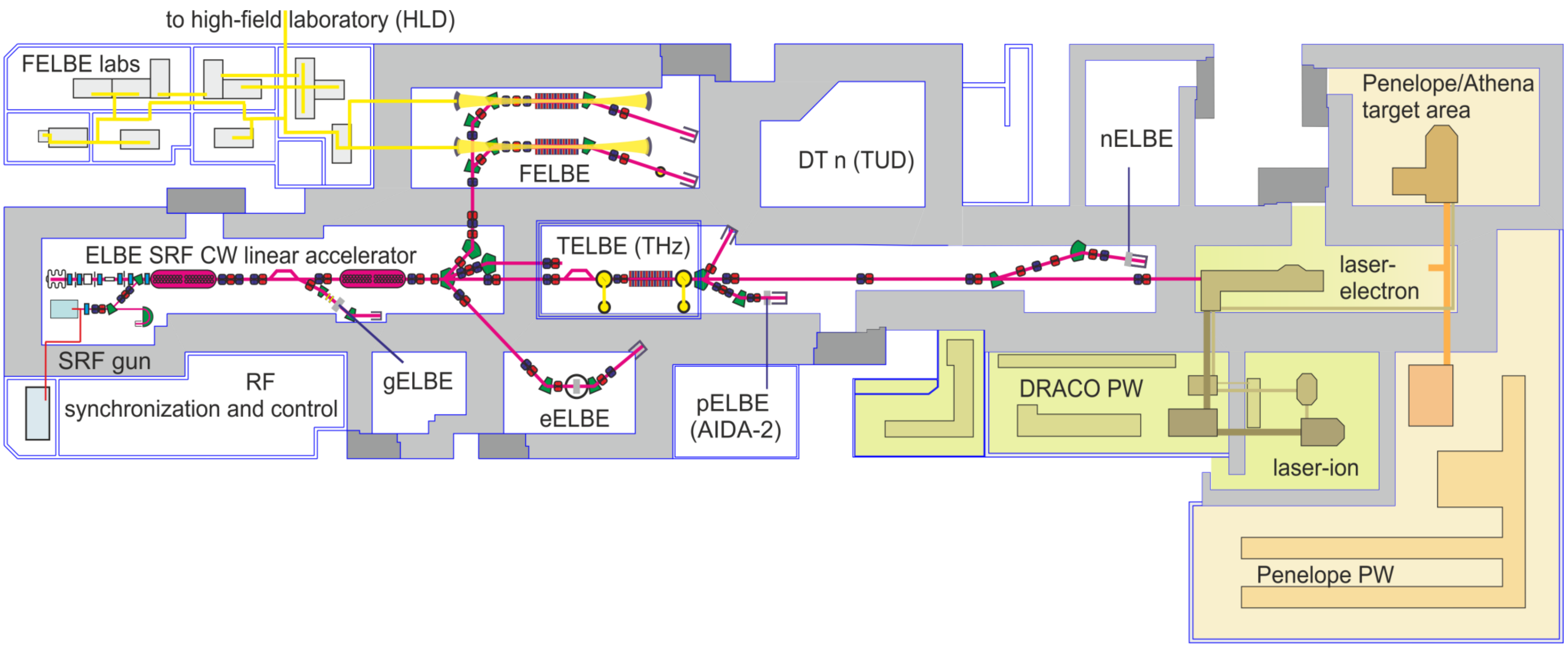

ELBE center for high power radiation sources

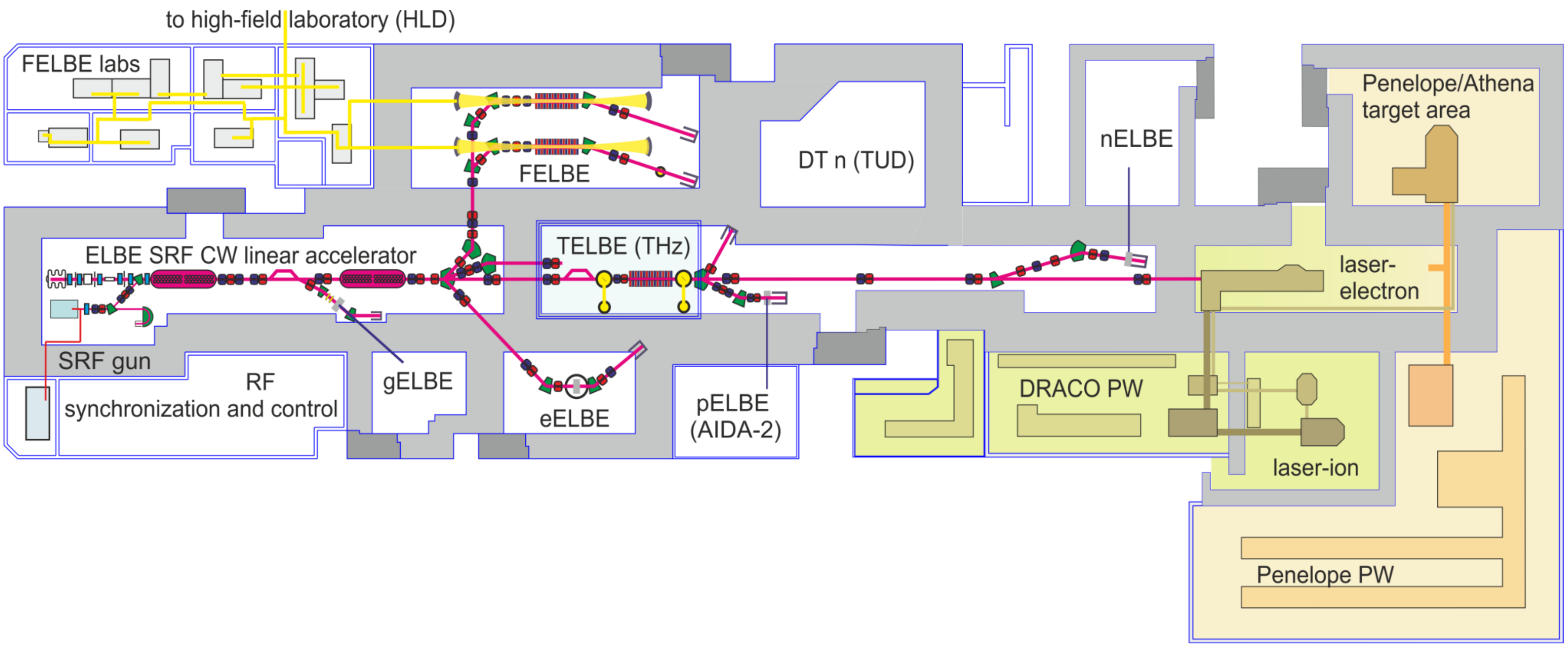

ELBE center for high power radiation sources

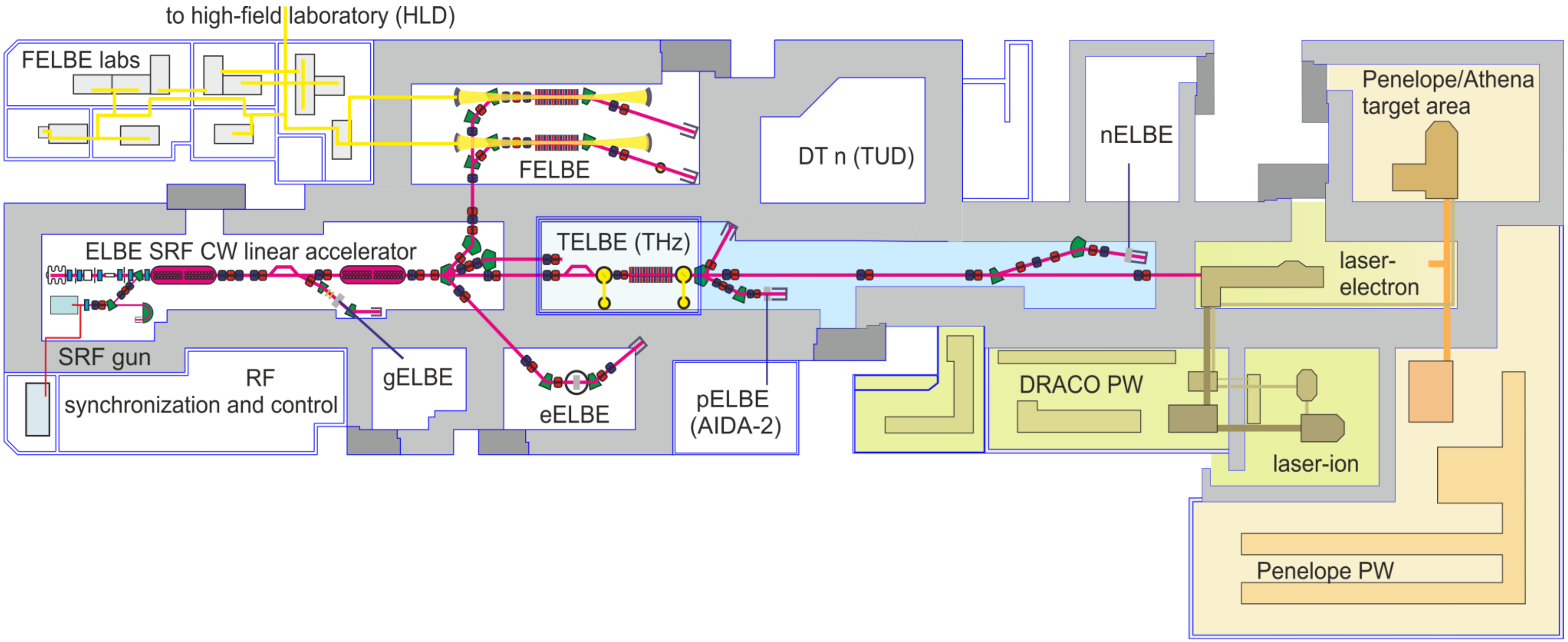

ELBE center for high power radiation sources

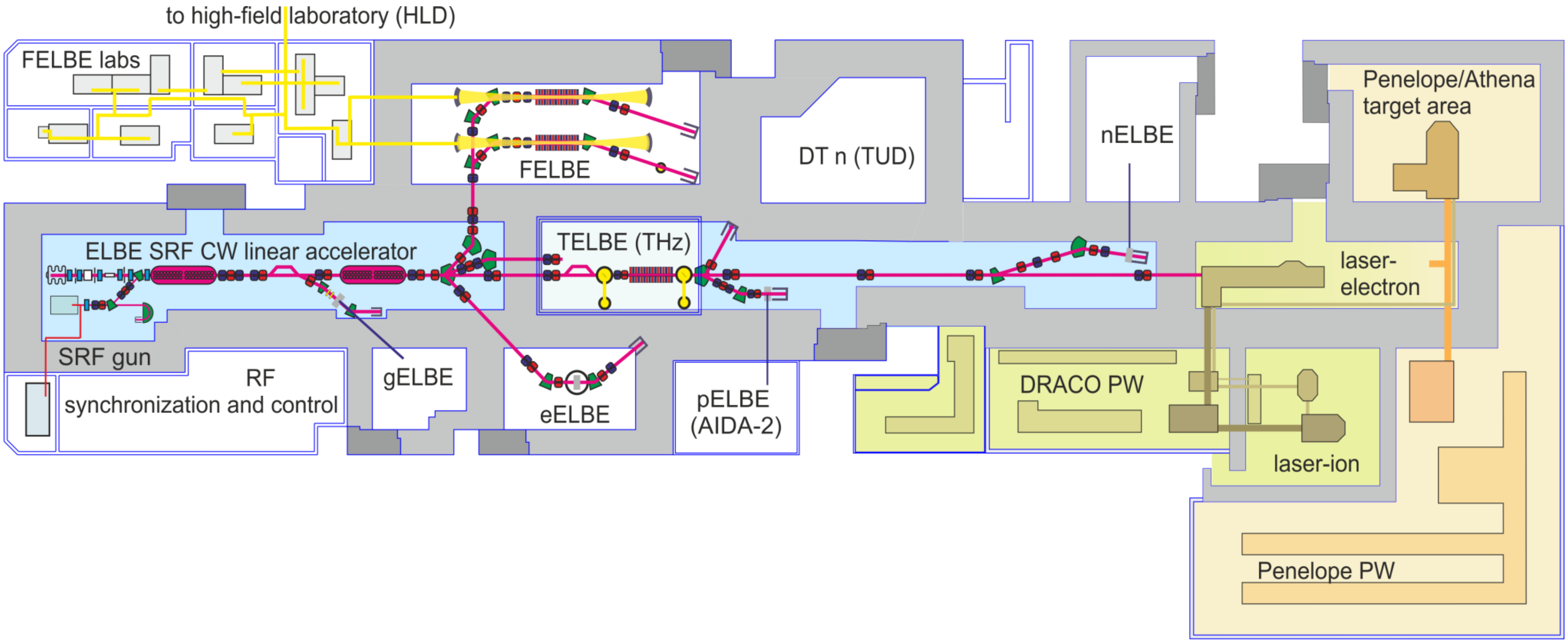

ELBE center for high power radiation sources

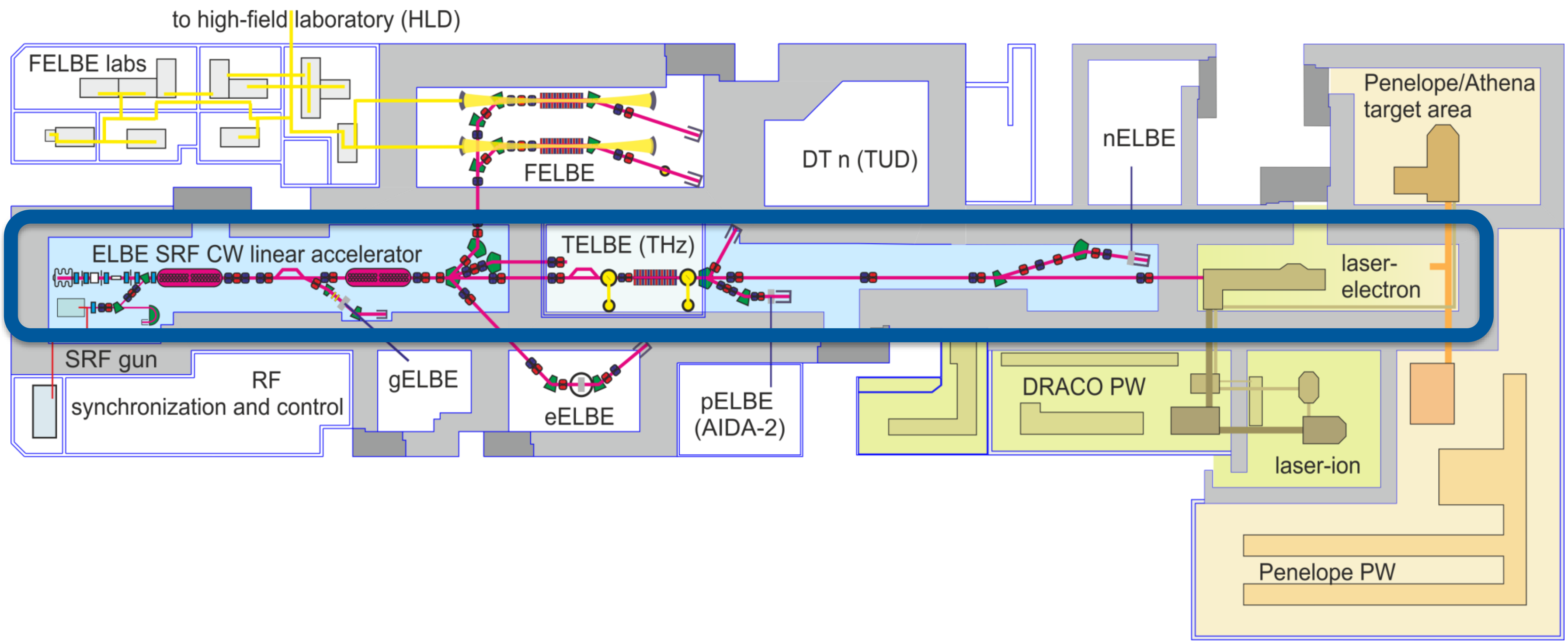

ELBE center for high power radiation sources

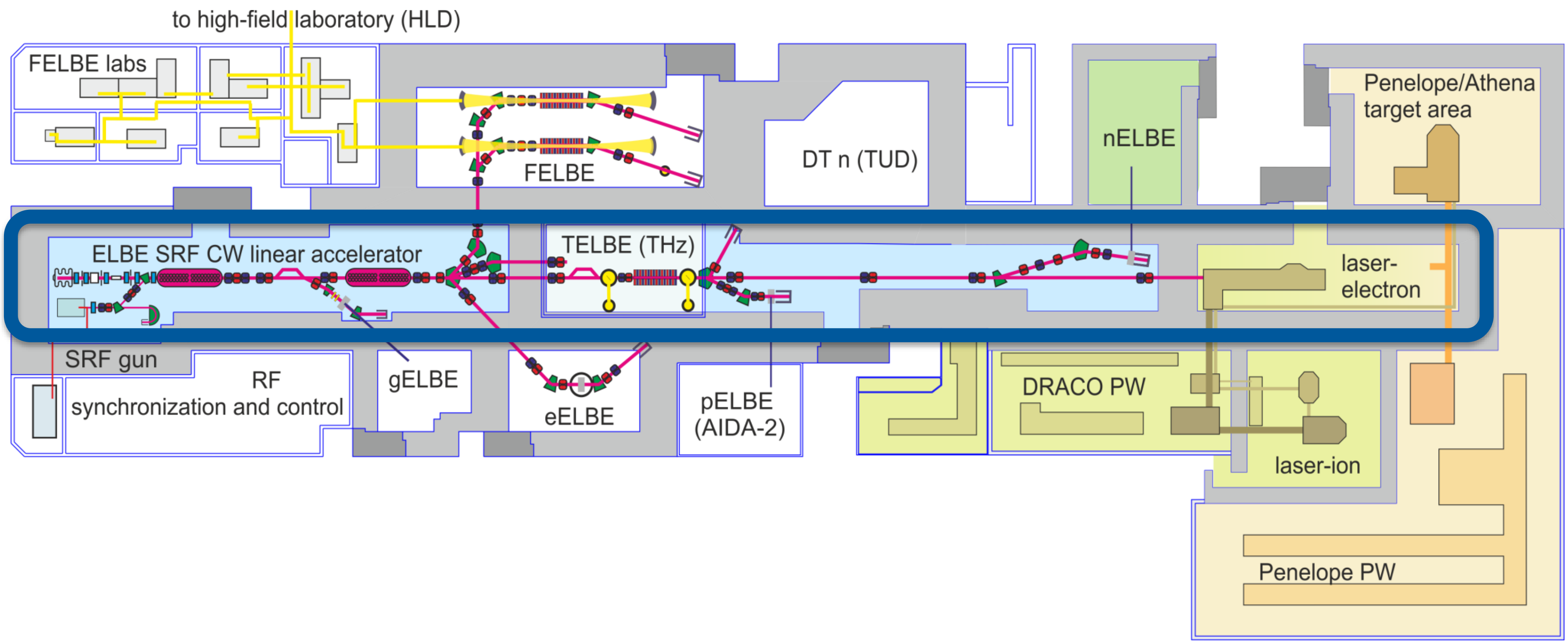

ELBE center for high power radiation sources

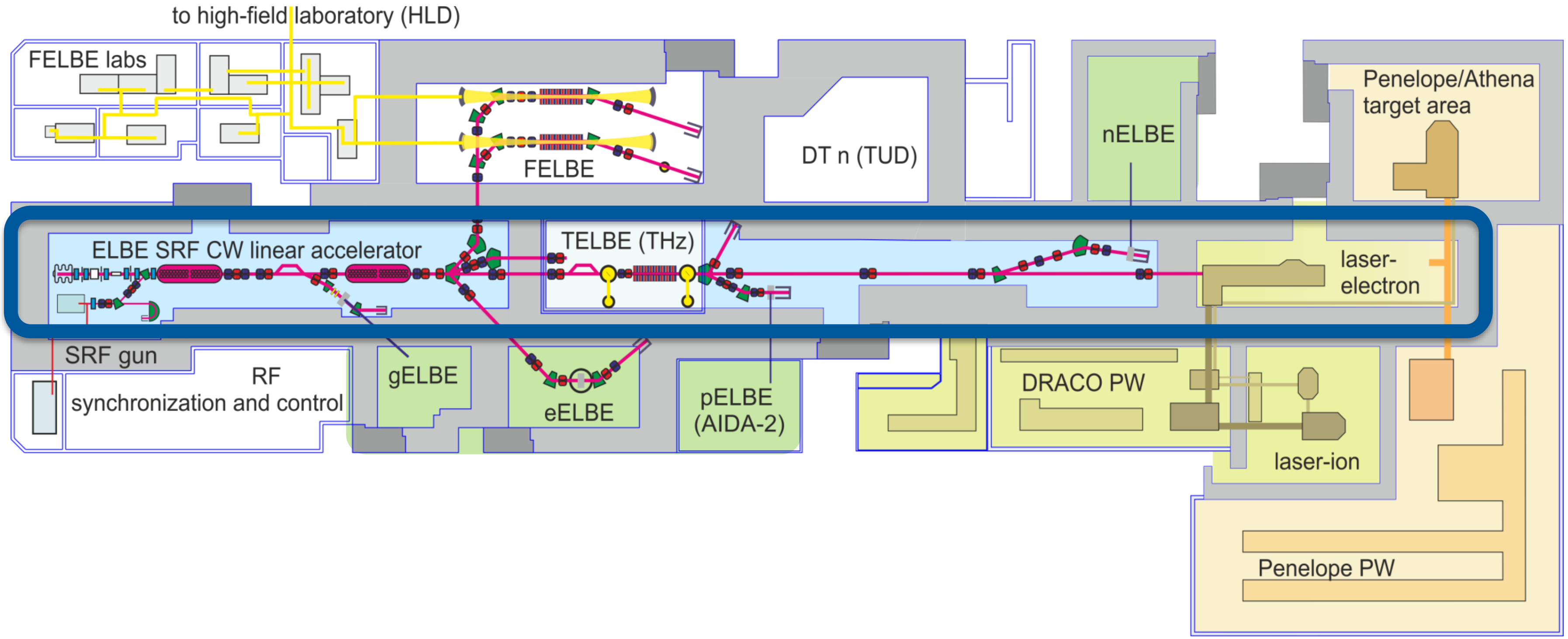

ELBE center for high power radiation sources

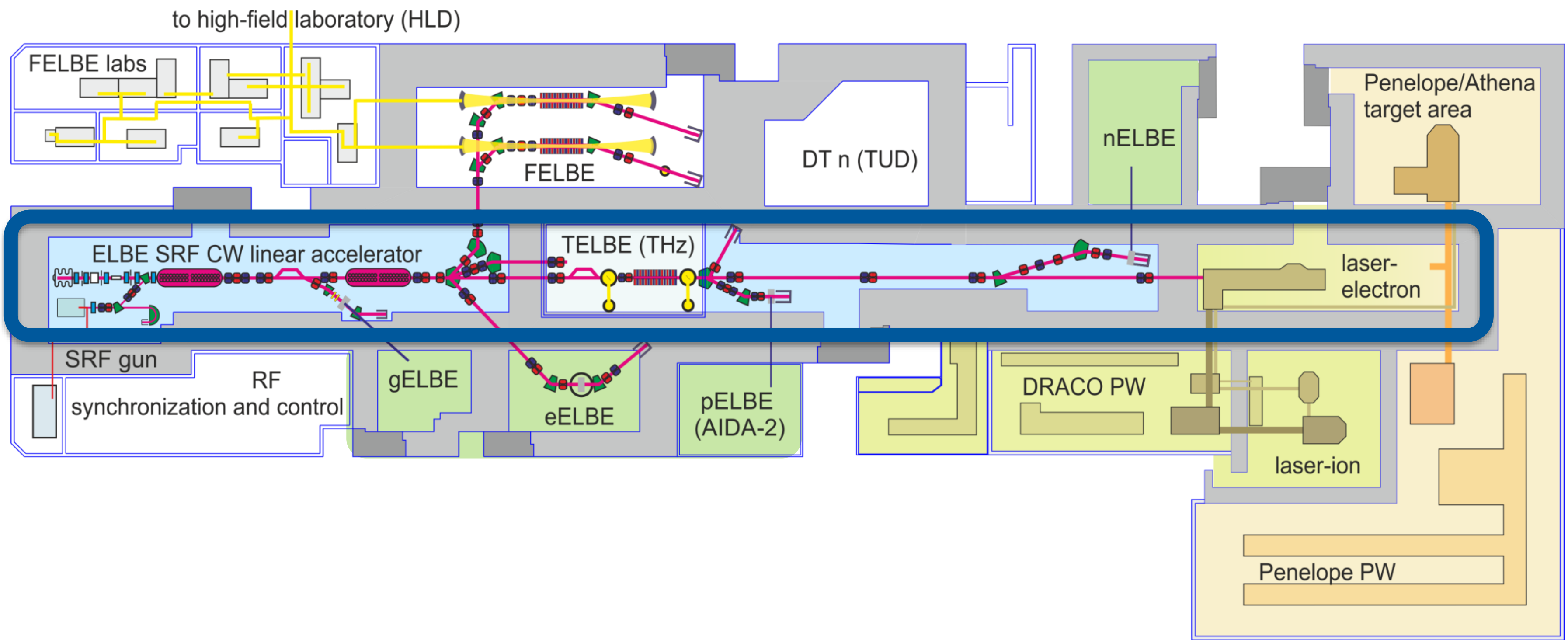

Variable pulse rate (up to 13 MHz) and charge (**up to 0.3 nC**) in 40 MeV ps pulses

ELBE center for high power radiation sources

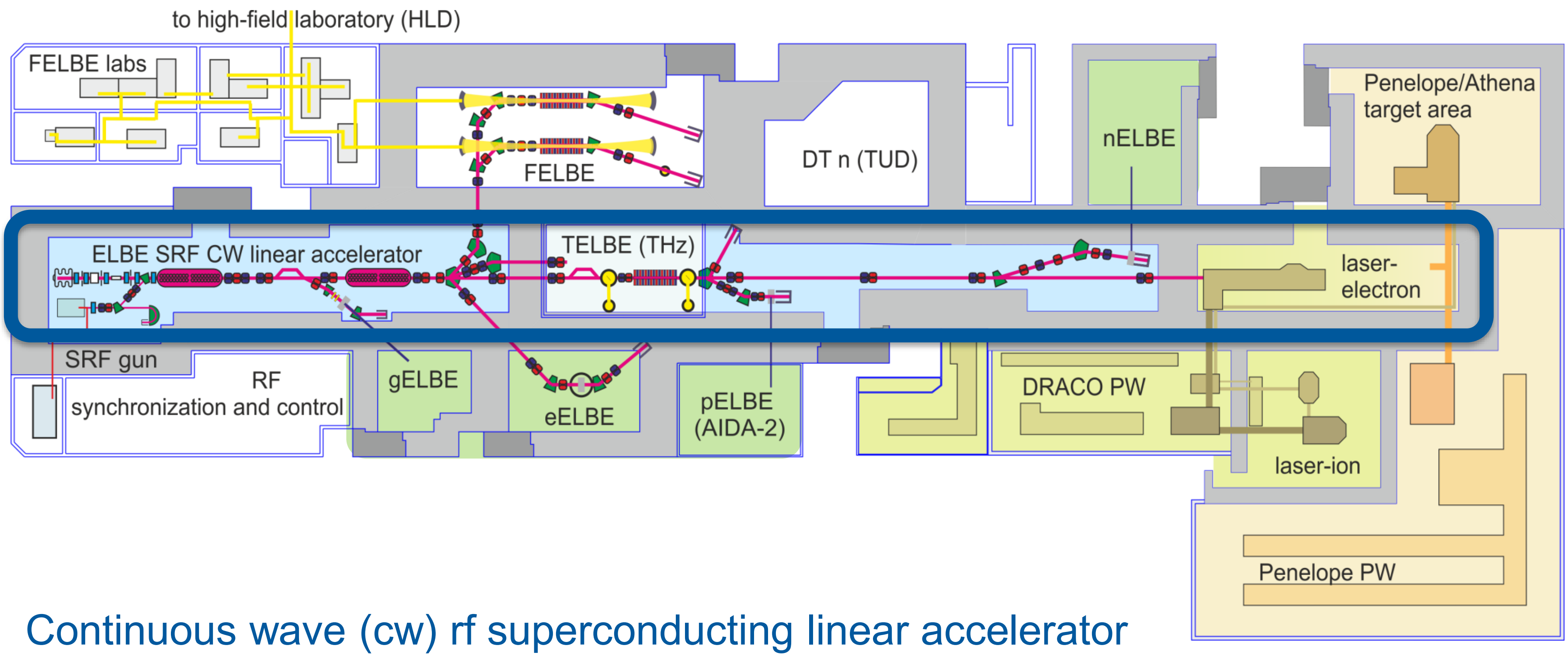

- Continuous wave (cw) rf superconducting linear accelerator

  Variable pulse rate (up to 13 MHz) and charge (**up to 0.3 nC**) in 40 MeV ps pulses

ELBE center for high power radiation sources

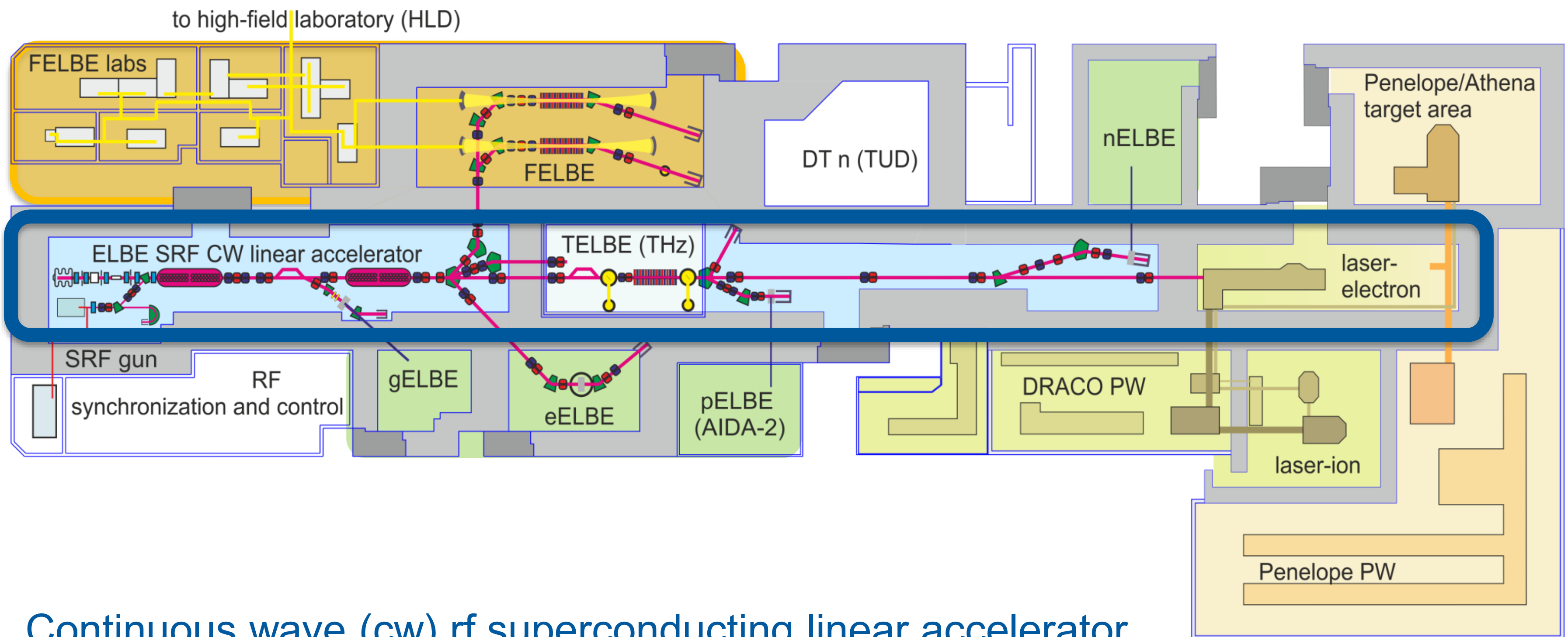

- Continuous wave (cw) rf superconducting linear accelerator

  Variable pulse rate (up to 13 MHz) and charge (**up to 0.3 nC**) in 40 MeV ps pulses

ELBE center for high power radiation sources

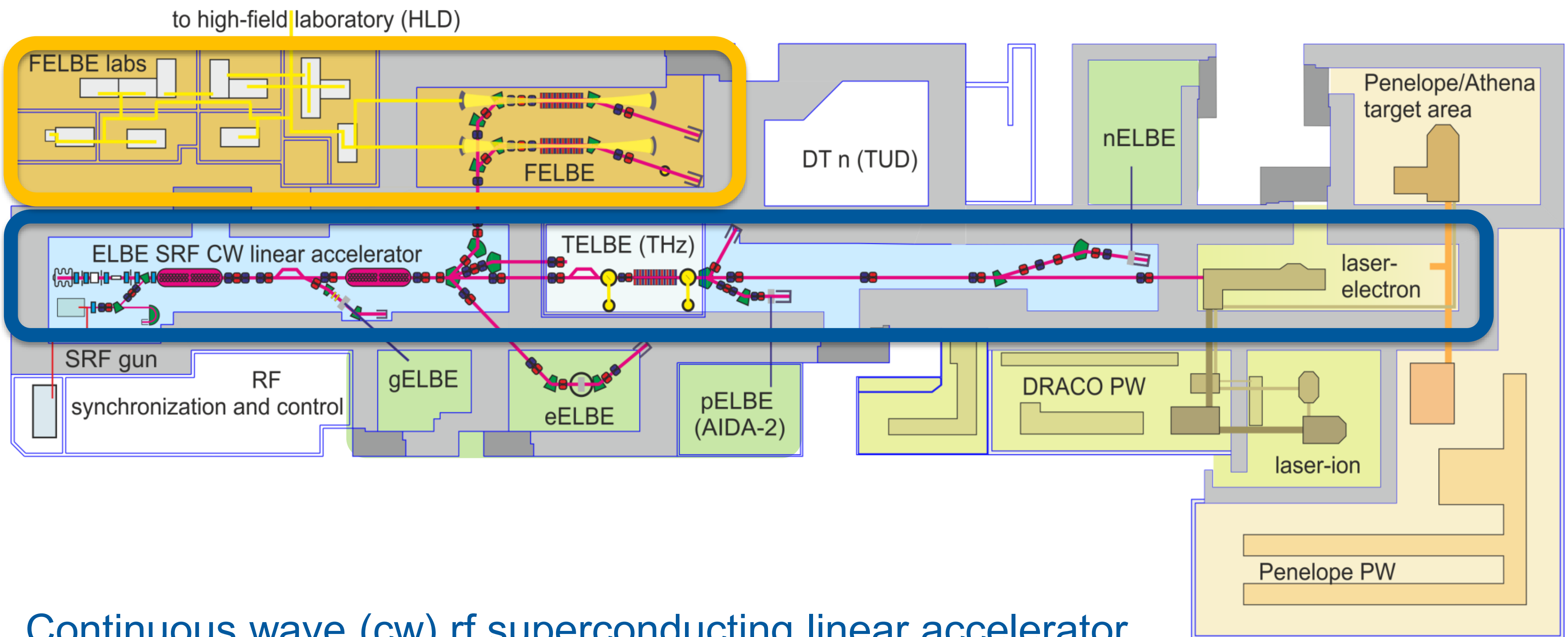

- Continuous wave (cw) rf superconducting linear accelerator

  Variable pulse rate (up to 13 MHz) and charge (**up to 0.3 nC**) in 40 MeV ps pulses

ELBE center for high power radiation sources

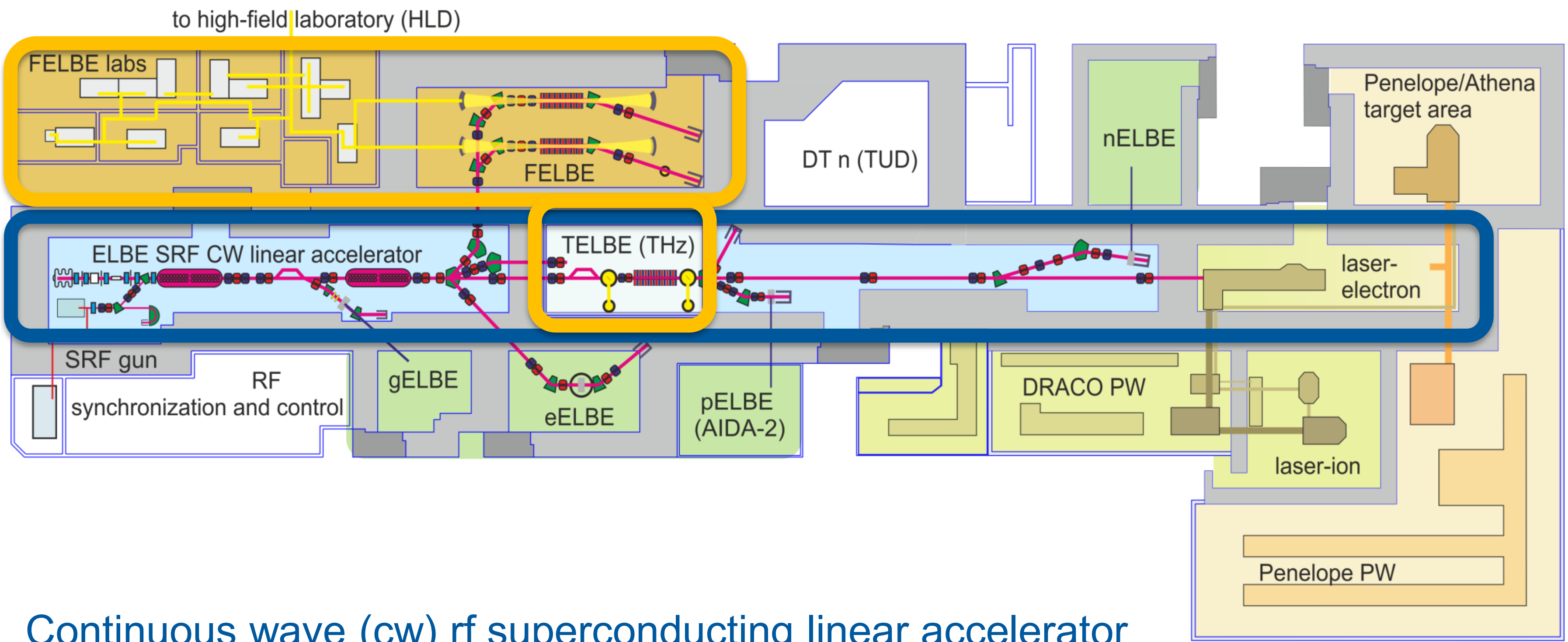

- Continuous wave (cw) rf superconducting linear accelerator

  Variable pulse rate (up to 13 MHz) and charge (**up to 0.3 nC**) in 40 MeV ps pulses

ELBE center for high power radiation sources

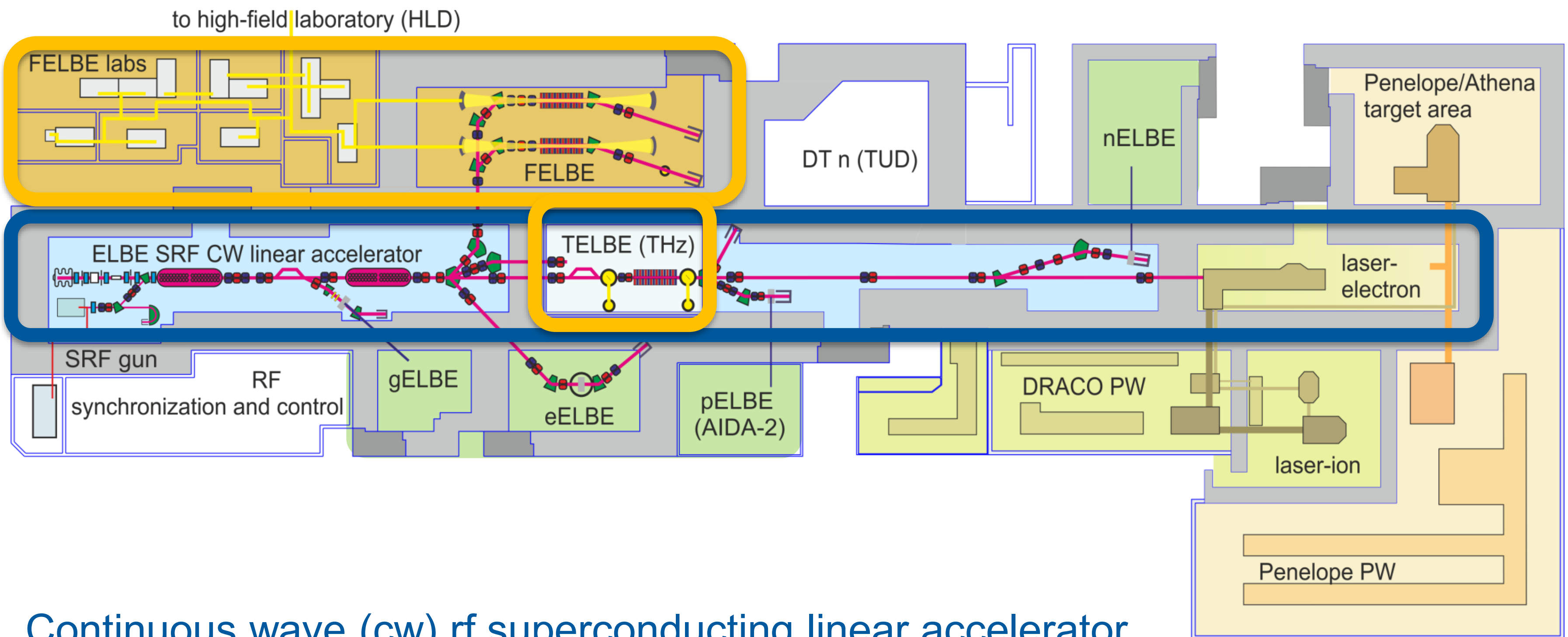

- Continuous wave (cw) rf superconducting linear accelerator

  Variable pulse rate (up to 13 MHz) and charge (**up to 0.3 nC**) in 40 MeV ps pulses

- IR-FEL and **superradiant THz** for IR spectroscopy and high field applications

ELBE center for high power radiation sources

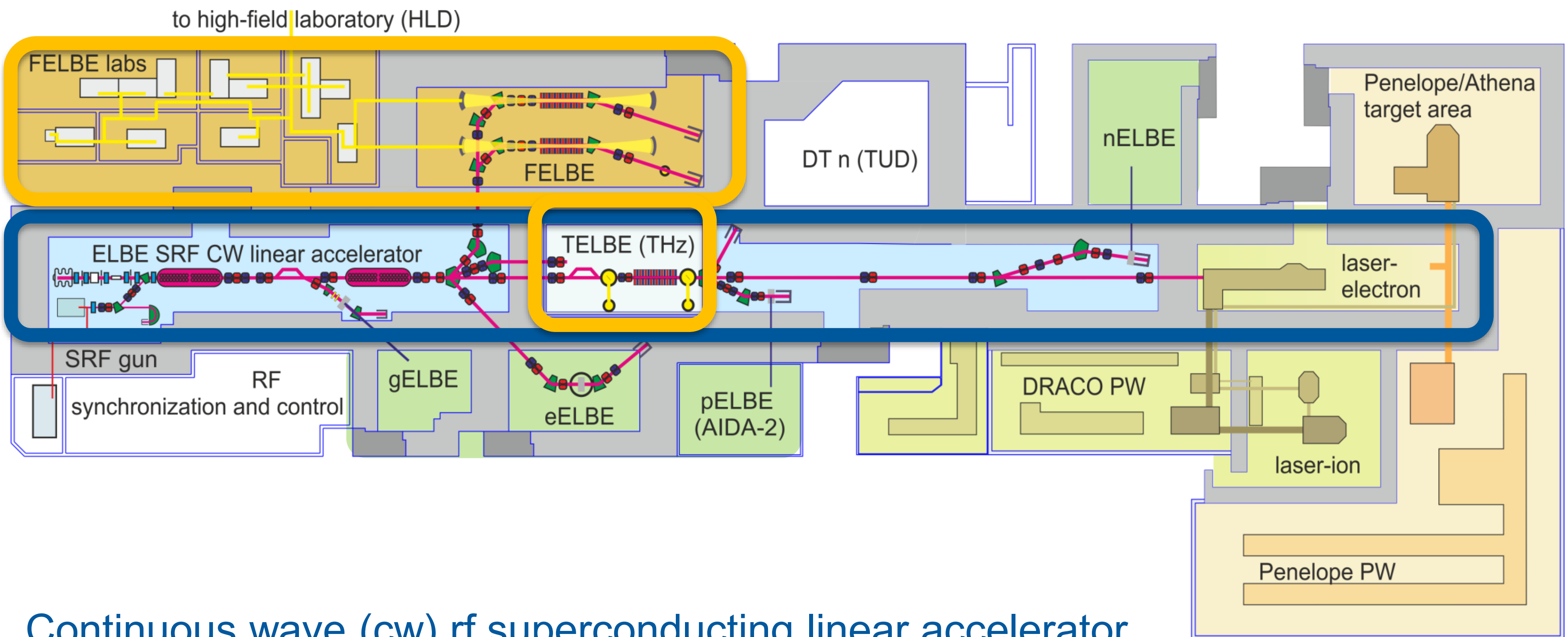

- Continuous wave (cw) rf superconducting linear accelerator

  Variable pulse rate (up to 13 MHz) and charge (**up to 0.3 nC**) in 40 MeV ps pulses
- IR-FEL and **superradiant THz** for IR spectroscopy and high field applications
- Test bench for advanced accelerator research, focus on **laser plasma accelerators** with 150 TW / PW dual beam ultrashort-pulse laser DRACO
- Diode laser pumped PW project PENELOPE (150J/150fs)

ELBE center for high power radiation sources

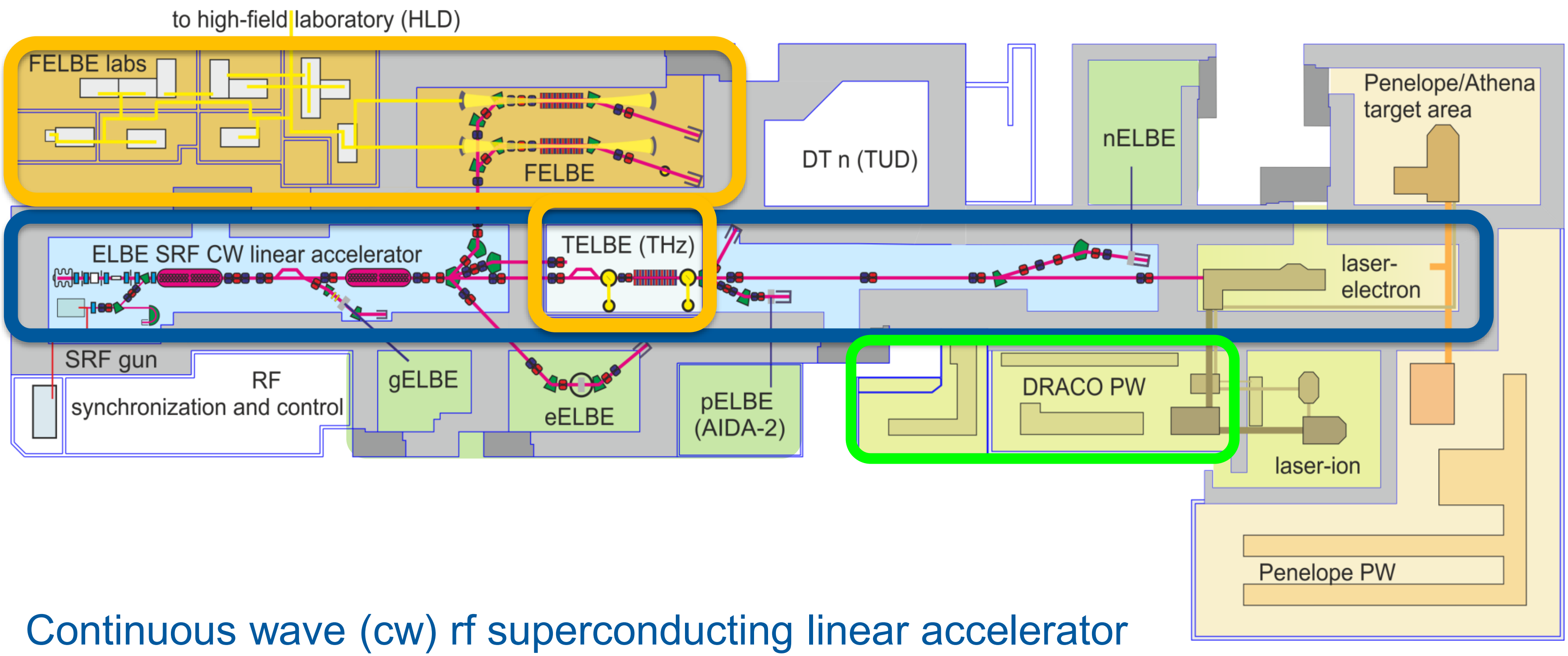

- Continuous wave (cw) rf superconducting linear accelerator

  Variable pulse rate (up to 13 MHz) and charge (**up to 0.3 nC**) in 40 MeV ps pulses
- IR-FEL and **superradiant THz** for IR spectroscopy and high field applications
- Test bench for advanced accelerator research, focus on **laser plasma accelerators** with 150 TW / PW dual beam ultrashort-pulse laser DRACO
- Diode laser pumped PW project PENELOPE (150J/150fs)

ELBE center for high power radiation sources

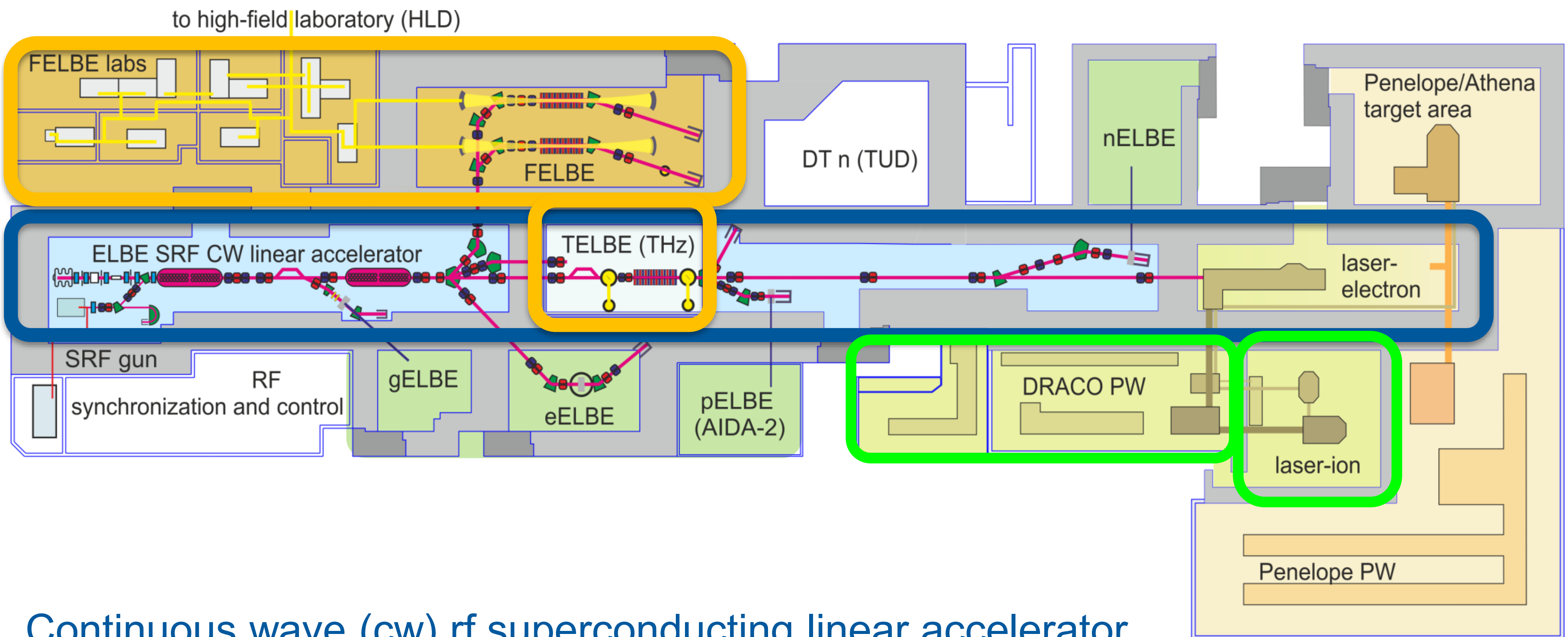

- Continuous wave (cw) rf superconducting linear accelerator

  Variable pulse rate (up to 13 MHz) and charge (**up to 0.3 nC**) in 40 MeV ps pulses

- IR-FEL and **superradiant THz** for IR spectroscopy and high field applications

- Test bench for advanced accelerator research, focus on **laser plasma accelerators** with 150 TW / PW dual beam ultrashort-pulse laser DRACO
- Diode laser pumped PW project PENELOPE (150J/150fs)

ELBE center for high power radiation sources

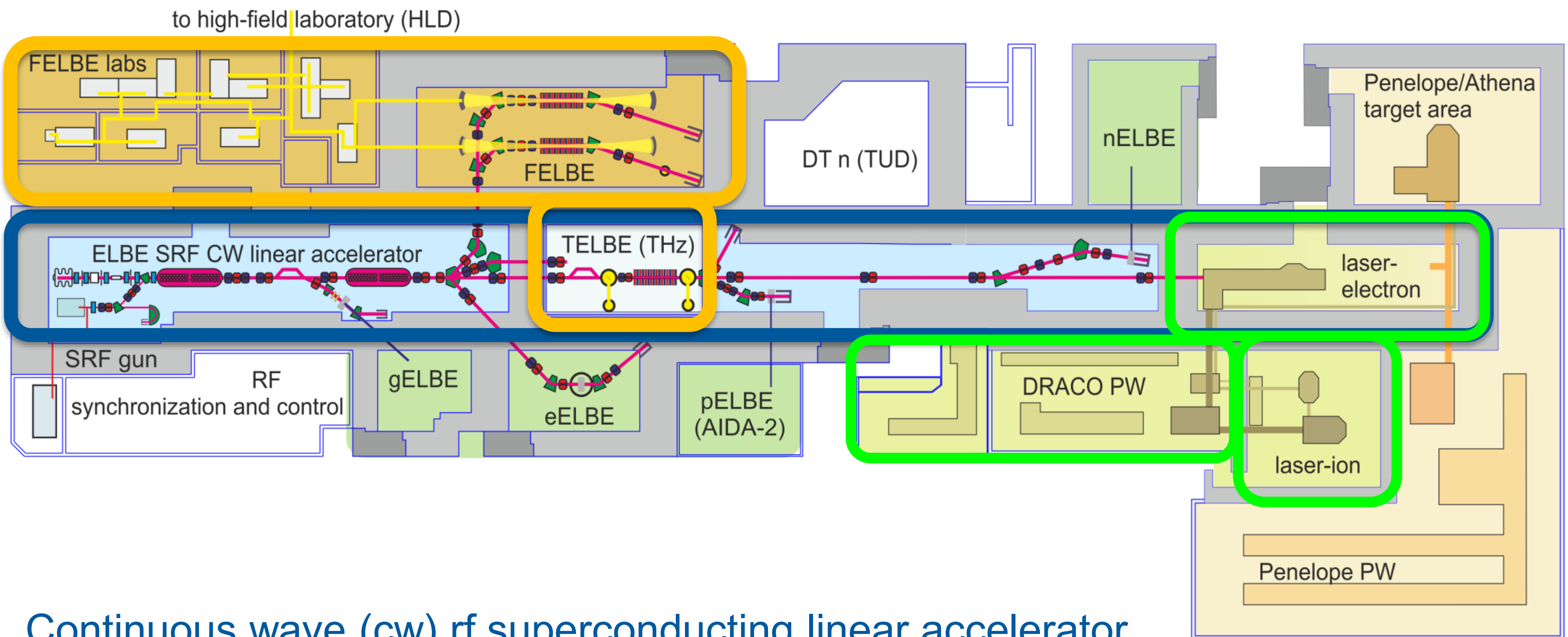

- Continuous wave (cw) rf superconducting linear accelerator

  Variable pulse rate (up to 13 MHz) and charge (**up to 0.3 nC**) in 40 MeV ps pulses

- IR-FEL and **superradiant THz** for IR spectroscopy and high field applications

- Test bench for advanced accelerator research, focus on **laser plasma accelerators** with 150 TW / PW dual beam ultrashort-pulse laser DRACO
- Diode laser pumped PW project PENELOPE (150J/150fs)

Accelerator (ELBE) based Thomson source

Laser wakefield acceleration

-> self truncated ionization injection

-> high charge / peak current regime

LWFA based light sources

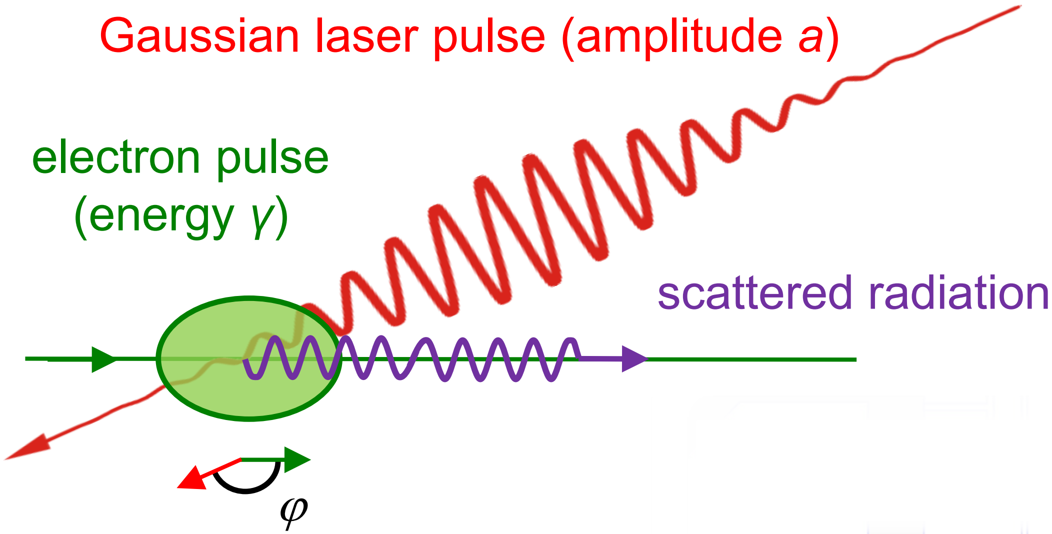
Gaussian laser pulse (amplitude *a*)
electron pulse
(energy *γ*)
scattered radiation
φ

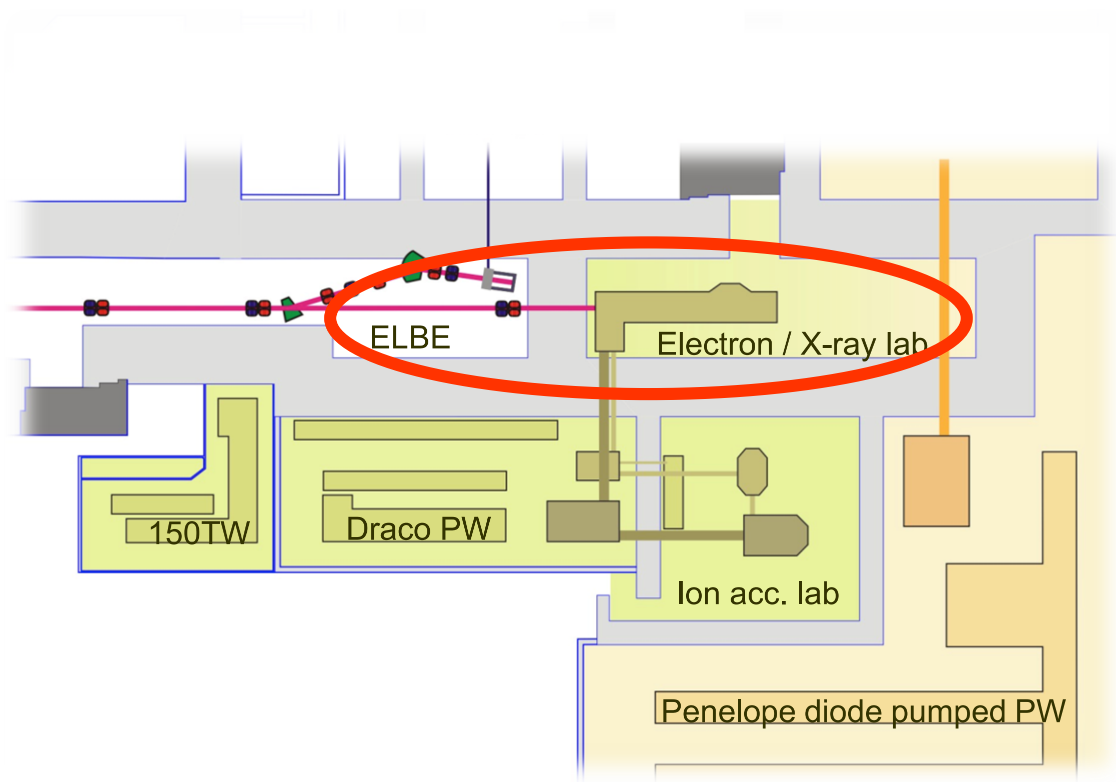
ELBE
Electron / X-ray lab
150TW
Draco PW
Ion acc. lab
Penelope diode pumped PW

Spectral distribution Thomson scattering

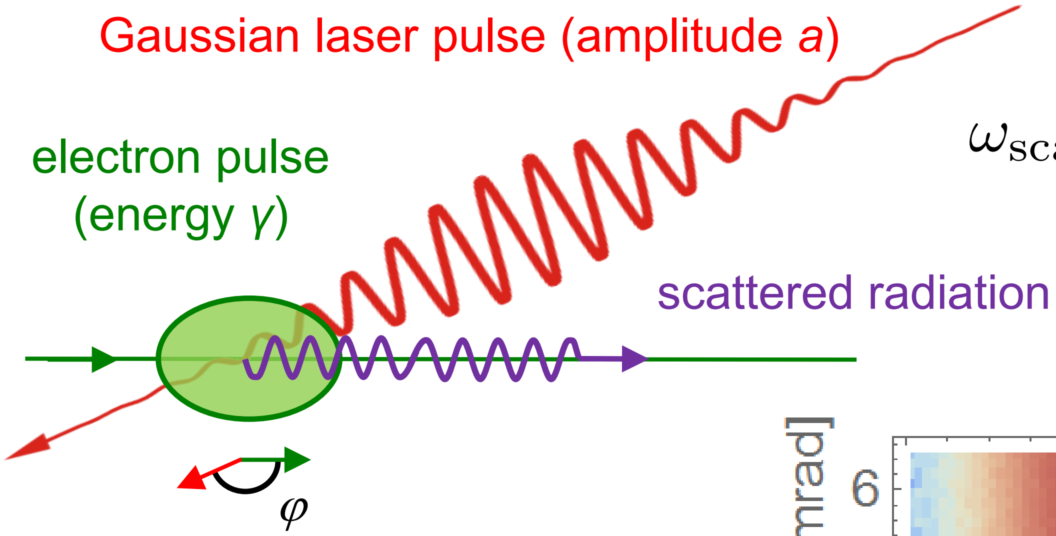

head-on

$$\omega_{\text{scatter}} = \frac{2\gamma^2\cancel{(1-\cos\varphi)}}{1+\frac{a_0^2}{2}+(\gamma\theta)^2}\,\omega_{\text{laser}}$$

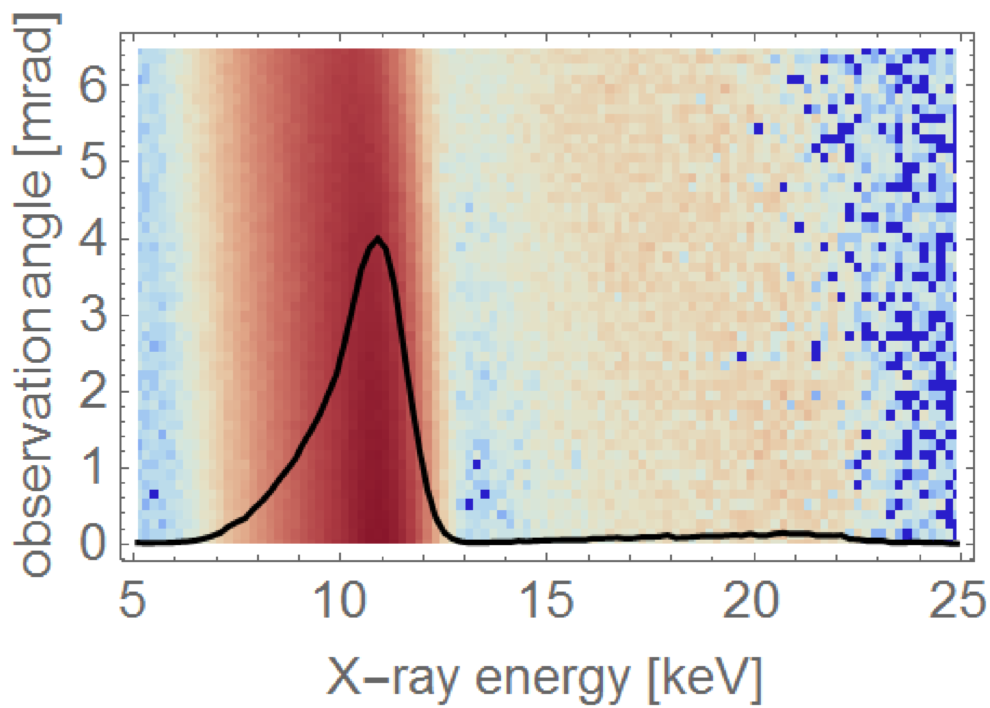

A. Debus, et al., Appl. Phys. B 100, 61 (2010)
A. Jochmann et al., PRL 111, 114803 (2013)
J. Krämer, Scientific Reports 8, 1398 (2018)

Spectral distribution Thomson scattering

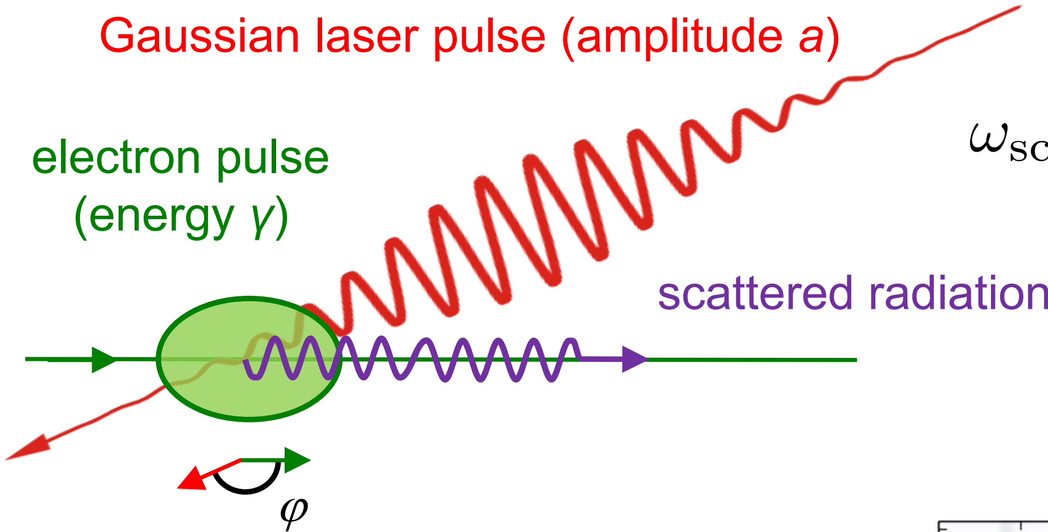

head-on

$$\omega_{\mathrm{scatter}} = \frac{2\gamma^2 \cancel{(1-\cos\varphi)}}{1+\frac{a_0^2}{2}+(\gamma\theta)^2}\,\omega_{\mathrm{laser}}$$

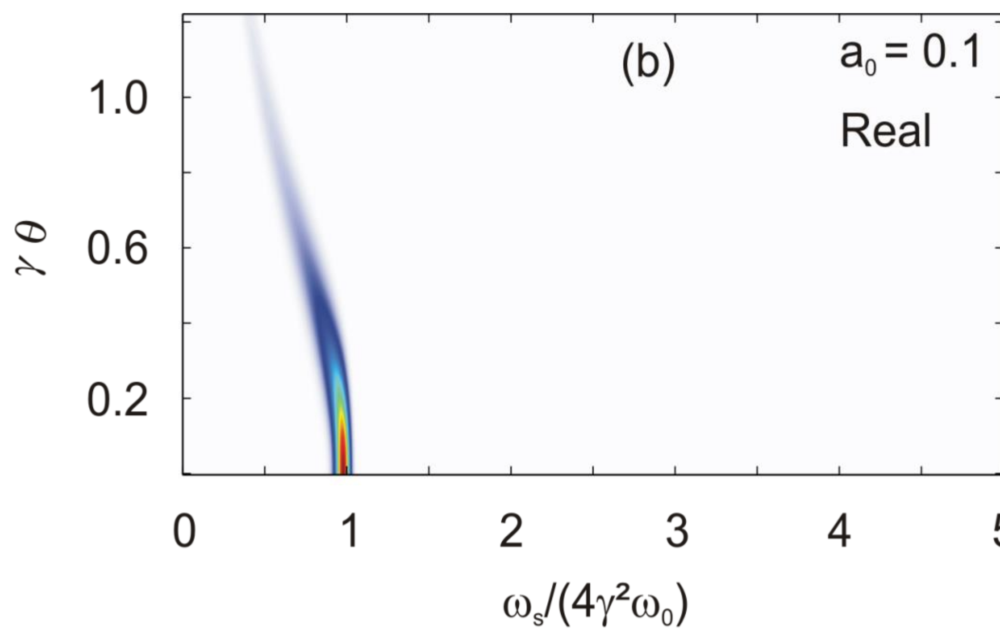

A. Debus, et al., Appl. Phys. B 100, 61 (2010)
A. Jochmann et al., PRL 111, 114803 (2013)
J. Krämer, Scientific Reports 8, 1398 (2018)

Spectral distribution Thomson scattering

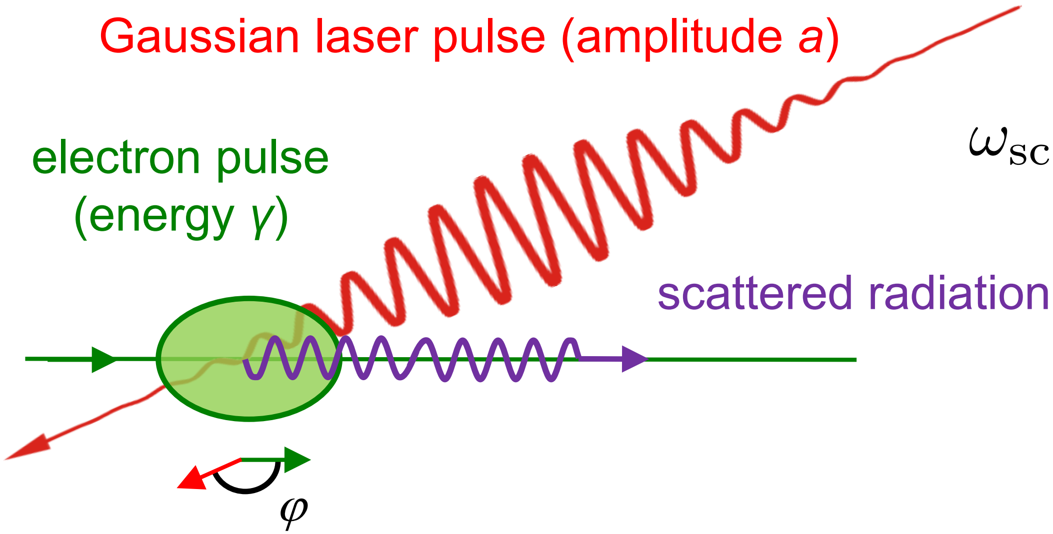

$$\omega_{\text{scatter}} = \frac{2\gamma^2(1-\cos\varphi)}{1+\frac{a_0^2}{2}+(\gamma\theta)^2}\,\omega_{\text{laser}}$$

Nonlinear case, Gaussian pulse

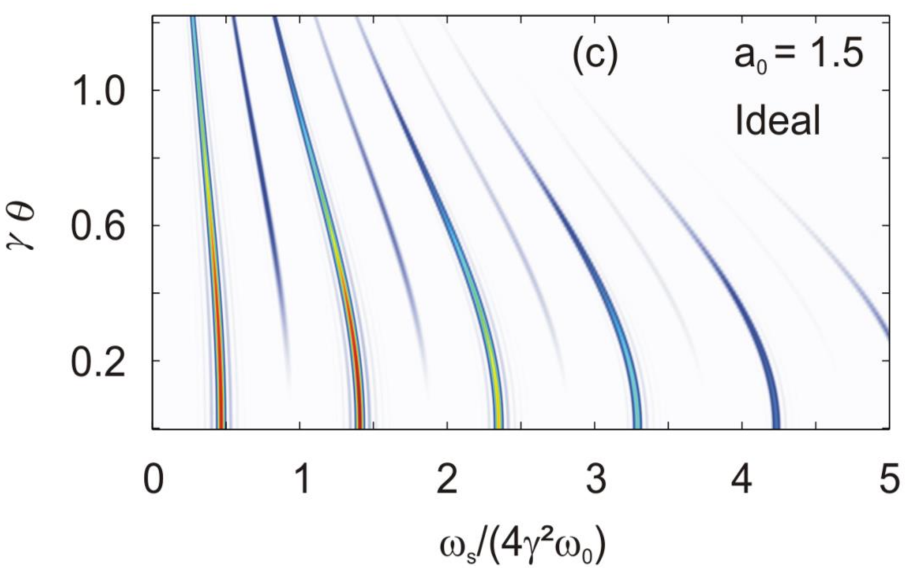

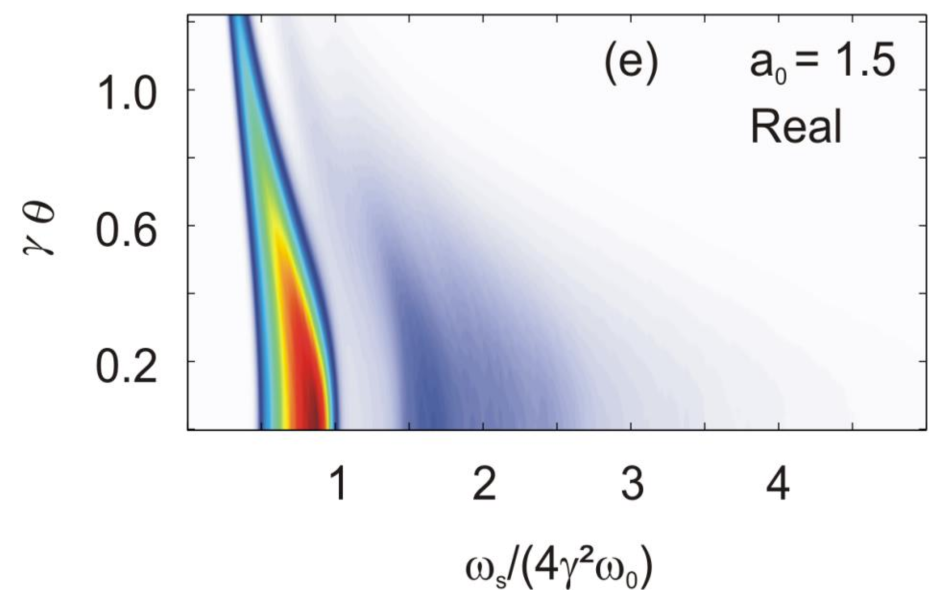

Accelerator based Thomson source

Nonlinear Thomson scattering

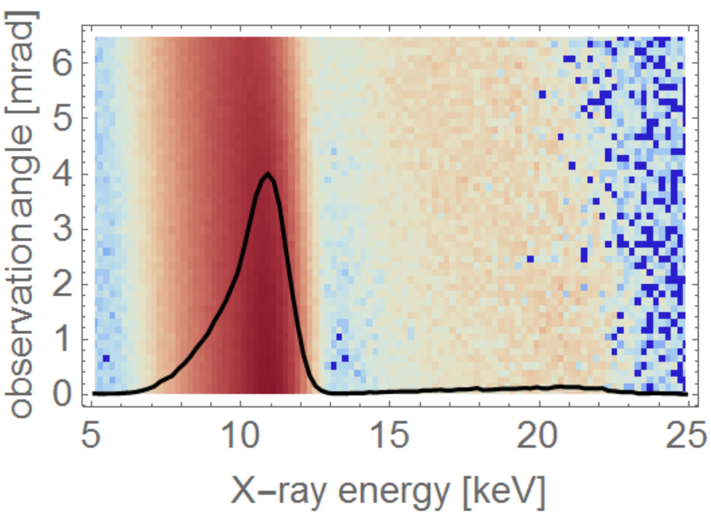

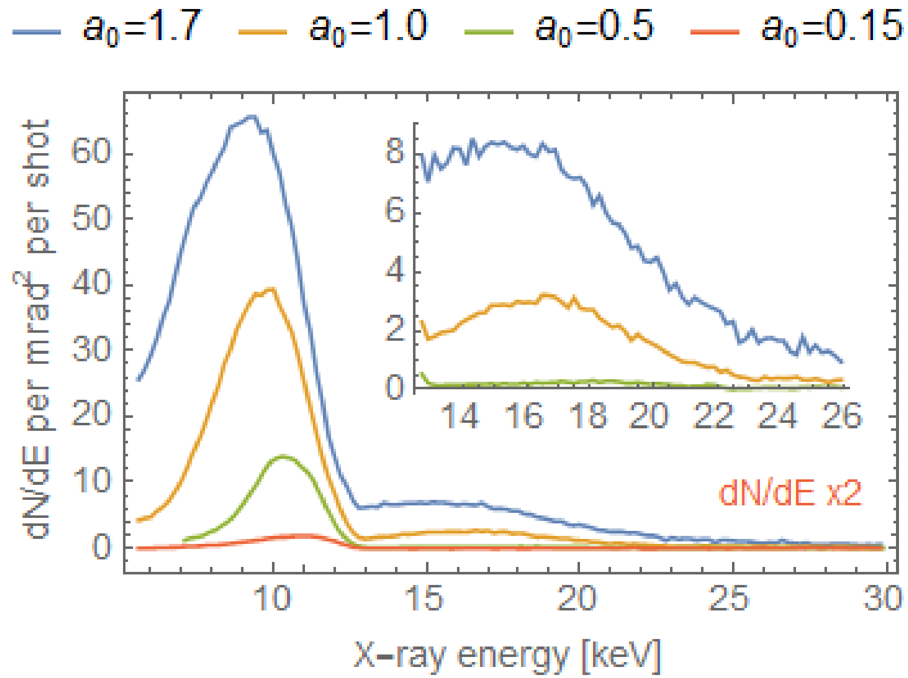

- red-shift and broadening of the fundamental with increasing a_0
- harmonics (pile up corrected) with increasing laser intensity a_0
- may serve as EUV to Xray light source

-> above 10^6 per shot
in $1/\gamma$ cone (a_0~1.5)
-> 10^9 with non-Gaussian pulse

- serves as high resolution in-situ diagnostics of angular distribution
(and with source size for emittance)

Accelerator based Thomson source

Laser wakefield acceleration

-> self truncated ionization injection

-> high charge / peak current regime

-> hybrid PWFA schemes

LWFA based light sources

Ionization injection in LWFA

- Ionization injection: accelerating medium (He) doped by a high-Z gas (N_2)

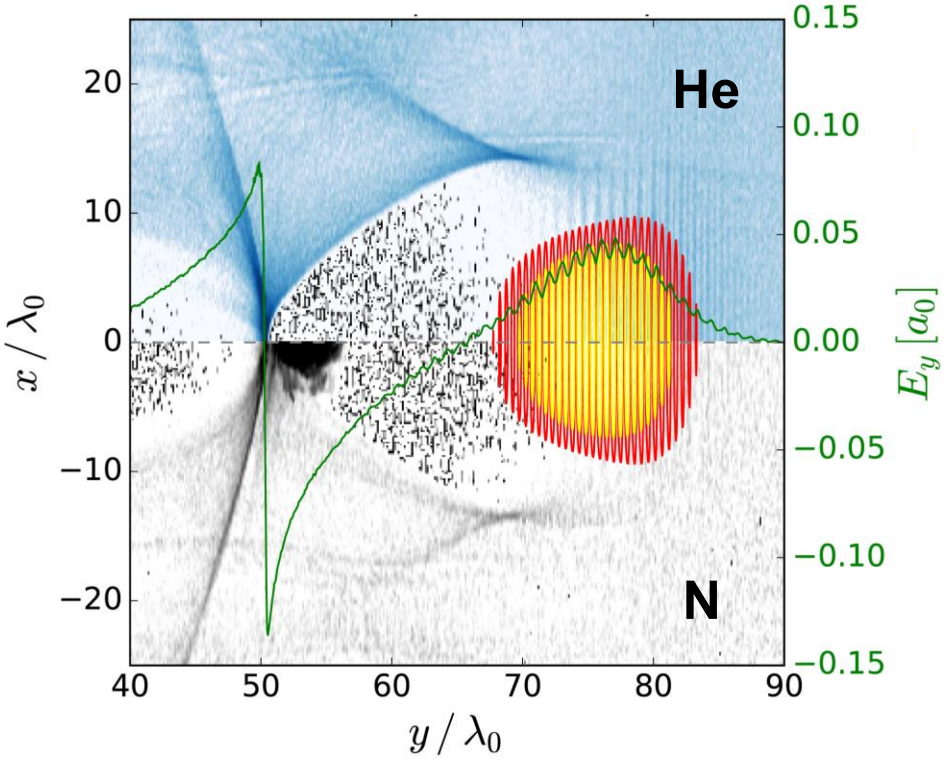

- Ionization injection: accelerating medium (He) doped by a high-Z gas (N_2)

Species	Ionisation energy (eV)
He^{1+}	24.6
He^{2+}	54.4
N^{1+}	14.5
N^{2+}	29.6
N^{3+}	47.4
N^{4+}	77.5
N^{5+}	97.9
N^{6+}	552
N^{7+}	667

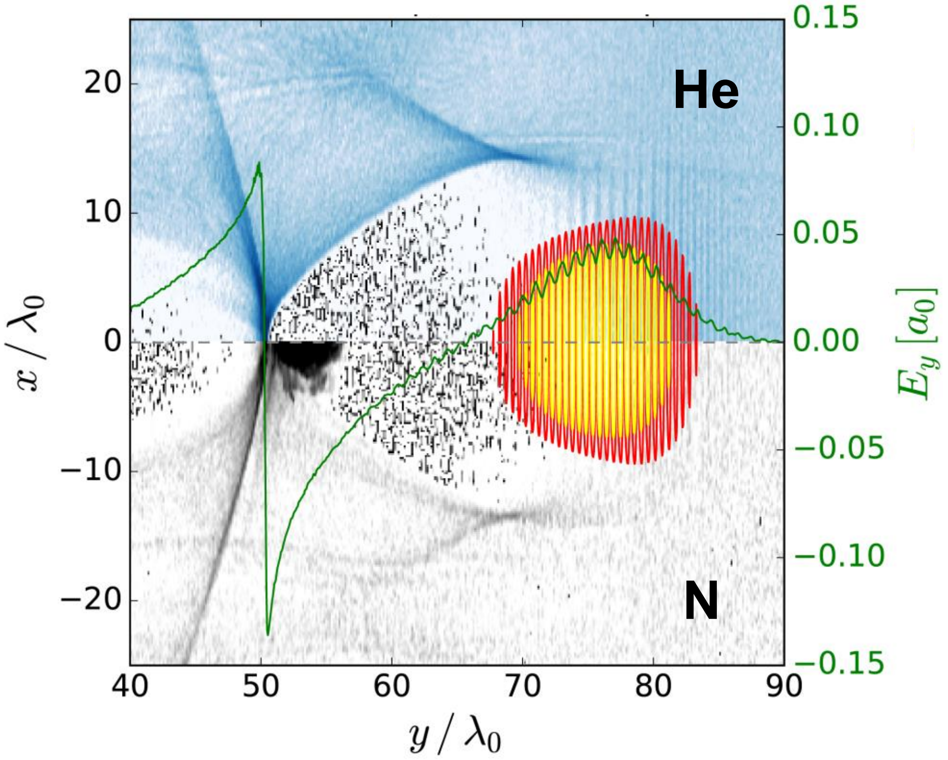

- Ionization injection: accelerating medium (He) doped by a high-Z gas (N_2)

Species	Ionisation energy (eV)
He^{1+}	24.6
He^{2+}	54.4
N^{1+}	14.5
N^{2+}	29.6
N^{3+}	47.4
N^{4+}	77.5
N^{5+}	97.9
N^{6+}	552
N^{7+}	667

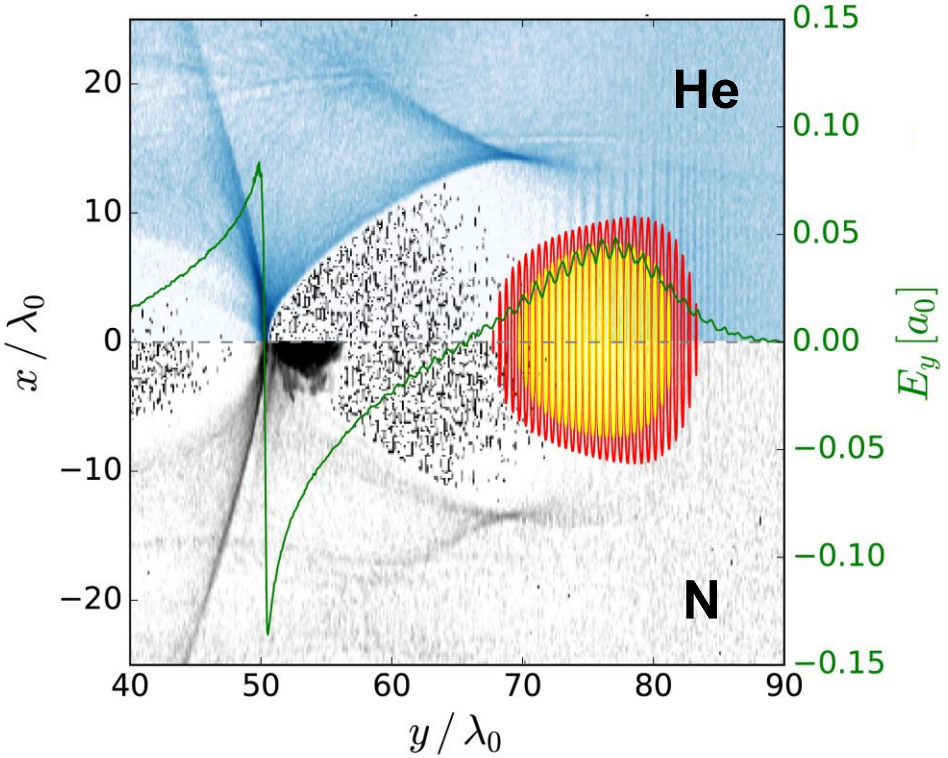

- Ionization injection: accelerating medium (He) doped by a high-Z gas (N_2)

Species	Ionisation energy (eV)
He^{1+}	24.6
He^{2+}	54.4
N^{1+}	14.5
N^{2+}	29.6
N^{3+}	47.4
N^{4+}	77.5
N^{5+}	97.9
N^{6+}	552
N^{7+}	667

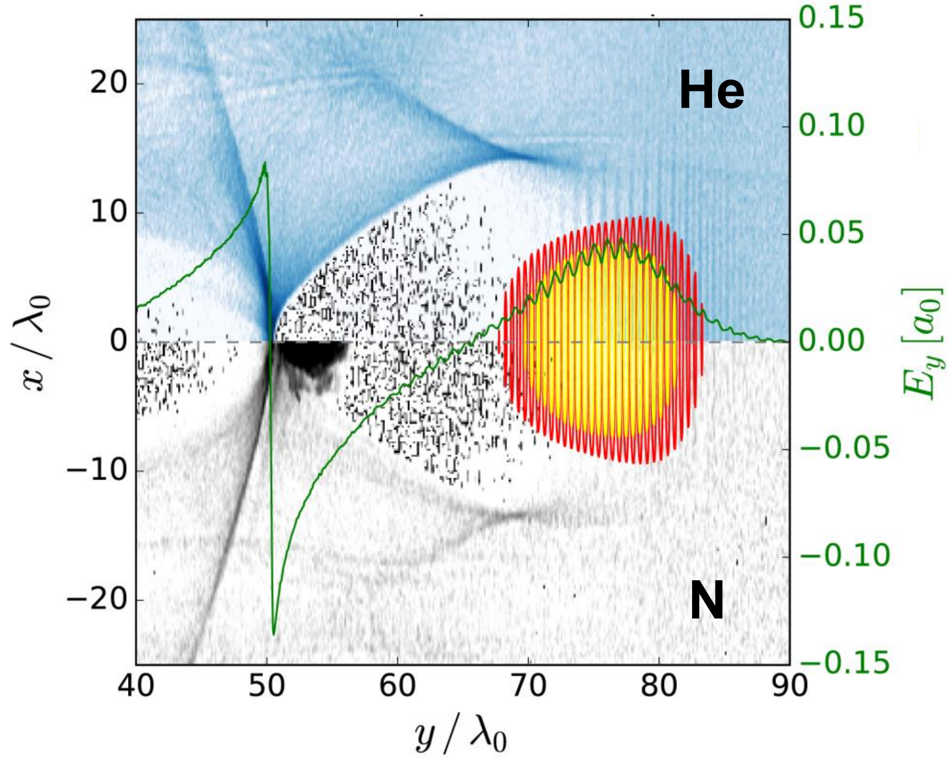

Ionized only near the laser peak intensity

Ionization injection in LWFA

- Ionization injection: accelerating medium (He) doped by a high-Z gas (N_2)

Species	Ionisation energy (eV)
He^{1+}	24.6
He^{2+}	54.4
N^{1+}	14.5
N^{2+}	29.6
N^{3+}	47.4
N^{4+}	77.5
N^{5+}	97.9
N^{6+}	552
N^{7+}	667

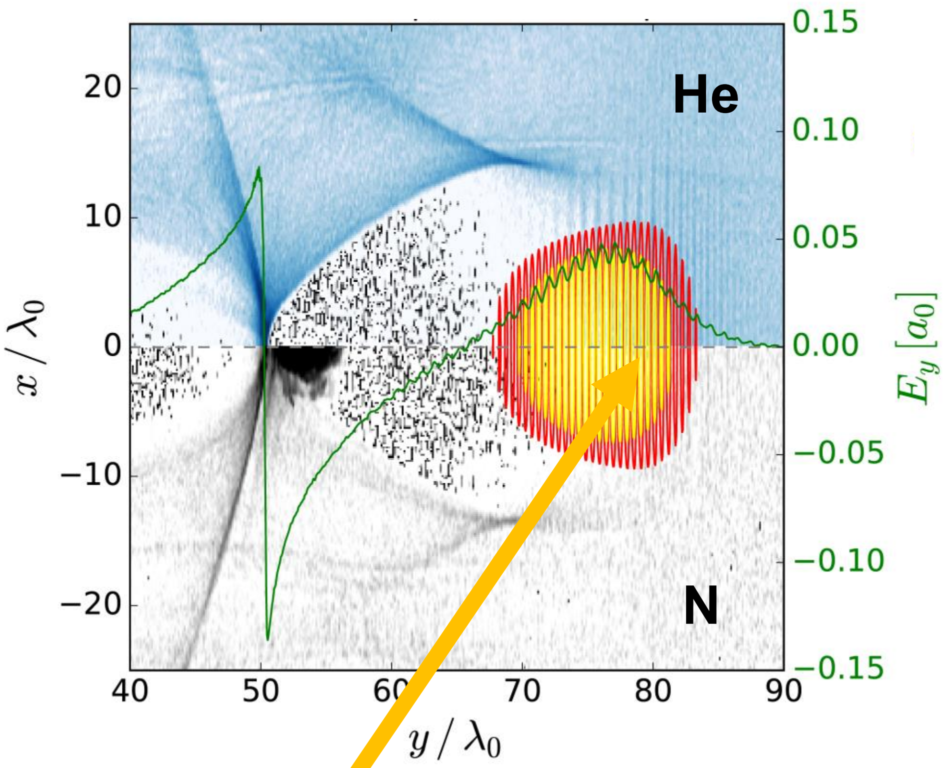

Ionized only near the laser peak intensity

Ionization injection in LWFA

- Ionization injection: accelerating medium (He) doped by a high-Z gas (N_2)

Species	Ionisation energy (eV)
He^{1+}	24.6
He^{2+}	54.4
N^{1+}	14.5
N^{2+}	29.6
N^{3+}	47.4
N^{4+}	77.5
N^{5+}	97.9
N^{6+}	552
N^{7+}	667

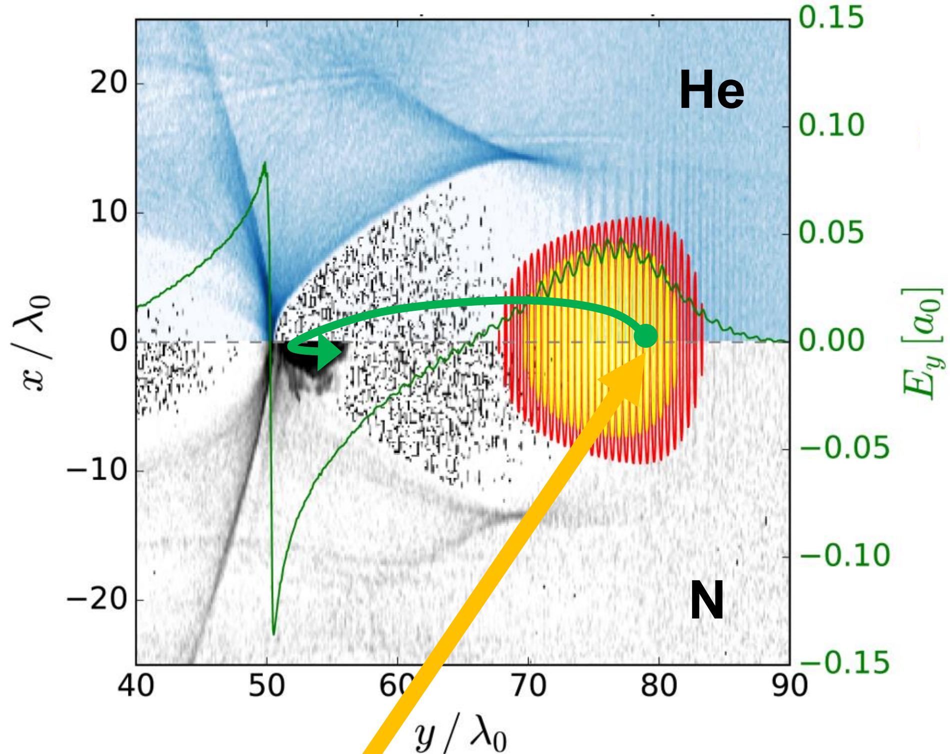

Ionized only near the laser peak intensity

- Ionization injection: accelerating medium (He) doped by a high-Z gas (N_2)

Species	Ionisation energy (eV)
He^{1+}	24.6
He^{2+}	54.4
N^{1+}	14.5
N^{2+}	29.6
N^{3+}	47.4
N^{4+}	77.5
N^{5+}	97.9
N^{6+}	552
N^{7+}	667

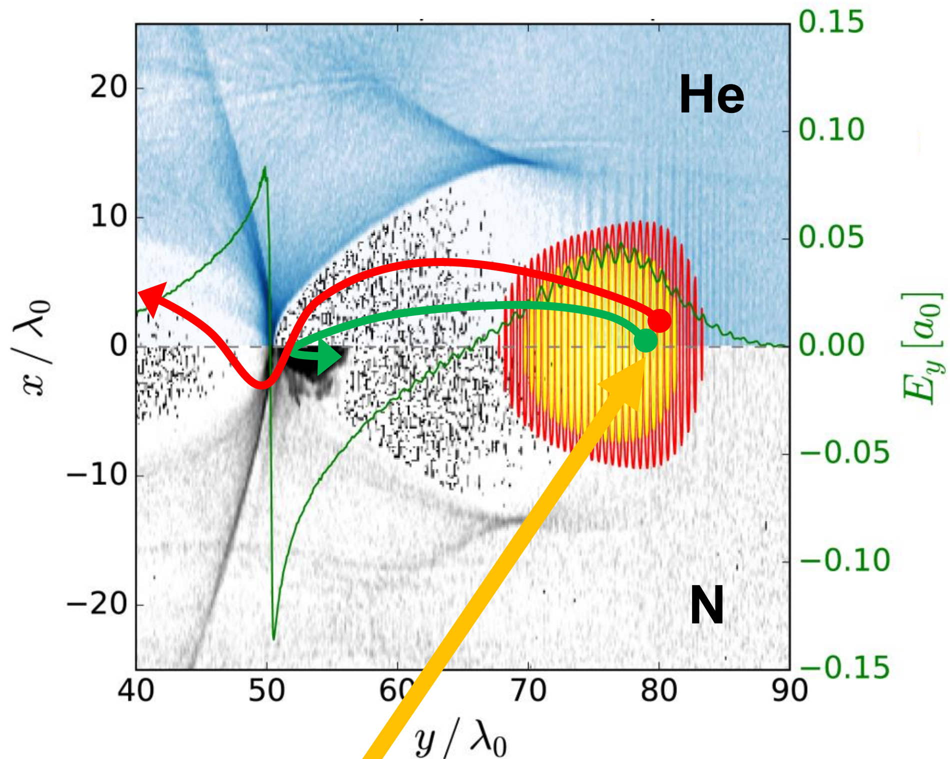

Ionized only near the laser peak intensity

Controlled self truncated ionization injection

- Injection can be limited by using an **unmatched laser spot**
- Laser modulation (external and self-focusing) influences the wakefield ending electron capture

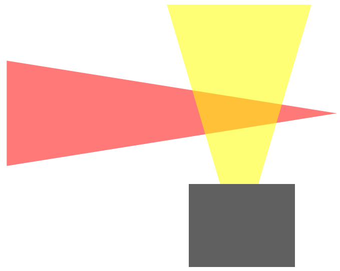

- **Injection only when**:
  - Laser intensity is high enough (valid over large distance)
  - Pseudo-potential difference allows trapping (can be tailored)

Controlled self truncated ionization injection

- Injection can be limited by using an **unmatched laser spot**
- Laser modulation (external and self-focusing) influences the wakefield ending electron capture

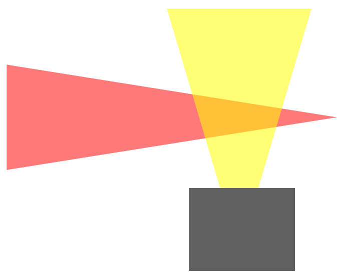

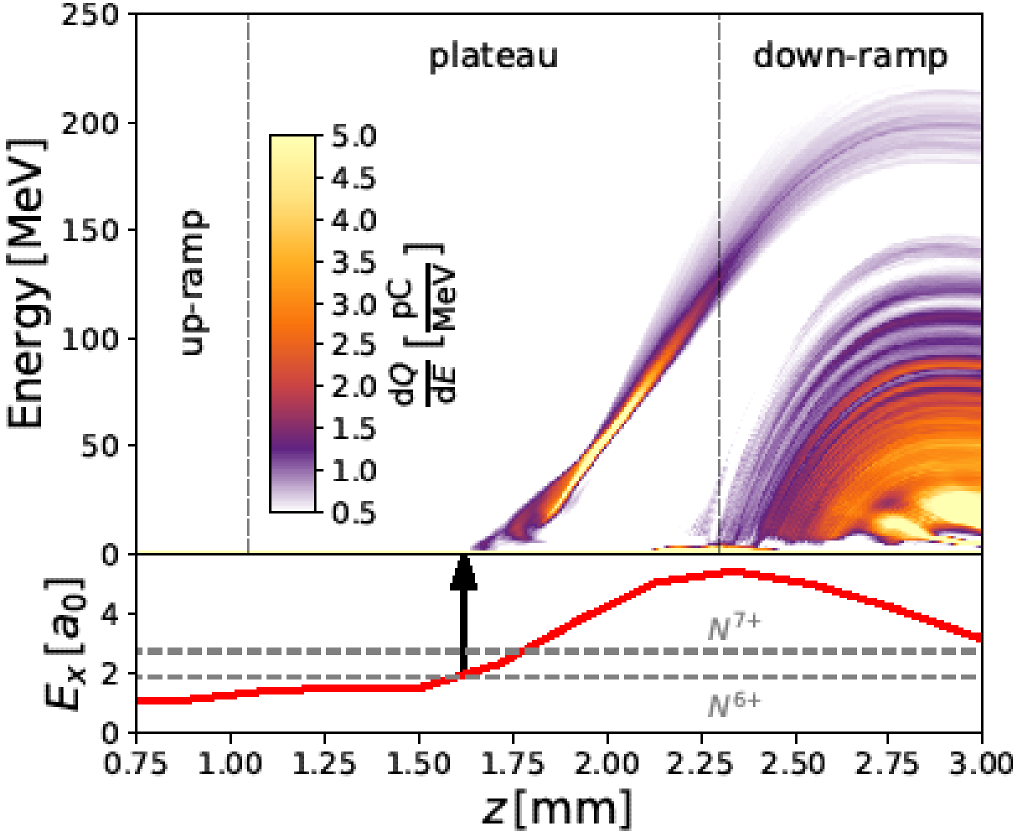

- **Injection only when**:
  - Laser intensity is high enough (valid over large distance)
  - Pseudo-potential difference allows trapping (can be tailored)

Controlled self truncated ionization injection

- Injection can be limited by using an **unmatched laser spot**
- Laser modulation (external and self-focusing) influences the wakefield ending electron capture

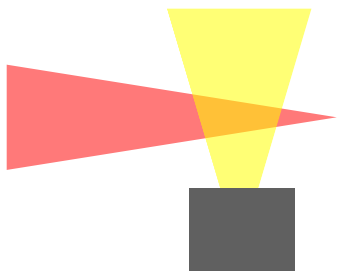

PIConGPU

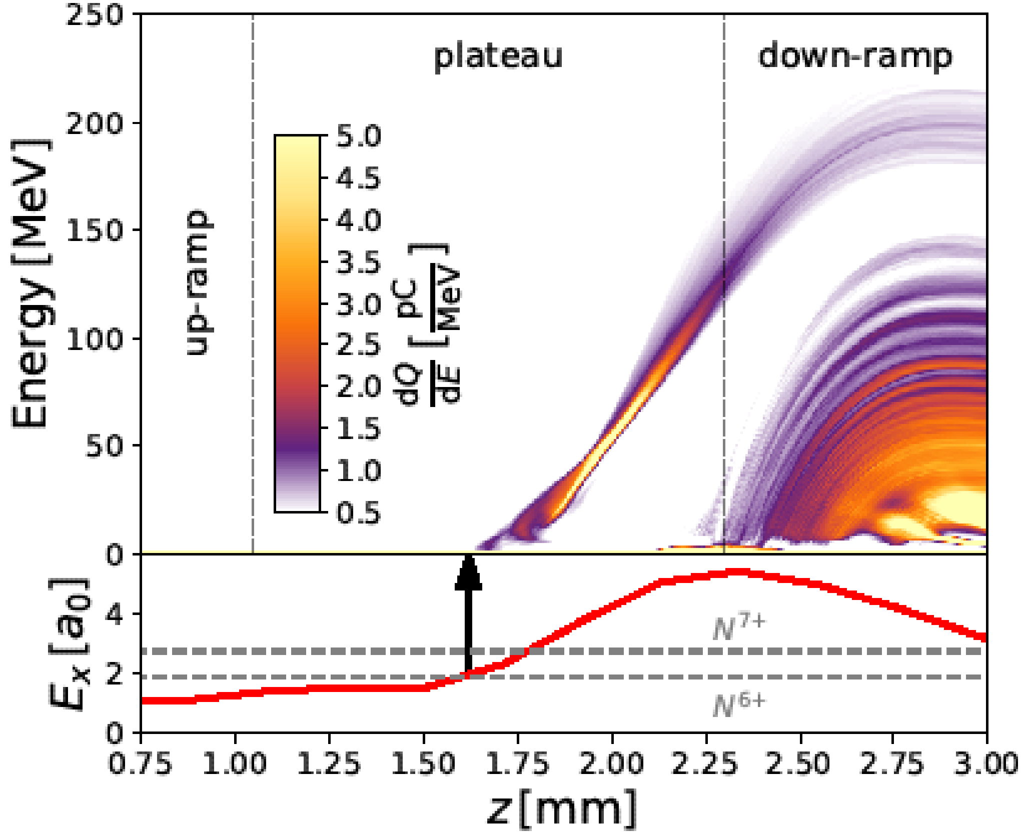

- **Injection only when**:
  - Laser intensity is high enough (valid over large distance)
  - Pseudo-potential difference allows trapping (can be tailored)

Controlled self truncated ionization injection

- Injection can be limited by using an **unmatched laser spot**
- Laser modulation (external and self-focusing) influences the wakefield ending electron capture

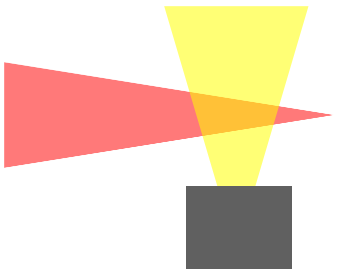

PIConGPU
picongpu.hzdr.de

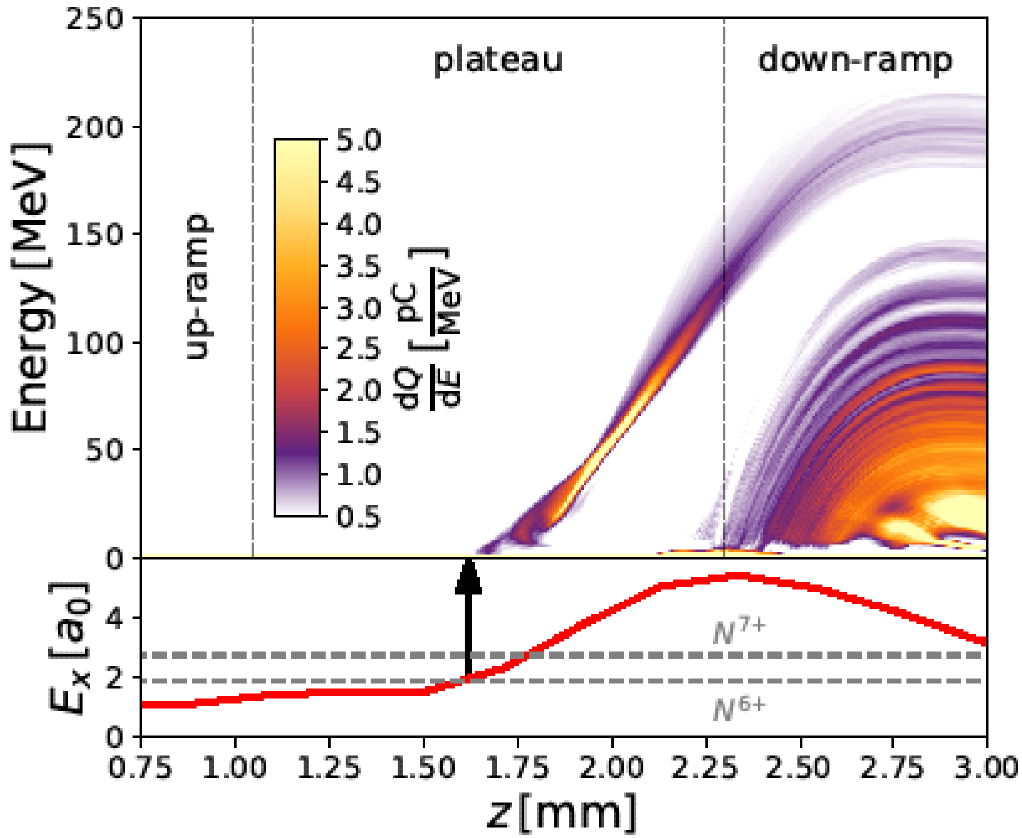

- **Injection only when**:
  - Laser intensity is high enough (valid over large distance)
  - Pseudo-potential difference allows trapping (can be tailored)

Controlled self truncated ionization injection

- Injection can be limited by using an **unmatched laser spot**
- Laser modulation (external and self-focusing) influences the wakefield ending electron capture

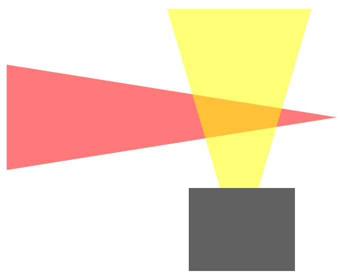

PIConGPU

picongpu.hzdr.de

(real beam propagation, ionization, 3D)

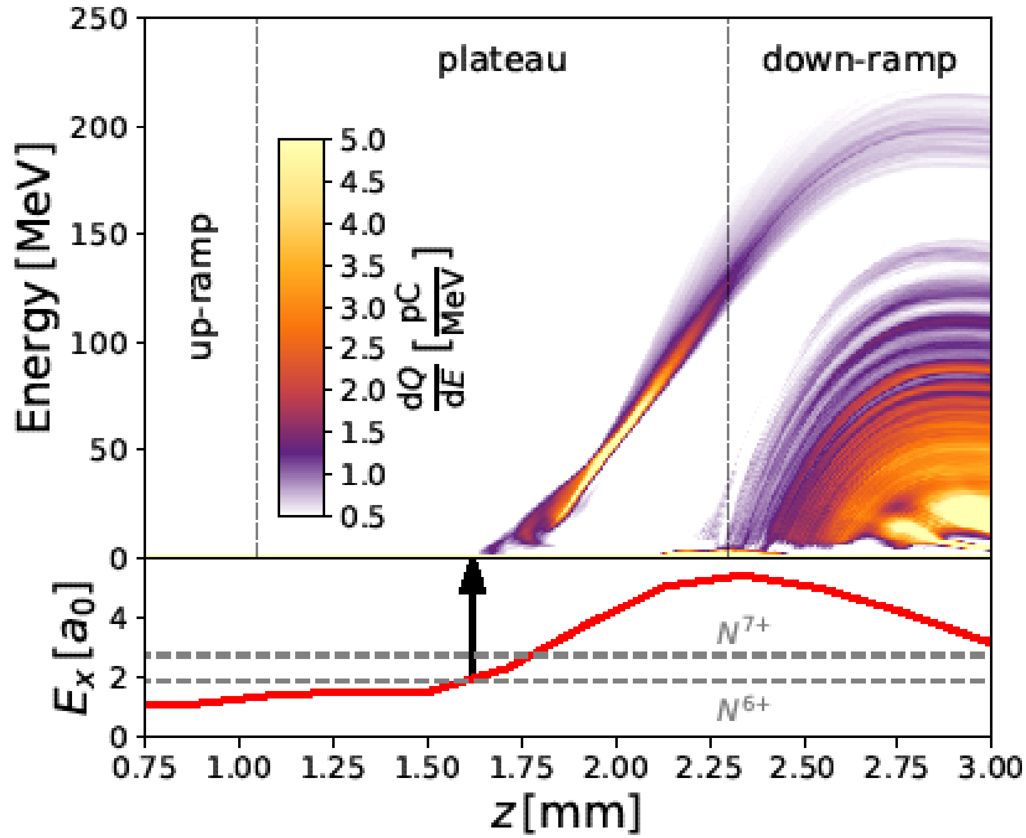

- **Injection only when**:
  - Laser intensity is high enough (valid over large distance)
  - Pseudo-potential difference allows trapping (can be tailored)

HZDR

nC-level charge in peaked low background distribution

2.5 J, 30 fs, a_0~2.6 (vac), plasma density 3.1×10^{18} cm^{-3}, mixed He + 1% N_2

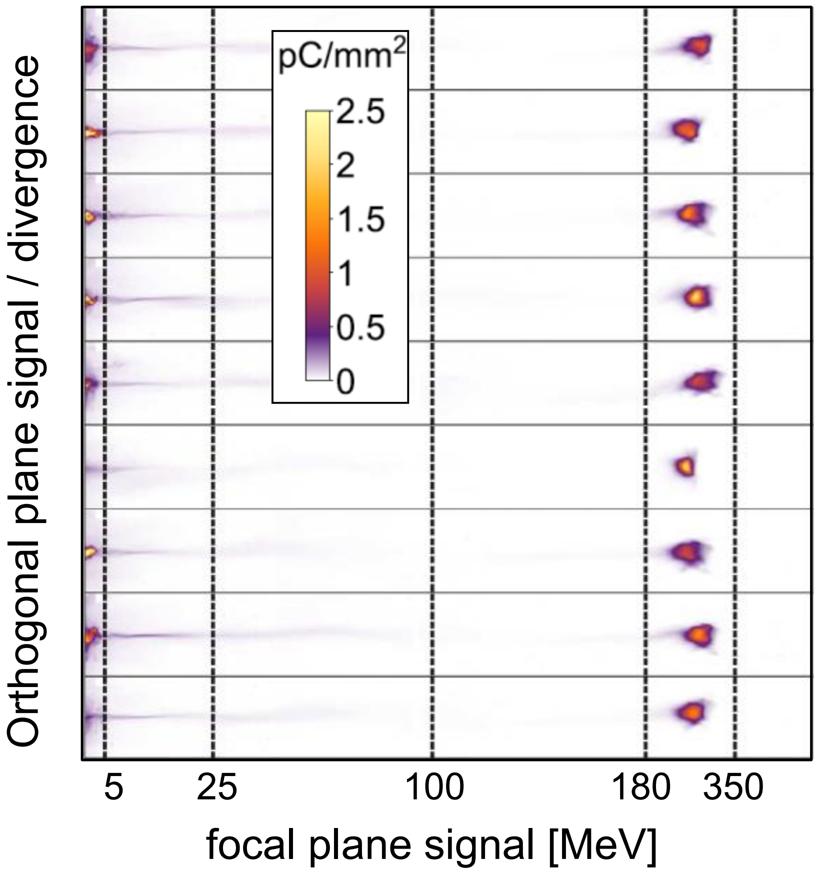

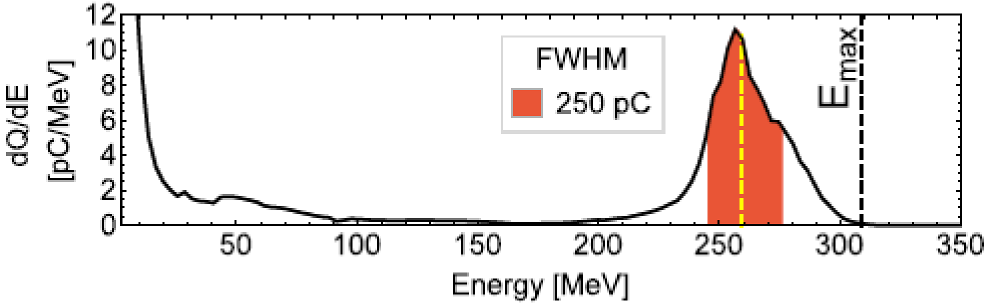

Parameters	Mean ± Shot-to-shot jitter
Mean peak energy	250 MeV ± 22.5 MeV
Charge in FWHM	250 pC ± 40 pC
Abs. energy width	36 MeV ± 11 MeV
Divergence	7 mrad ± 1 mrad

J. Couperus, et al., Nat. Commun. 8, 487 (2017), charge calibration revisited: T. Kurz in preparation (2017)

Charge tuning via Nitrogen doping

- We need to **tune** the **injected charge** at **equal plasma dynamics** in order to study beam loading effects

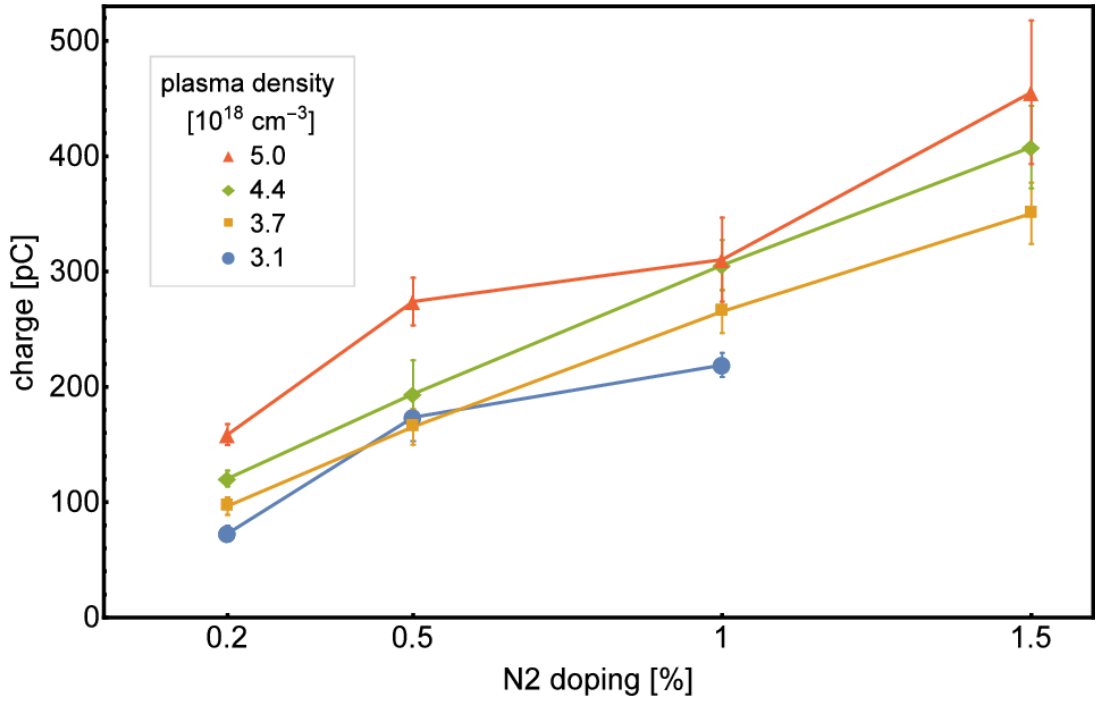

Charge tuning via Nitrogen doping

- We need to **tune** the **injected charge** at **equal plasma dynamics** in order to study beam loading effects

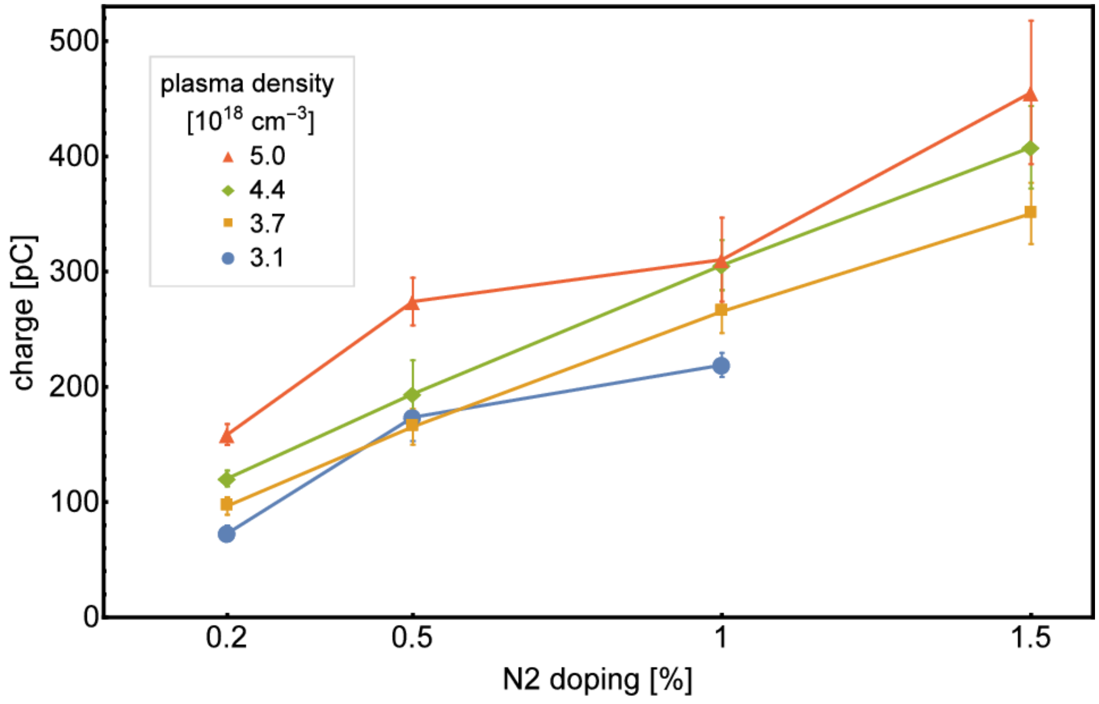

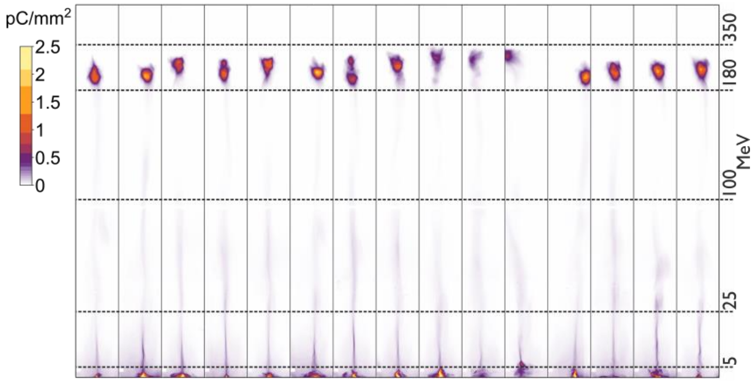

Charge tuning via Nitrogen doping

- We need to **tune** the **injected charge** at **equal plasma dynamics** in order to study beam loading effects

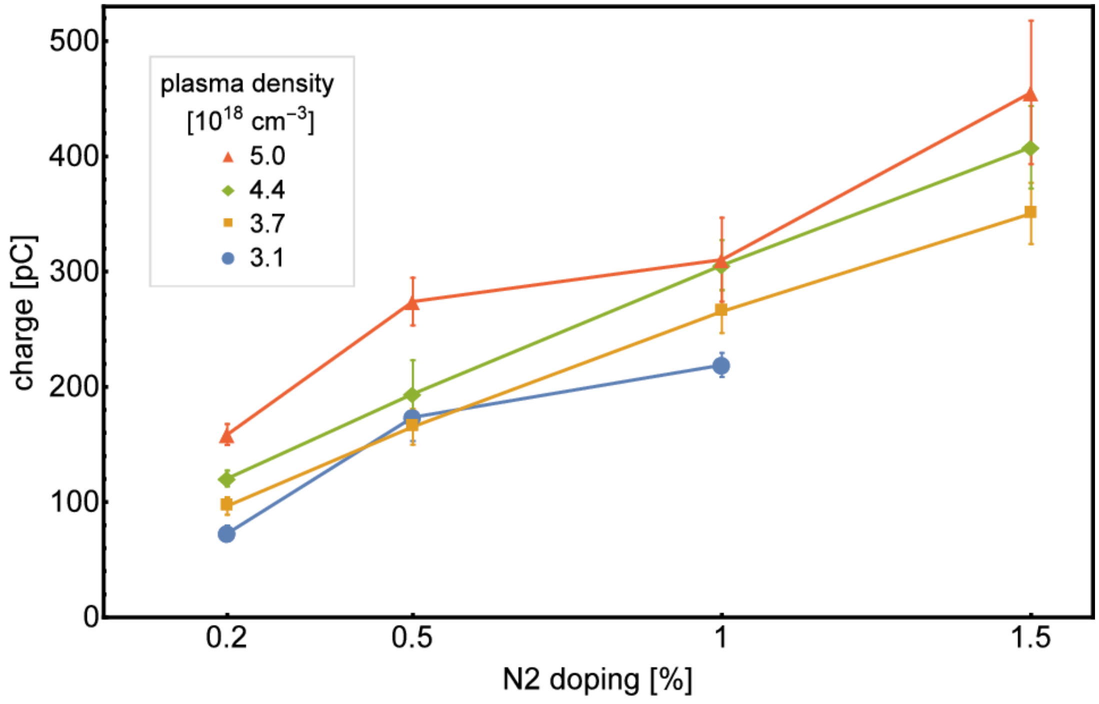

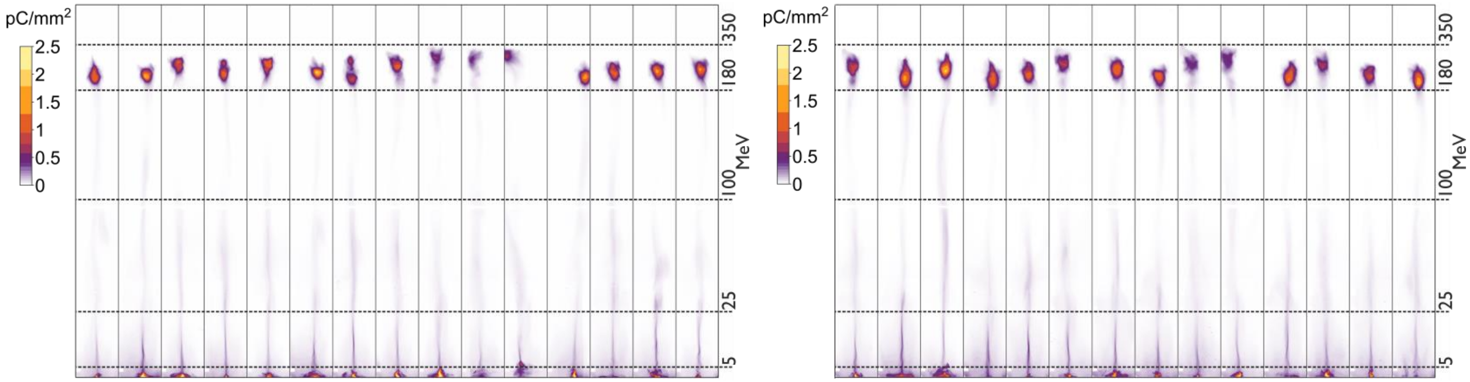

Charge tuning via Nitrogen doping

- We need to **tune** the **injected charge** at **equal plasma dynamics** in order to study beam loading effects

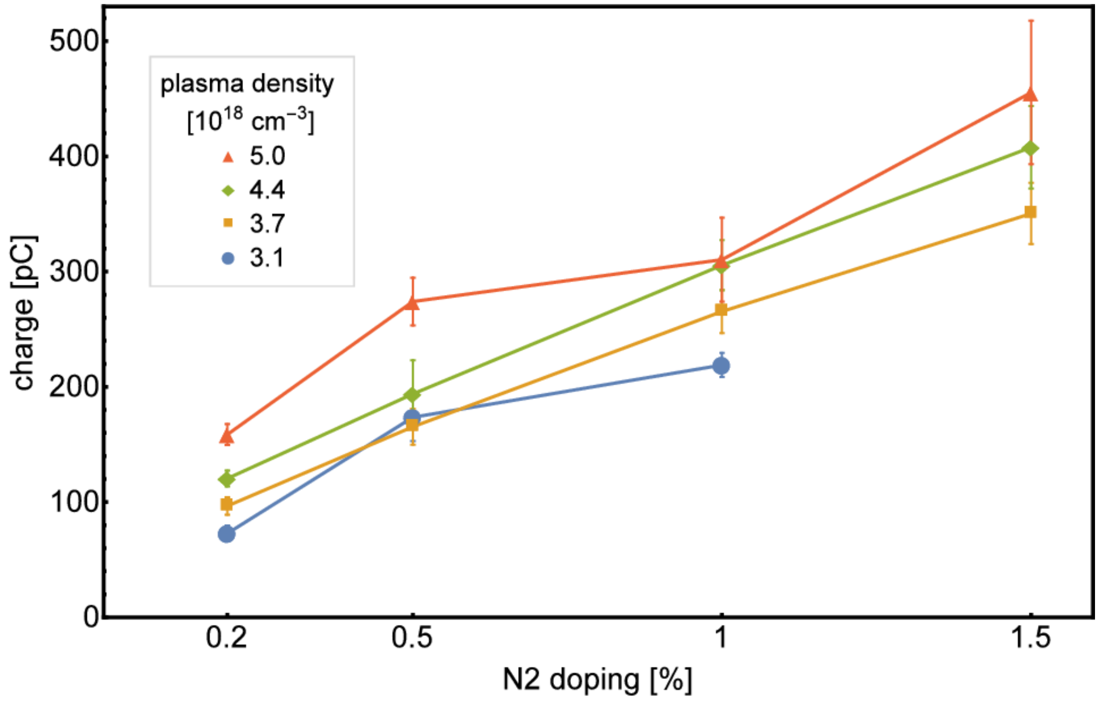

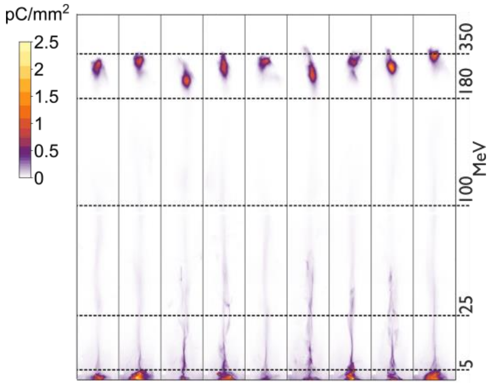

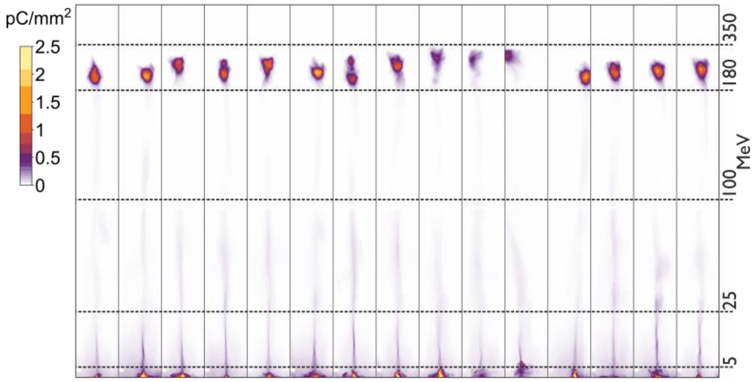

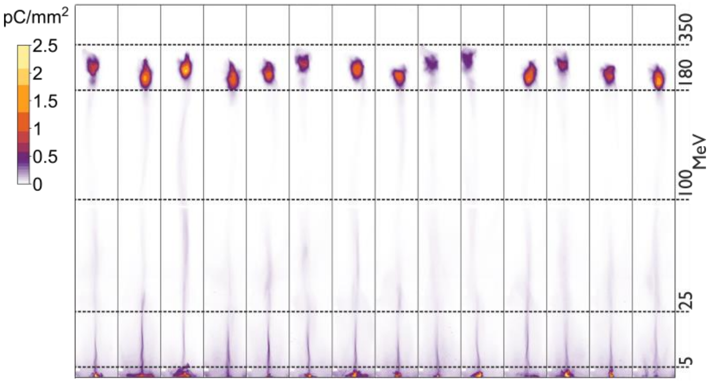

Charge tuning via Nitrogen doping

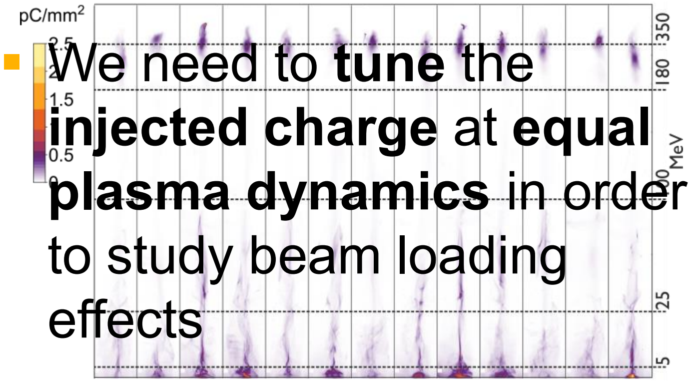

- We need to **tune** the **injected charge** at **equal plasma dynamics** in order to study beam loading effects

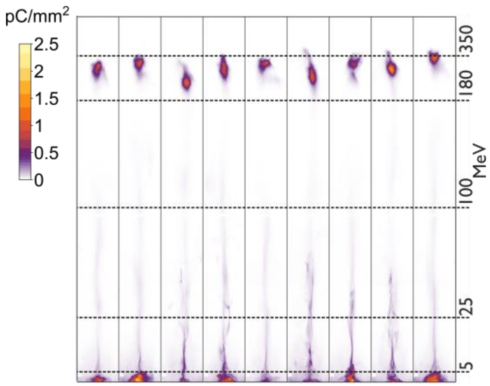

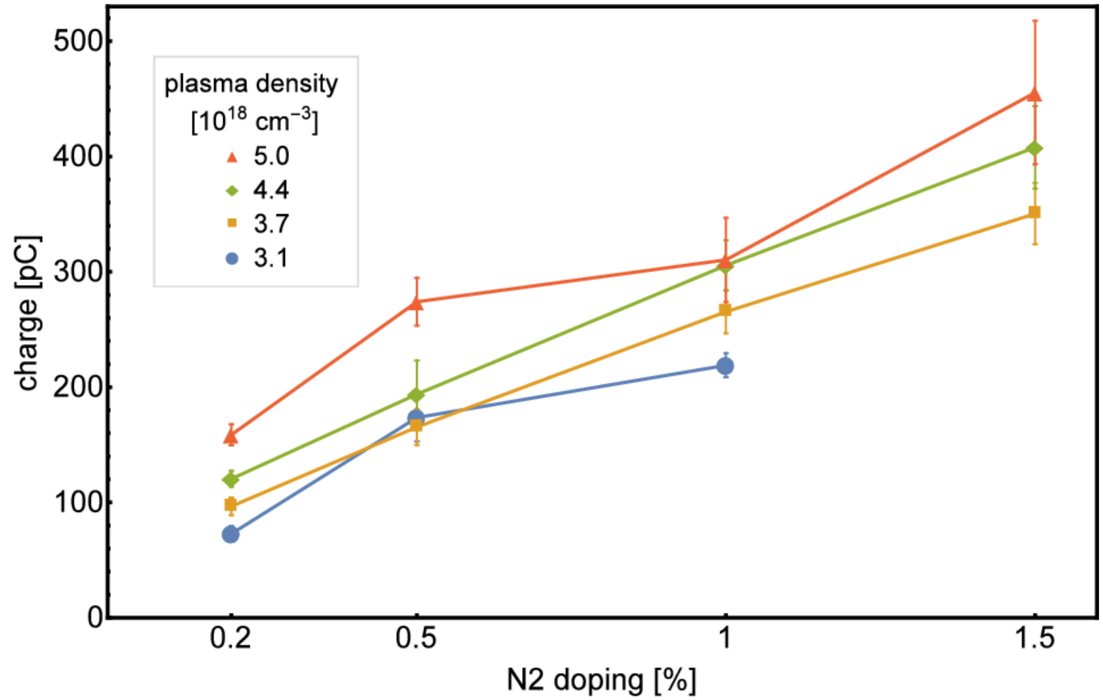

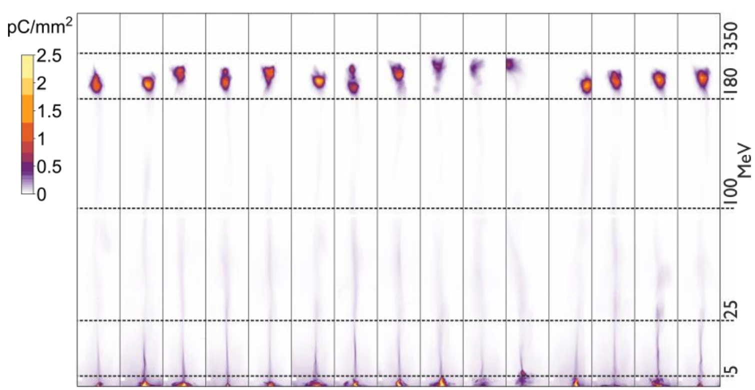

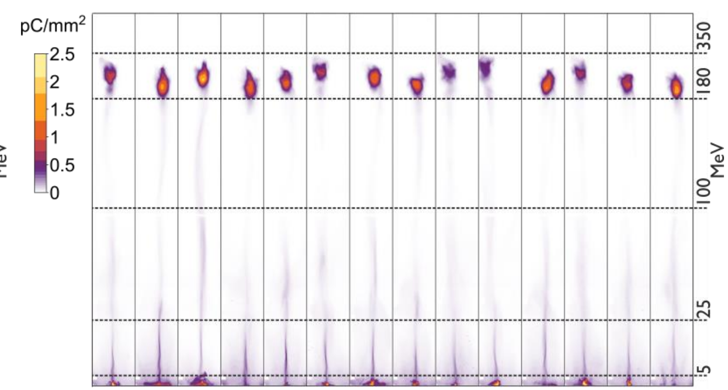

Charge tuning via Nitrogen doping

- We need to **tune** the **injected charge** at **equal plasma dynamics** in order to study beam loading effects

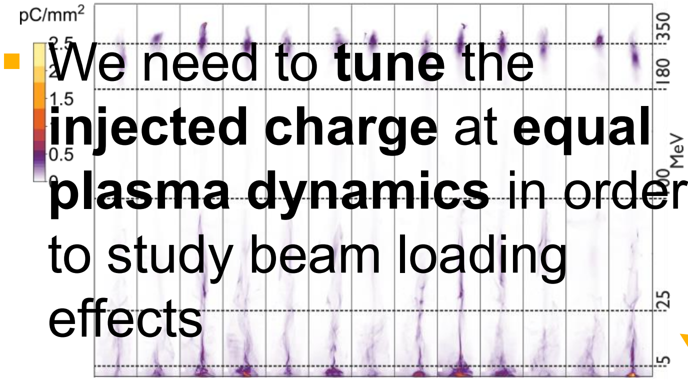

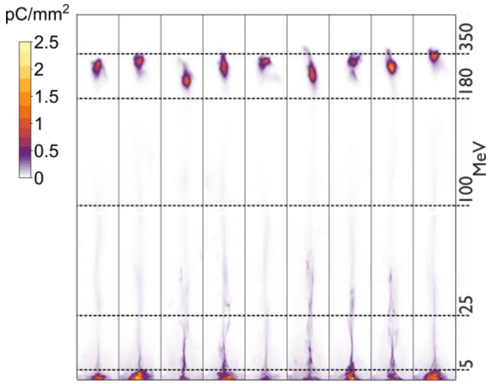

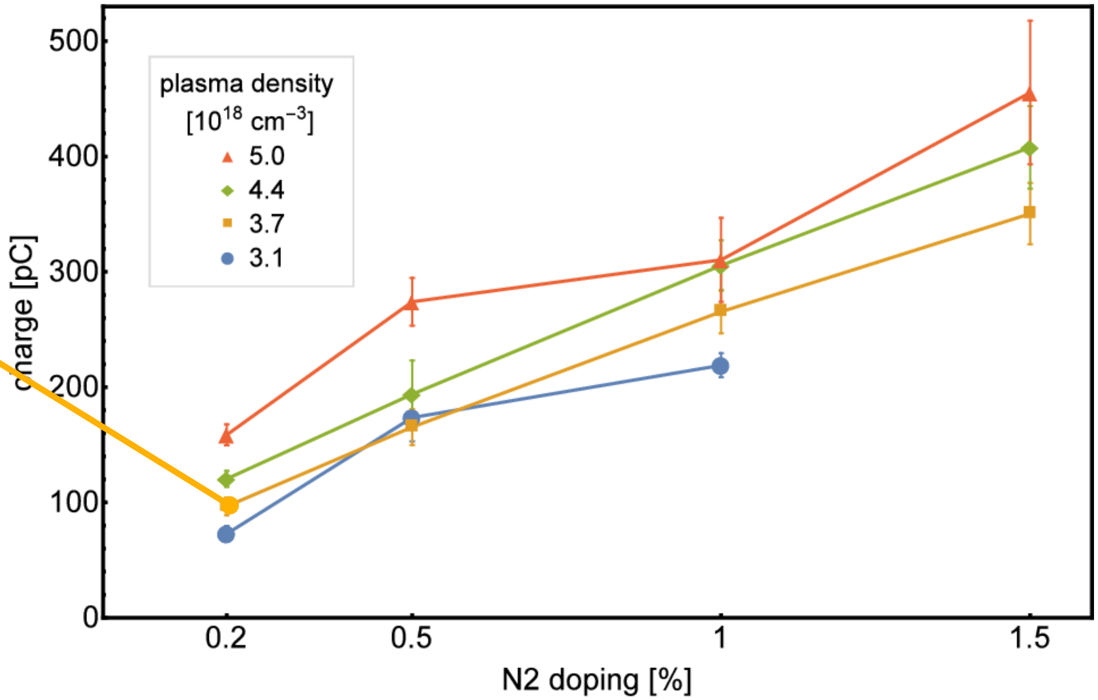

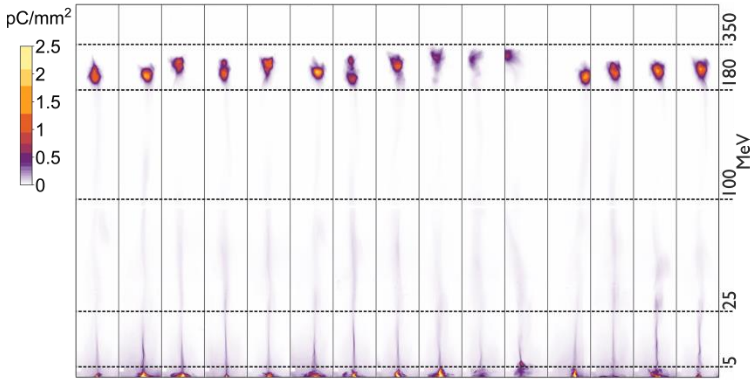

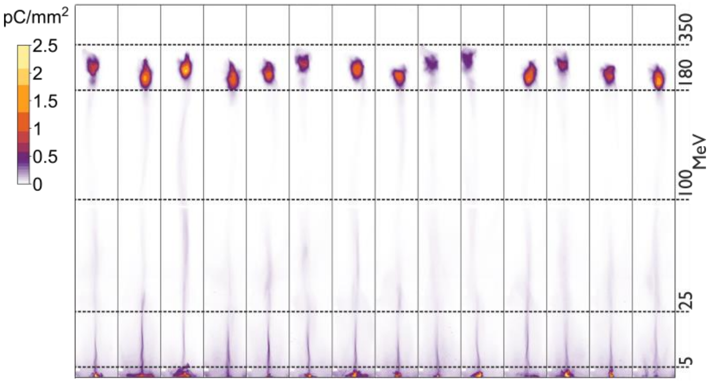

Charge tuning via Nitrogen doping

- We need to **tune** the **injected charge** at **equal plasma dynamics** in order to study beam loading effects

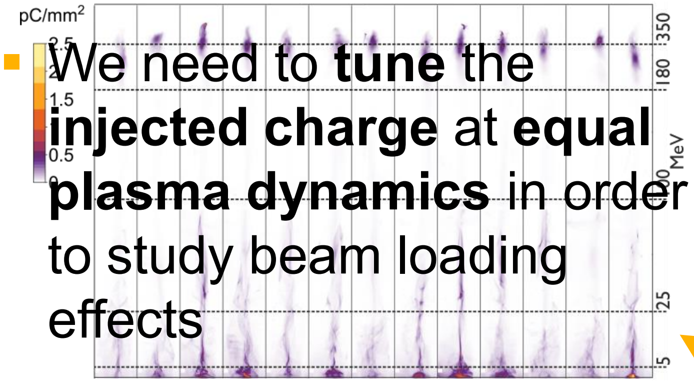

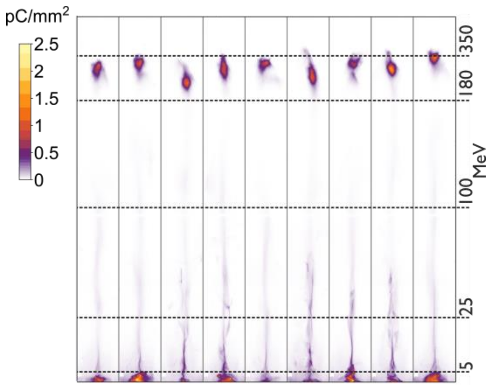

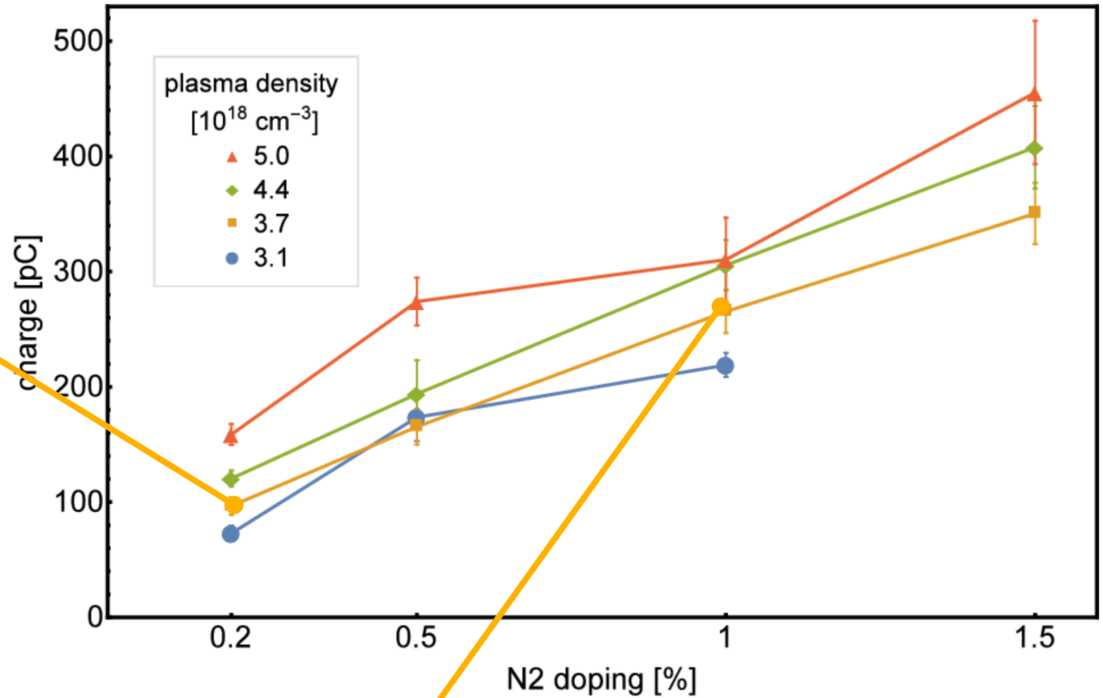

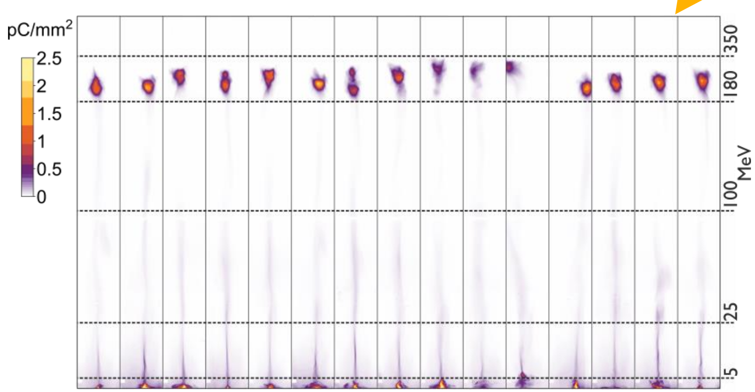

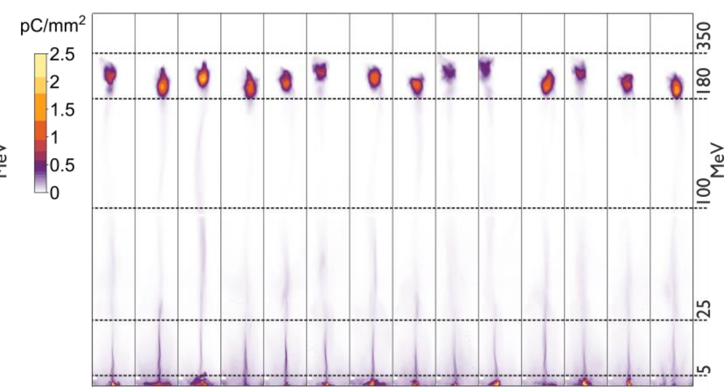

Charge tuning via Nitrogen doping

- We need to **tune** the **injected charge** at **equal plasma dynamics** in order to study beam loading effects

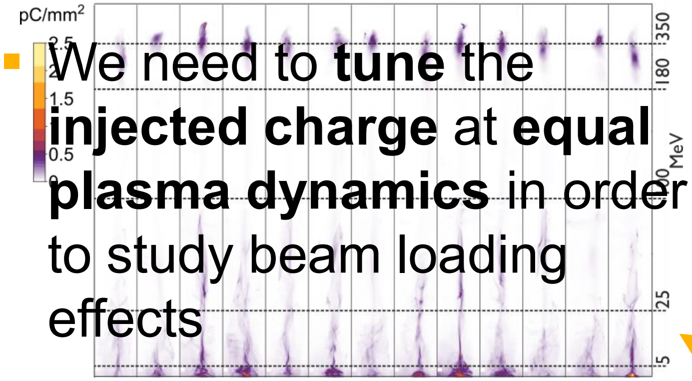

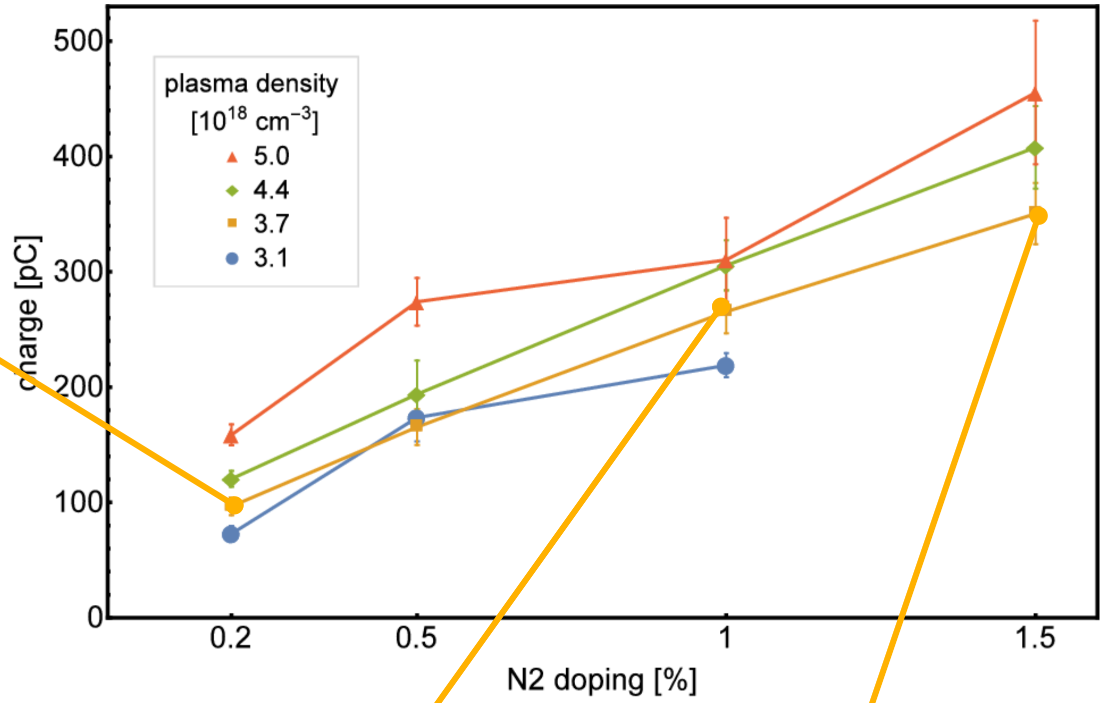

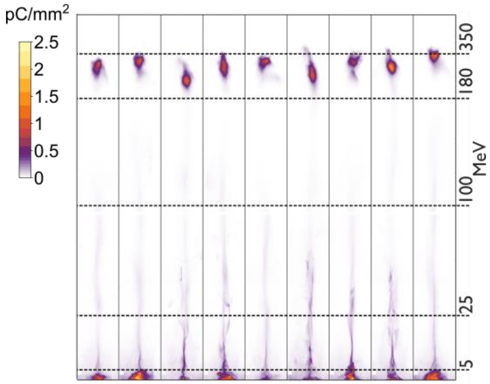

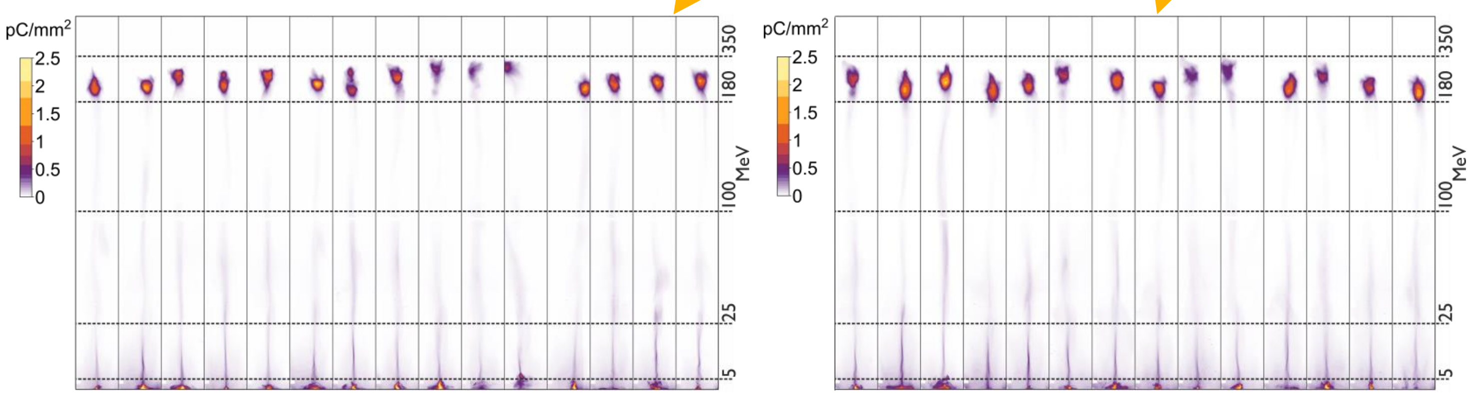

Charge tuning via Nitrogen doping

- We need to **tune** the **injected charge** at **equal plasma dynamics** in order to study beam loading effects

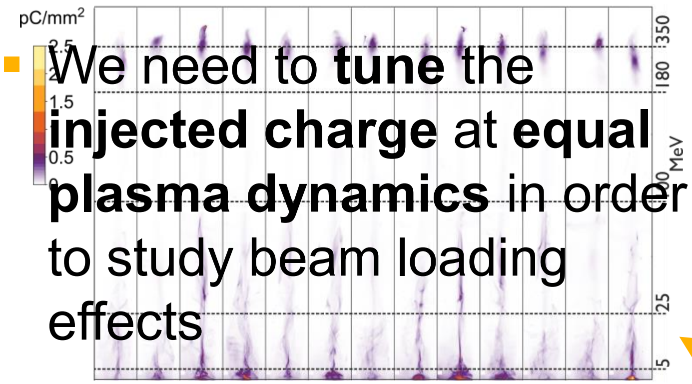

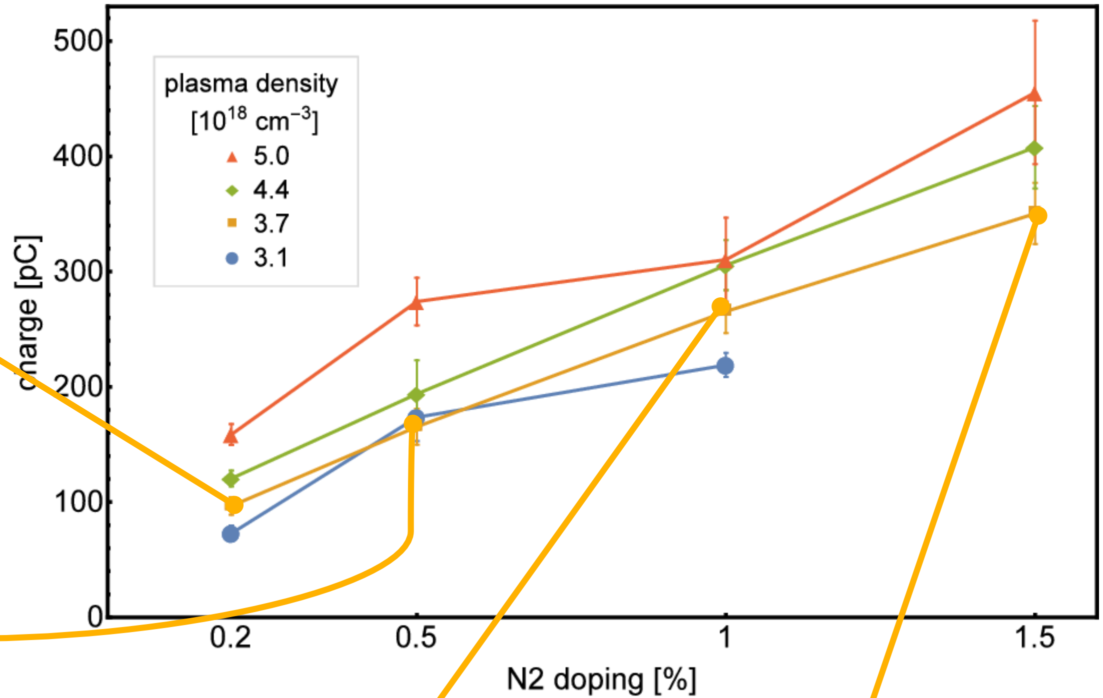

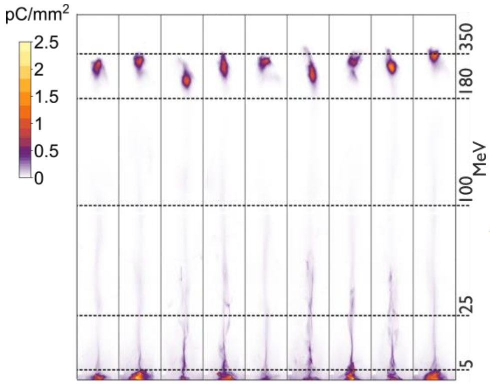

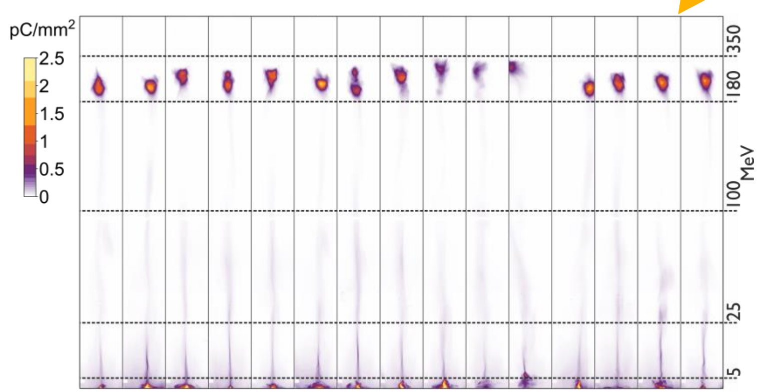

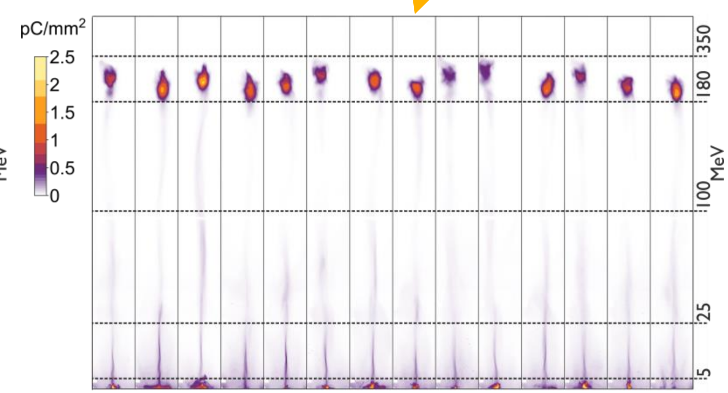

Beam loading improved beam quality

- With increasing charge energy and **energy spread decrease**

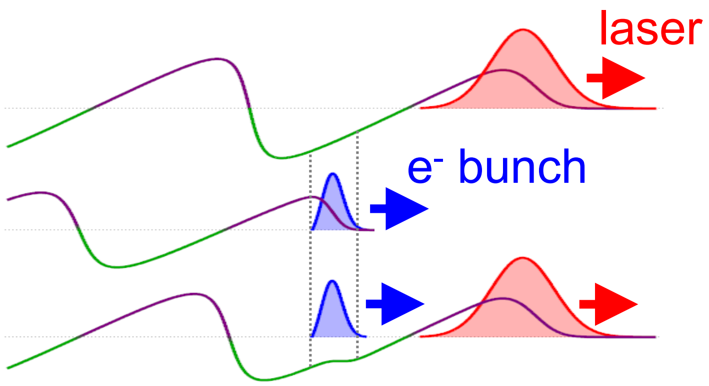

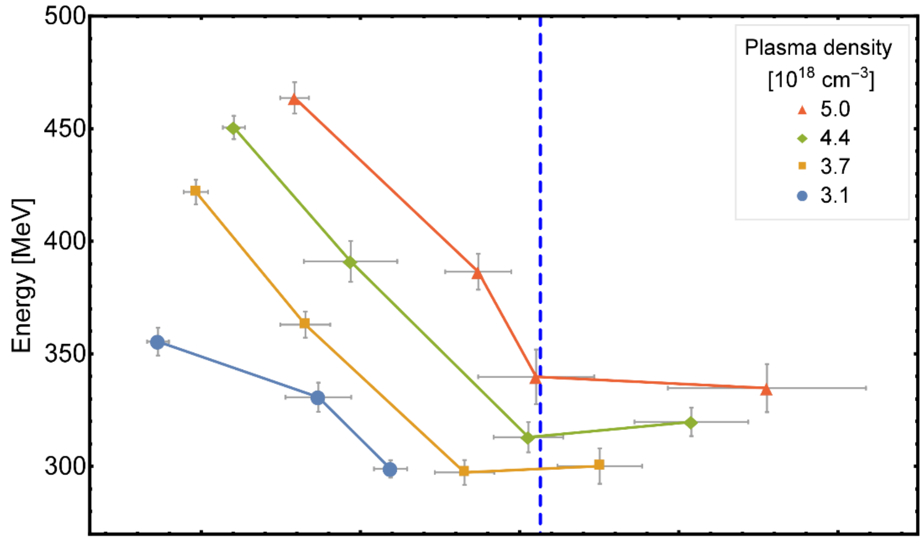

- Optimal charge ~300 pC, matching analytical model by Tzoufras et al. PRL 2008.
- Beam loading locally flattens potential distribution

J. Couperus, et al., Nat. Commun. 8, 487 (2017)
A. Irman, et al., PPCF online first (2018)

Beam loading improved beam quality

- With increasing charge energy and **energy spread decrease**

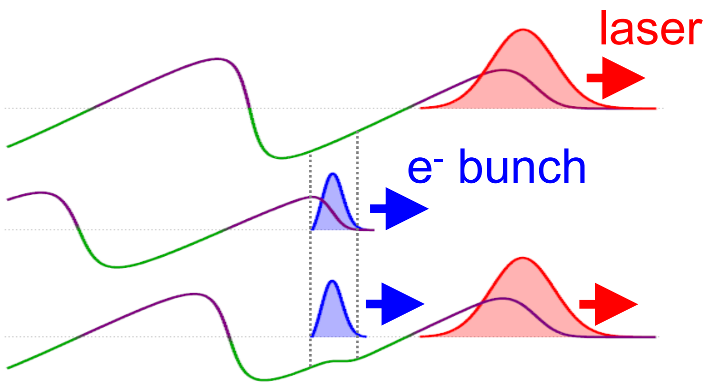

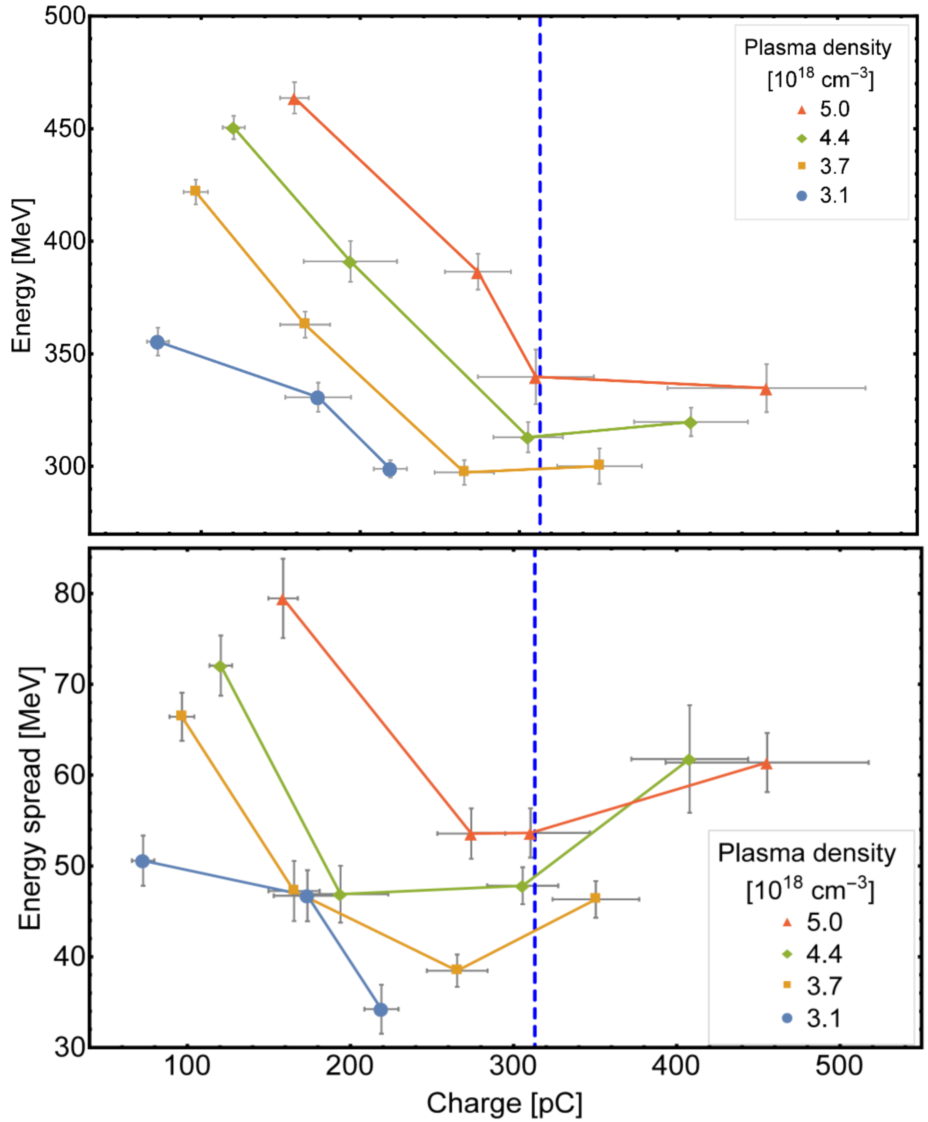

- Optimal charge ~300 pC, matching analytical model by Tzoufras et al. PRL 2008.
- Beam loading locally flattens potential distribution

J. Couperus, et al., Nat. Commun. 8, 487 (2017)
A. Irman, et al., PPCF online first (2018)

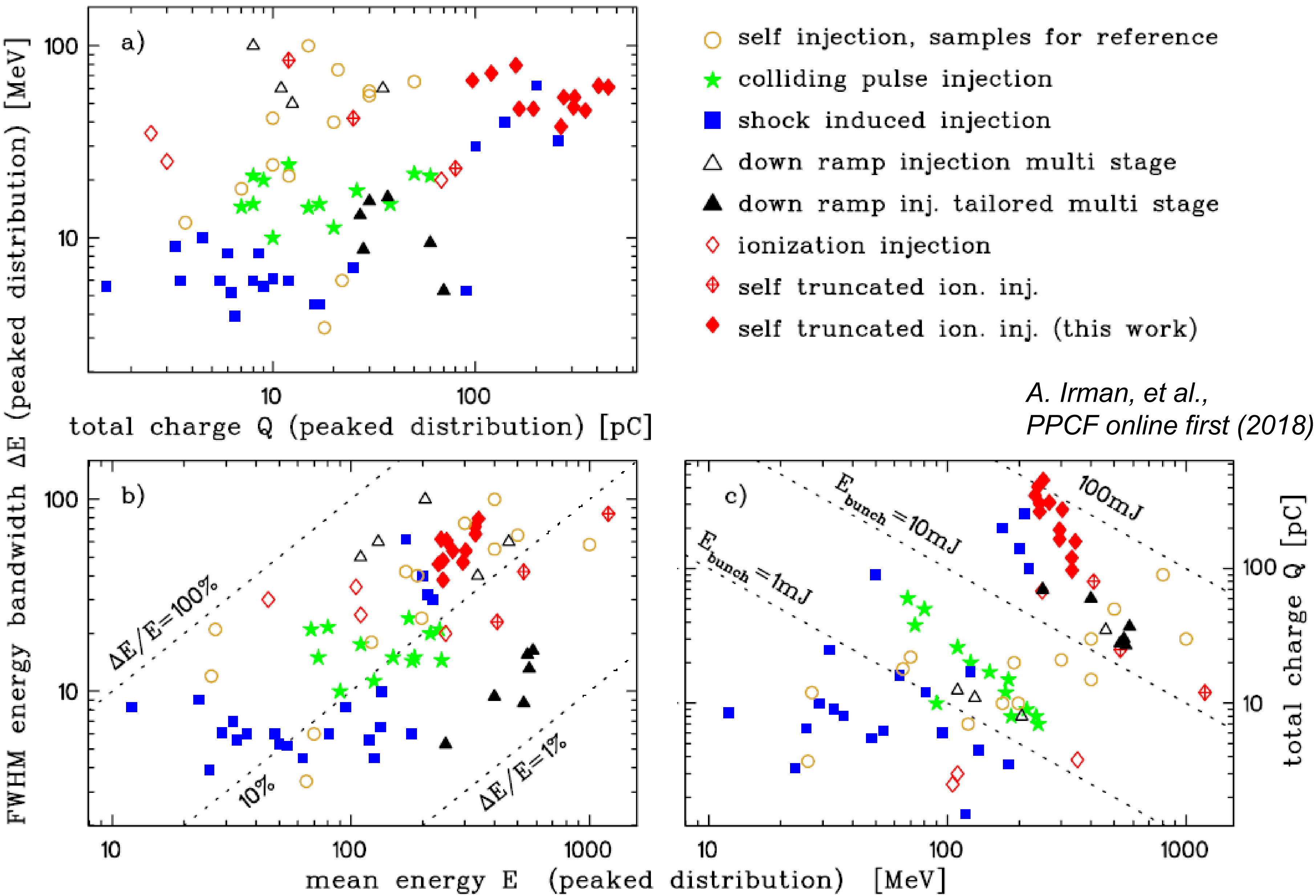

A. Irman, et al., PPCF online first (2018)

Measure coherent optical transition radiation -> reconstruct pulse duration

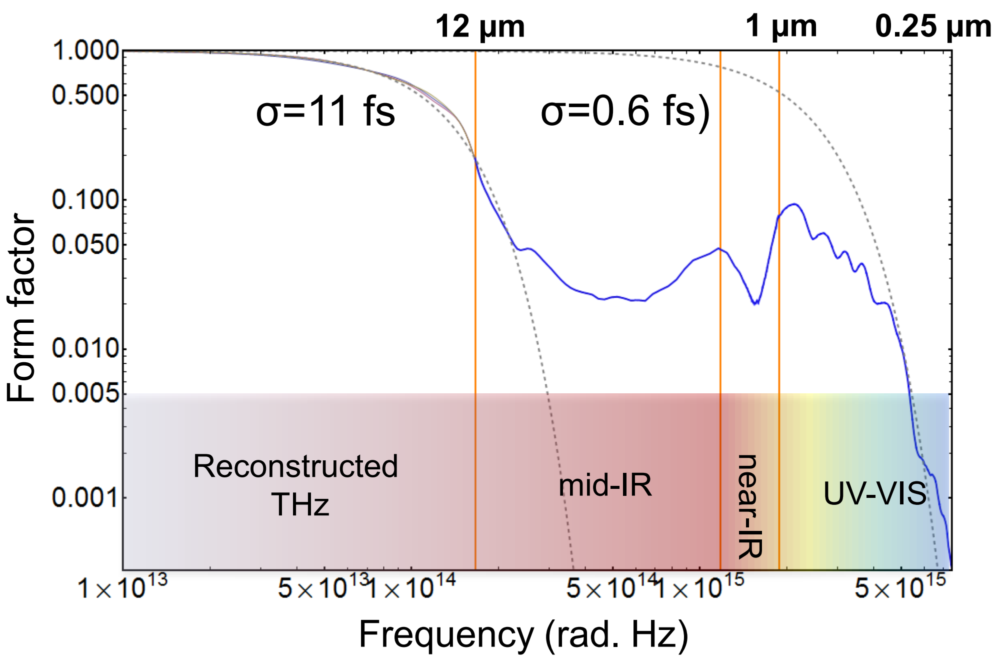

- single-shot capability
- 6 octaves frequency range
- detection limit ~ 50 fC
- time resolution ~ 0.5 fs

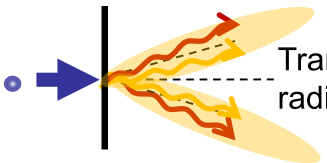

Highest peak-current in laser wakefield acceleration

HZDR

Measure coherent optical transition radiation -> reconstruct pulse duration

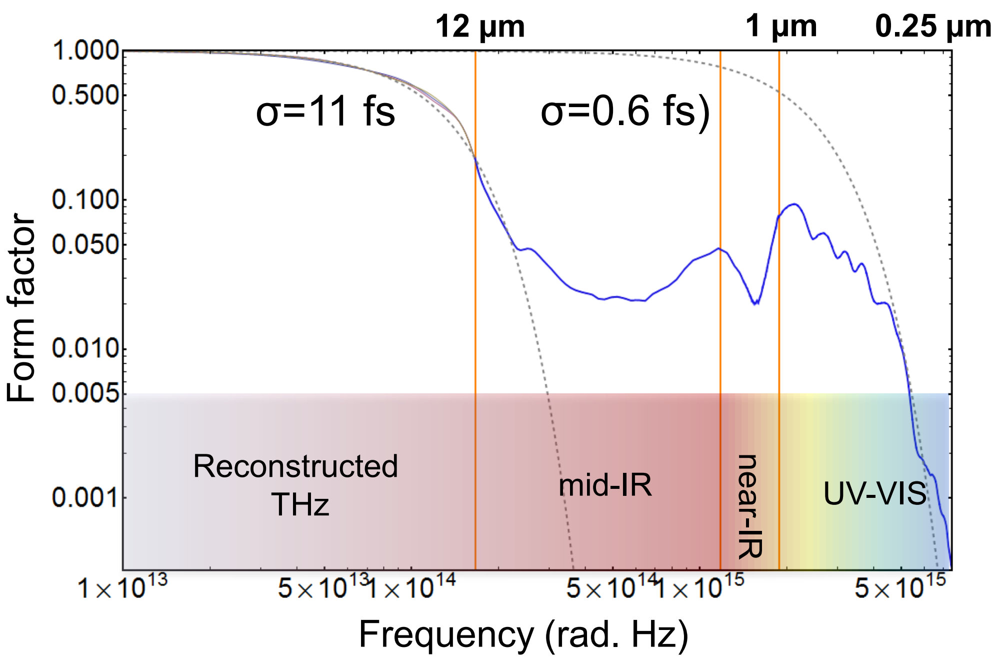

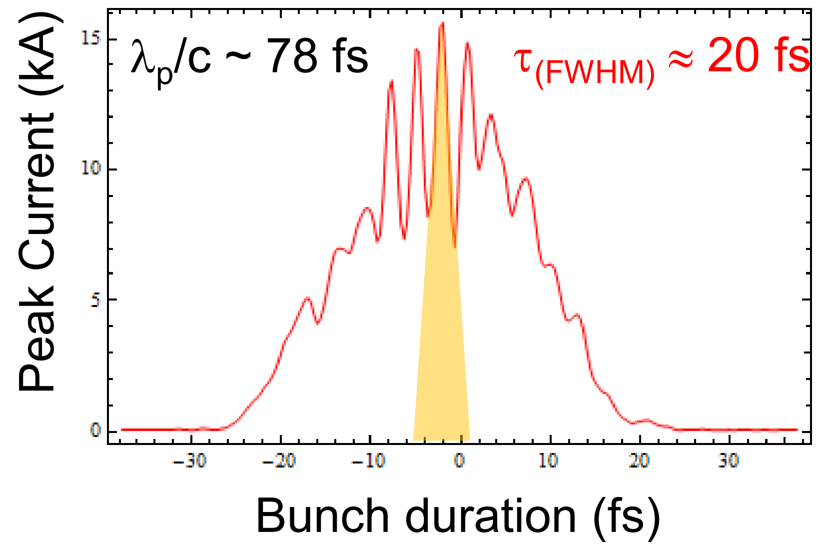

- single-shot capability
- 6 octaves frequency range
- detection limit ~ 50 fC
- time resolution ~ 0.5 fs

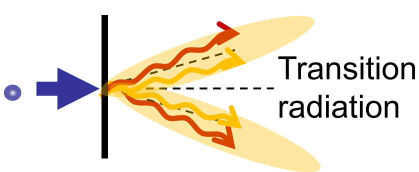

Highest peak-current in laser wakefield acceleration

Measure coherent optical transition radiation -> reconstruct pulse duration

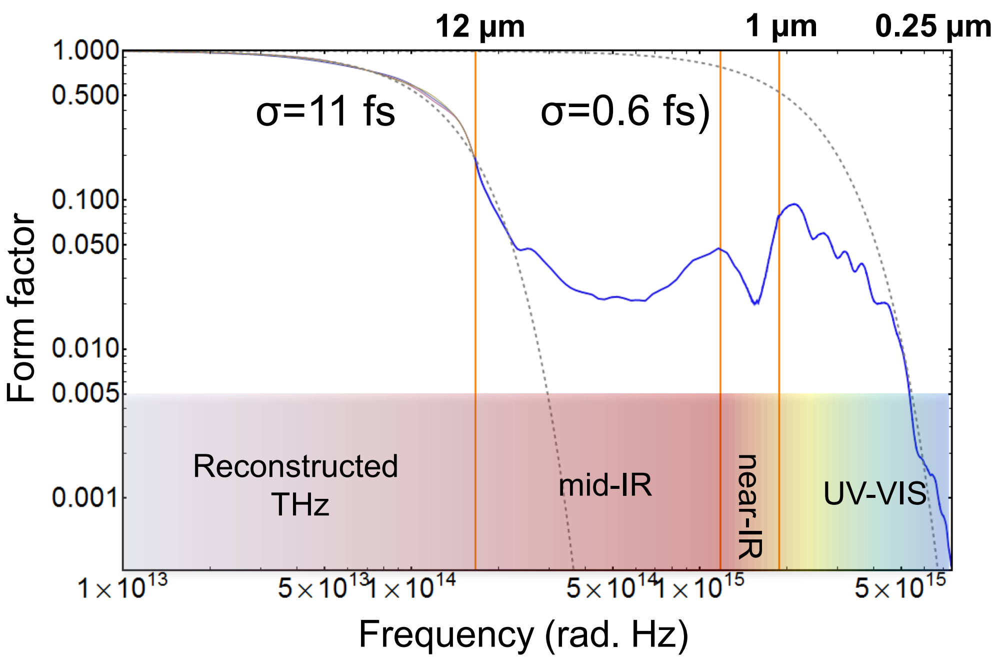

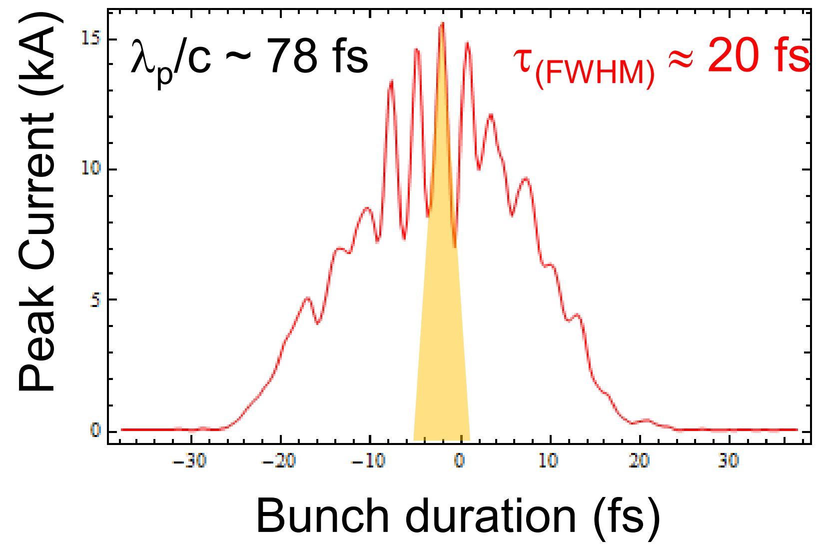

730 nm

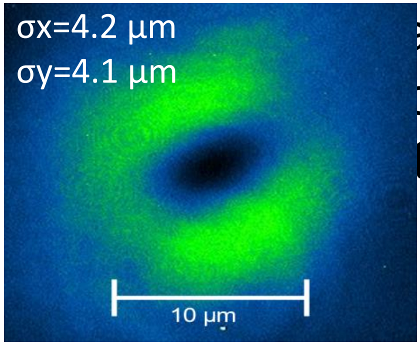

600 nm

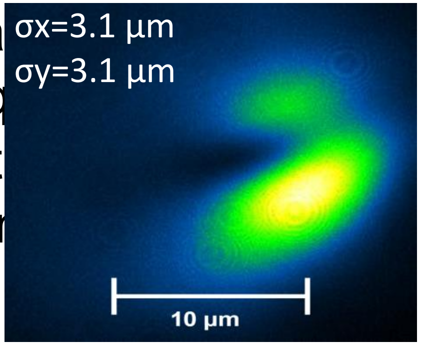

400 nm

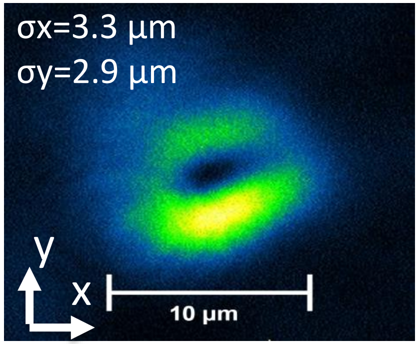

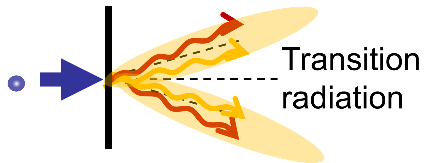

Hybrid plasma accelerator scheme (very preliminary)

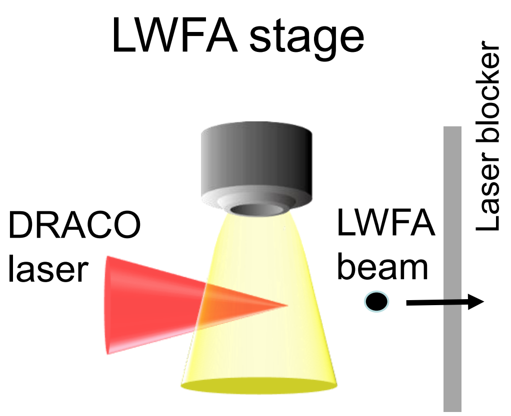

Hybrid plasma accelerator scheme (very preliminary)

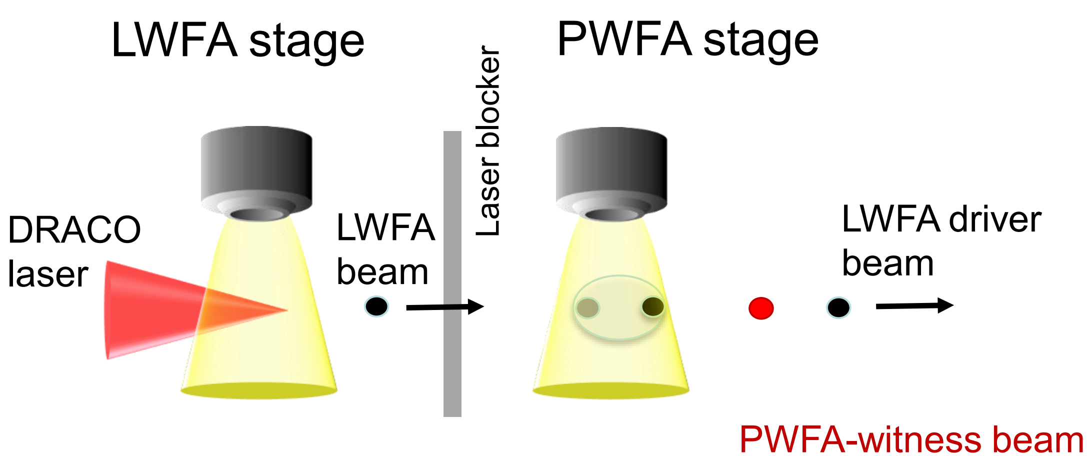

Hybrid plasma accelerator scheme (very preliminary)

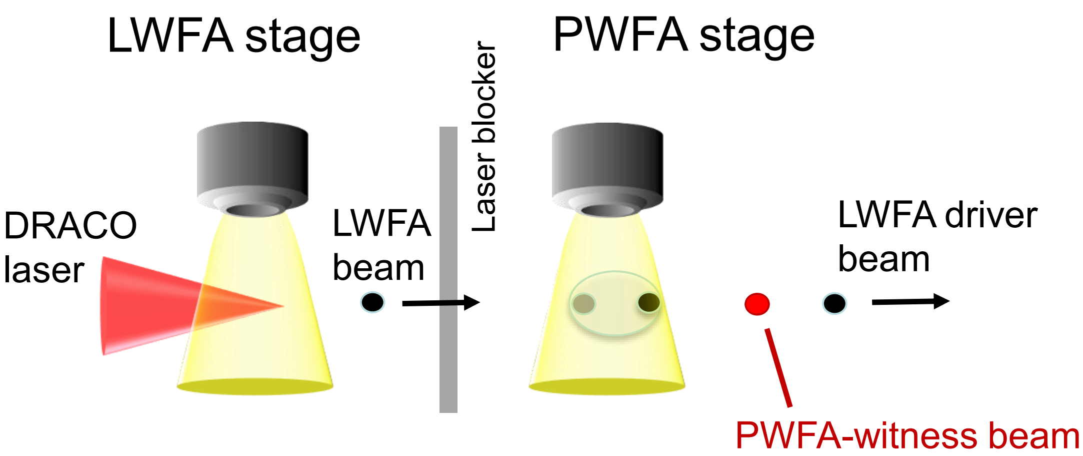

Hybrid plasma accelerator scheme (very preliminary)

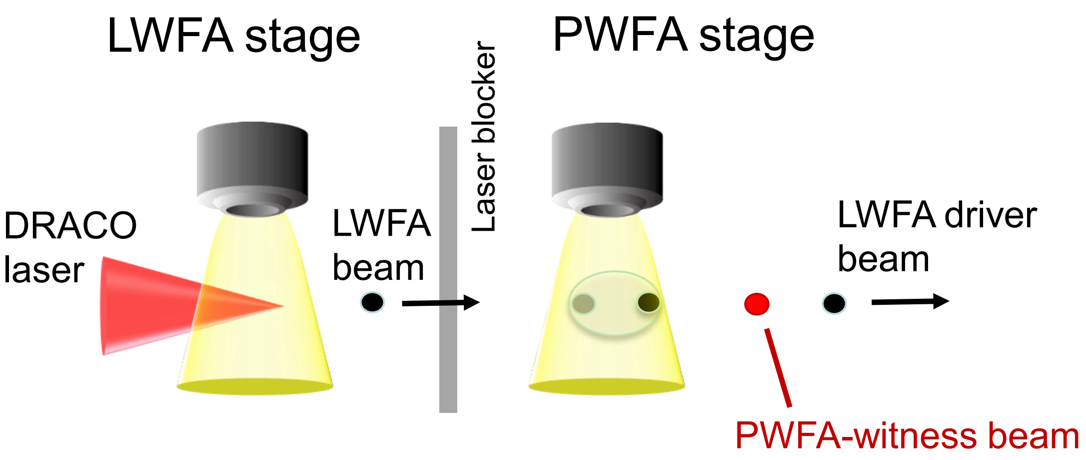

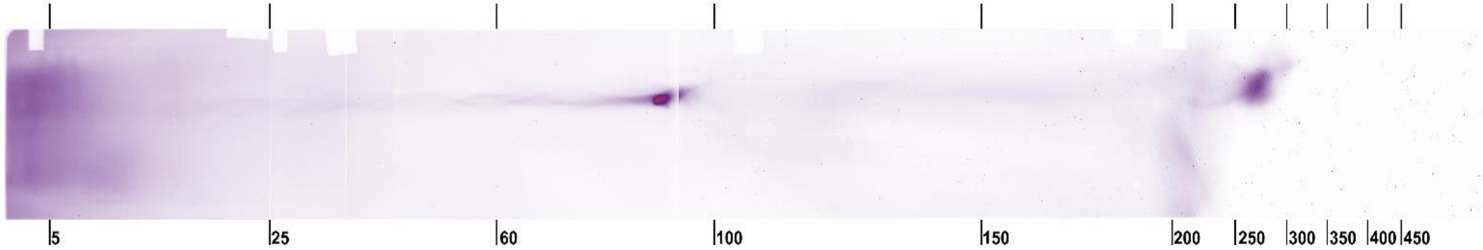

Hybrid plasma accelerator scheme (very preliminary)

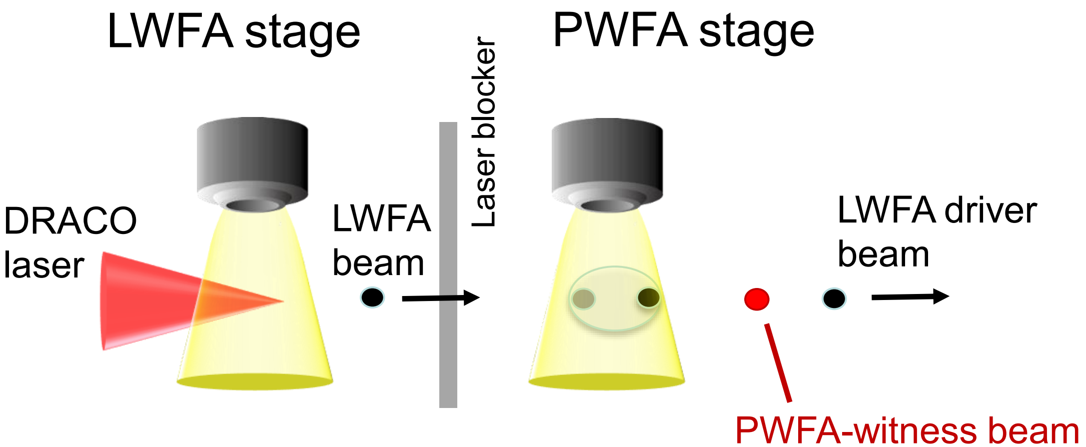

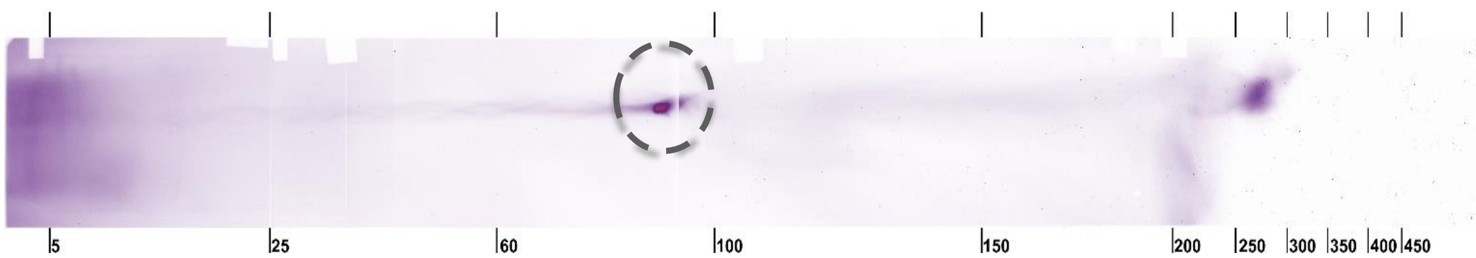

Hybrid plasma accelerator scheme (very preliminary)

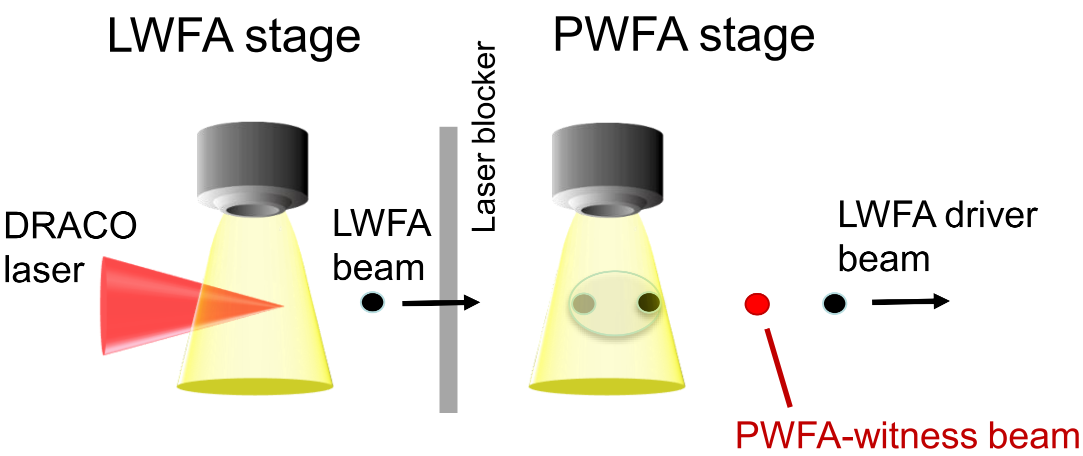

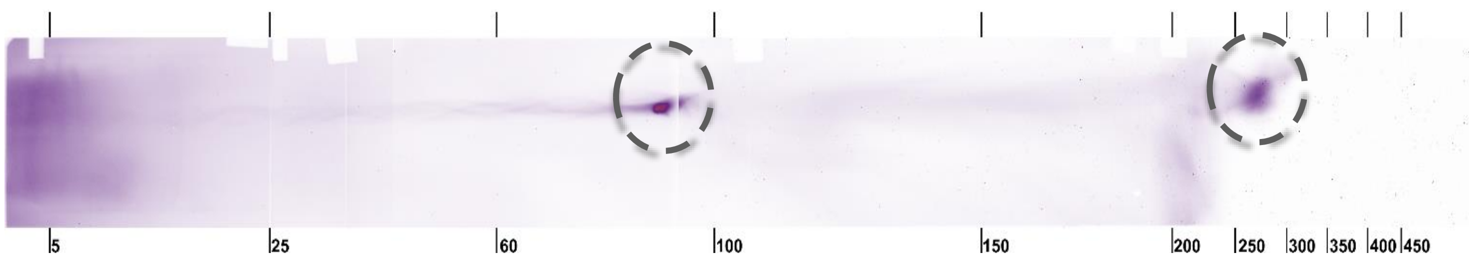

Hybrid plasma accelerator scheme (very preliminary)

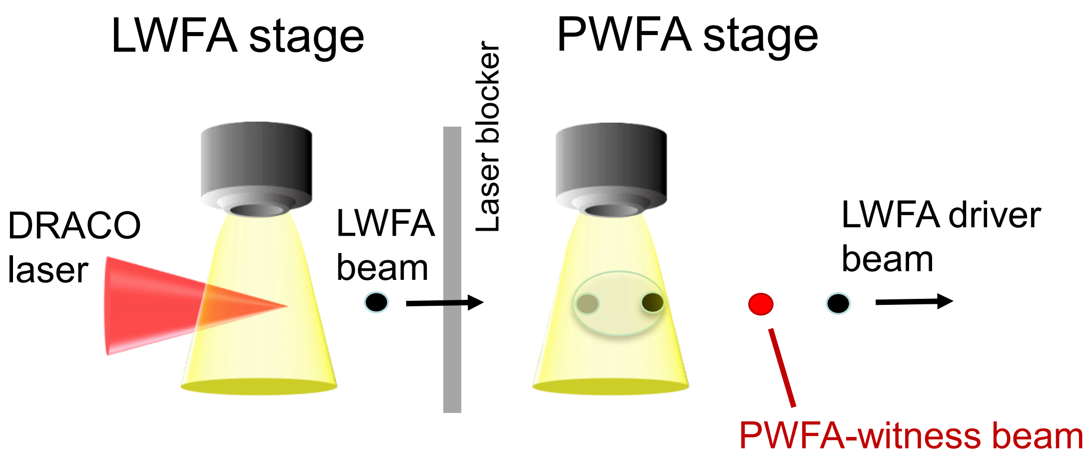

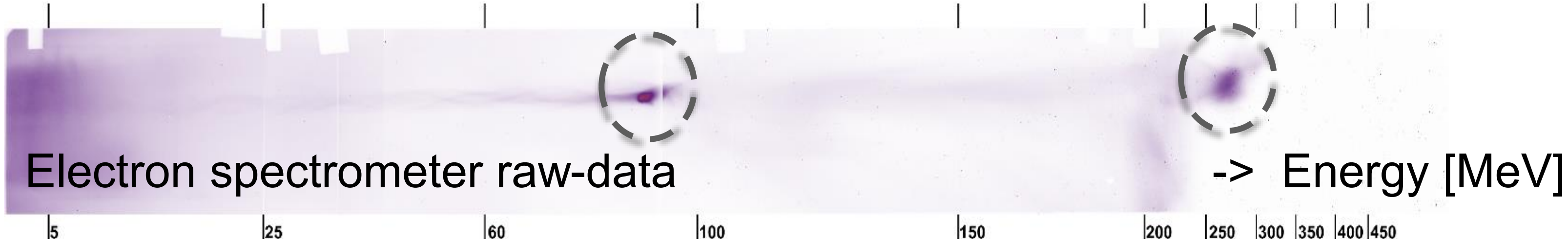

Hybrid plasma accelerator scheme (very preliminary)

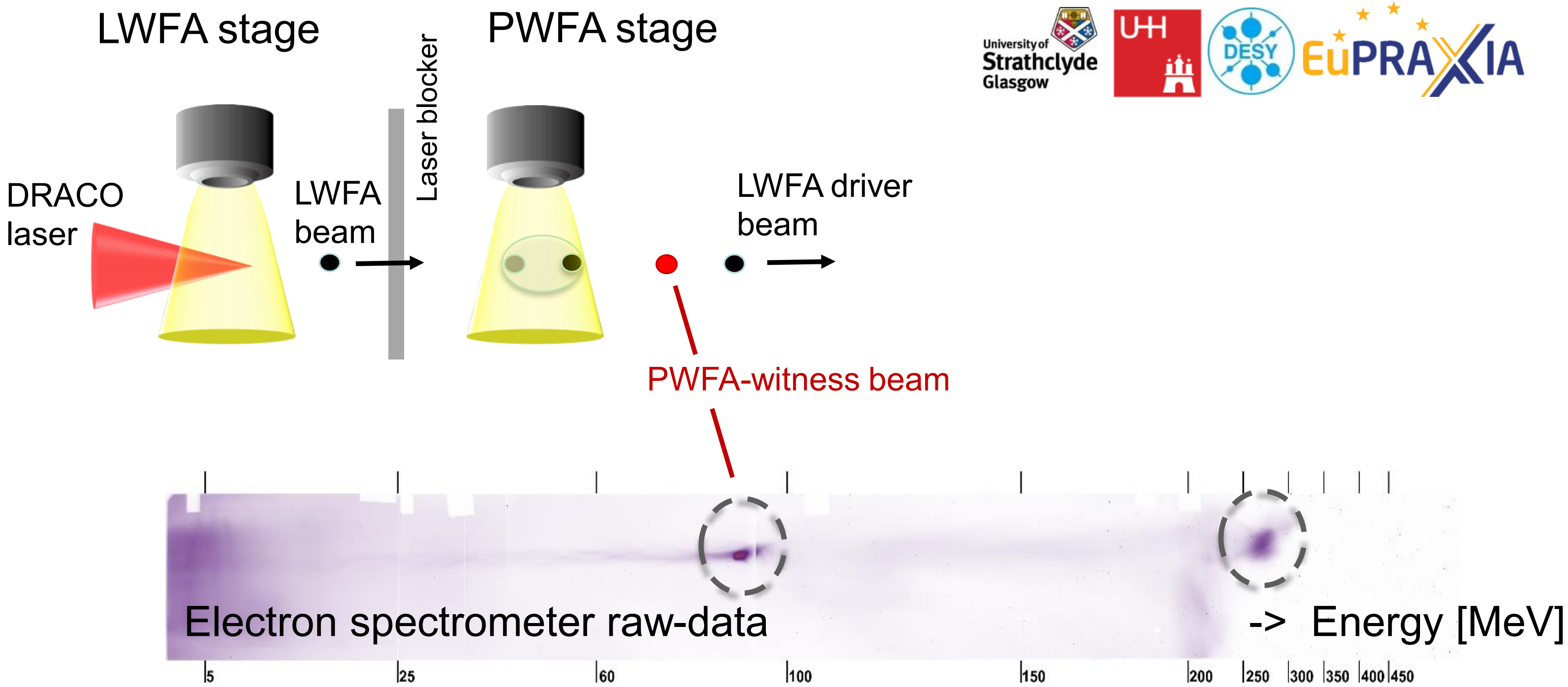

Hybrid plasma accelerator scheme (very preliminary)

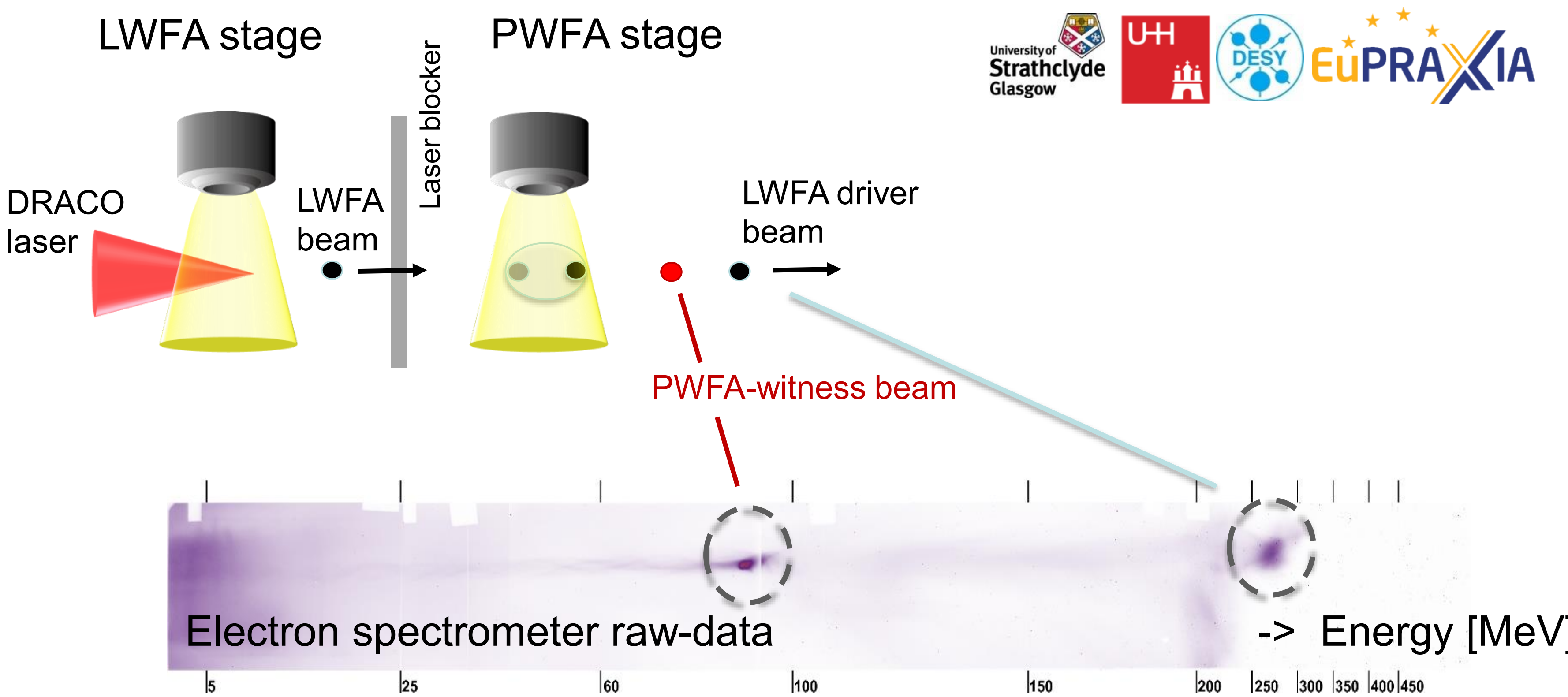

Broad-band „betatron“ radiation source

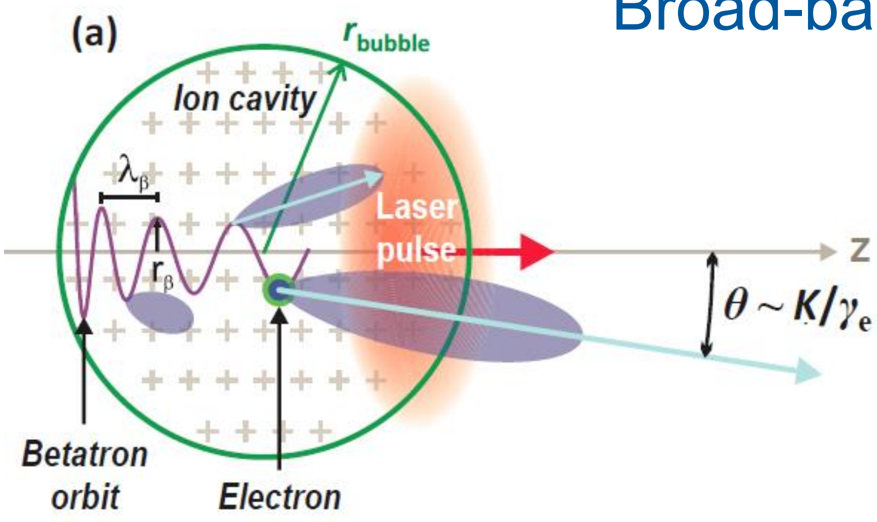

- Intrinsic efficient source
- Energy and oscillation amplitude vary with z
- Micron source size
- Diagnostics for „radius“

Broad-band „betatron“ radiation source

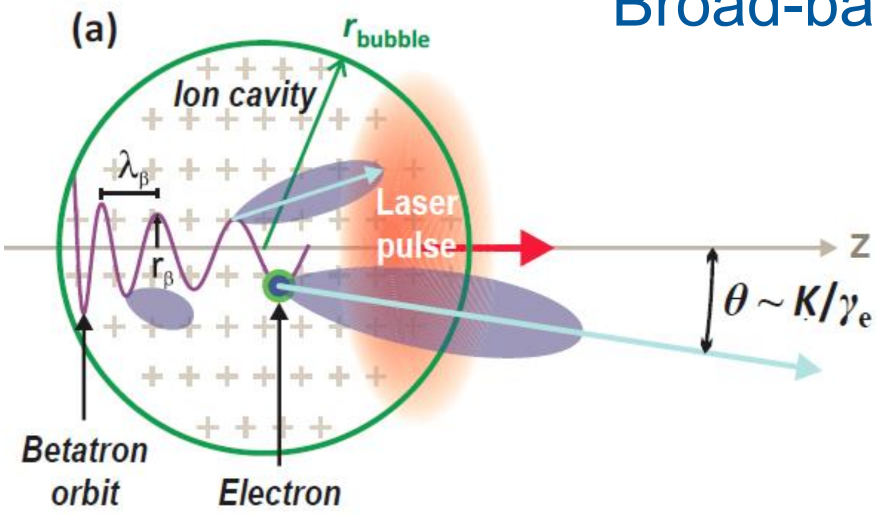

- Intrinsic efficient source
- Energy and oscillation amplitude vary with z
- Micron source size
- Diagnostics for „radius“

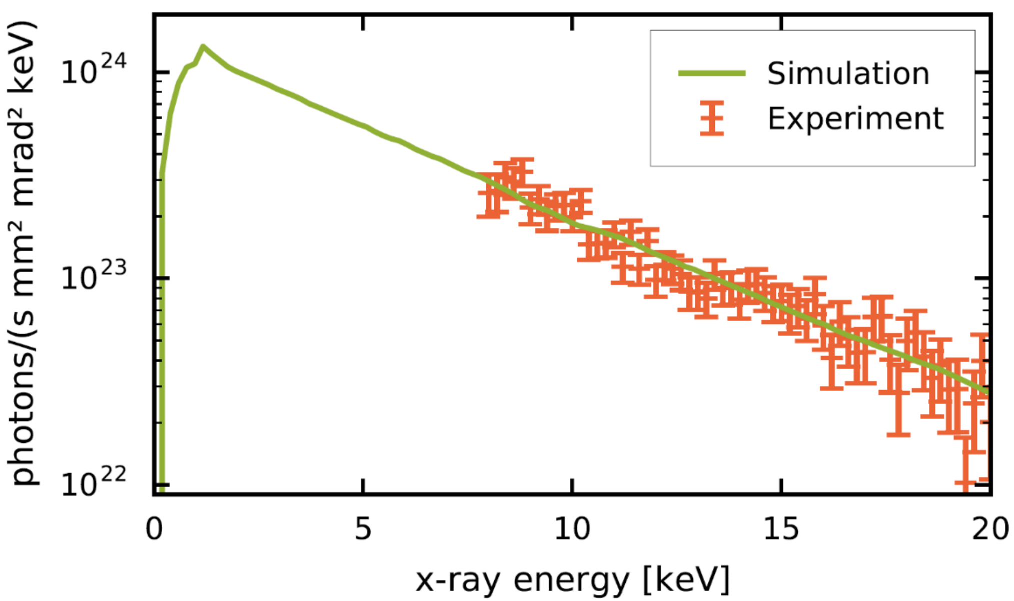

Applications of laser wakefield acceleration

Broad-band „betatron“ radiation source

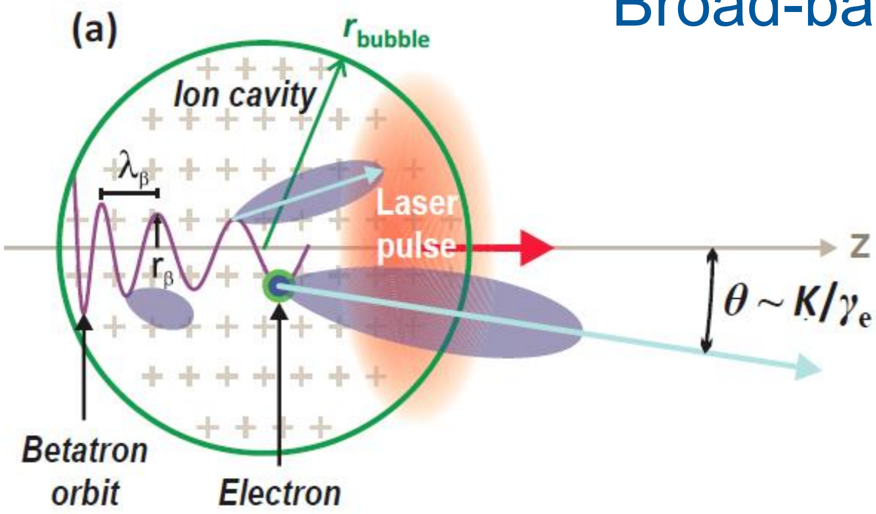

- Intrinsic efficient source
- Energy and oscillation amplitude vary with z
- Micron source size
- Diagnostics for „radius“

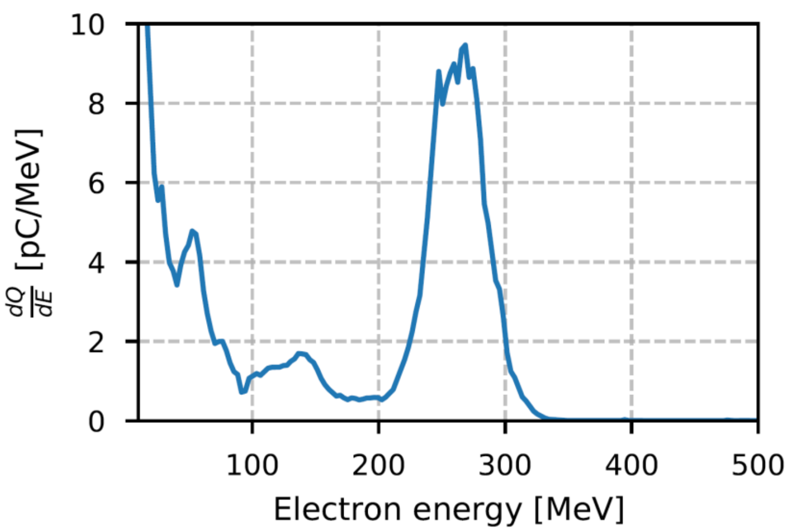

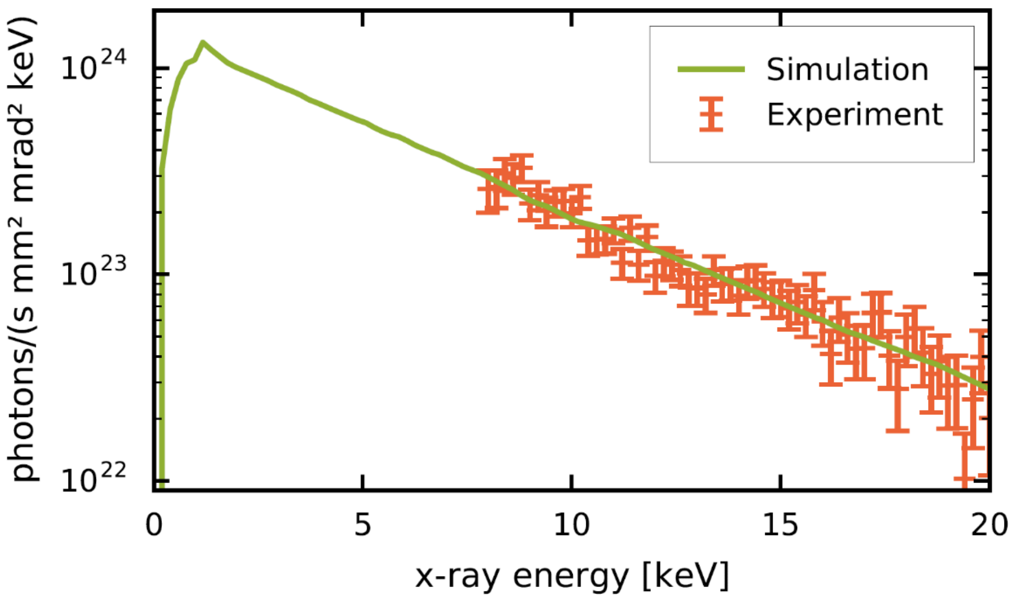

Broad-band „betatron“ radiation source

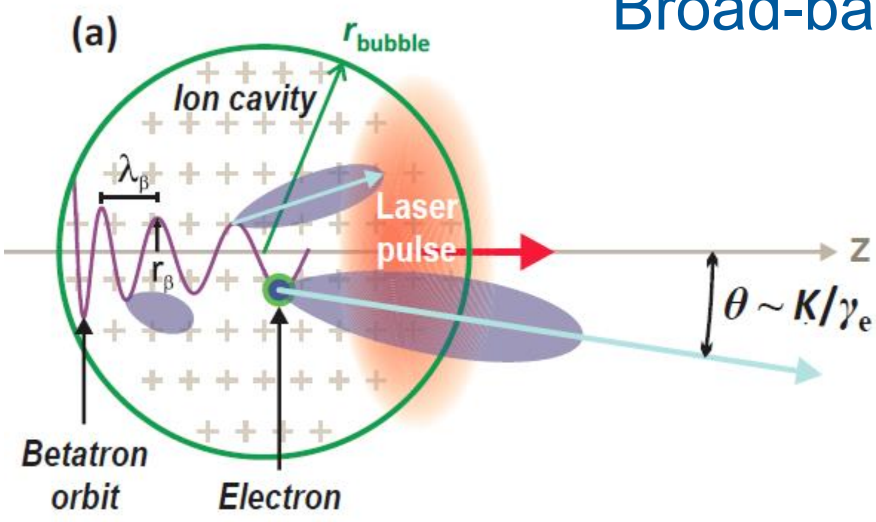

- Intrinsic efficient source
- Energy and oscillation amplitude vary with z
- Micron source size
- Diagnostics for „radius“

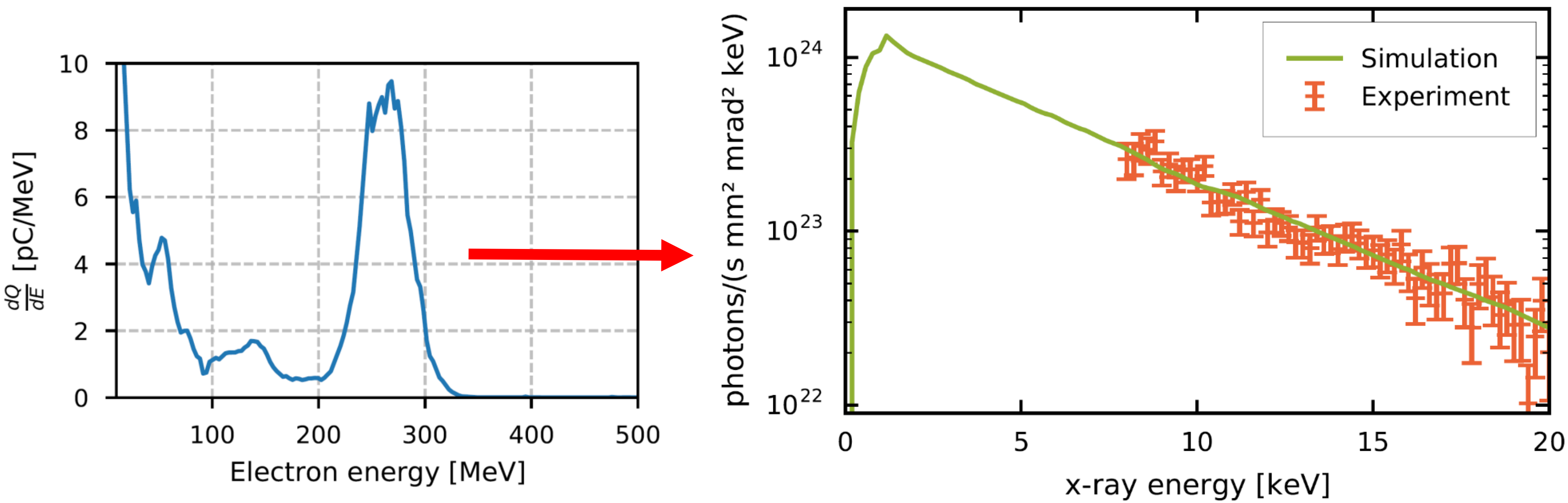

Integrated Thomson (inverse Compton) source

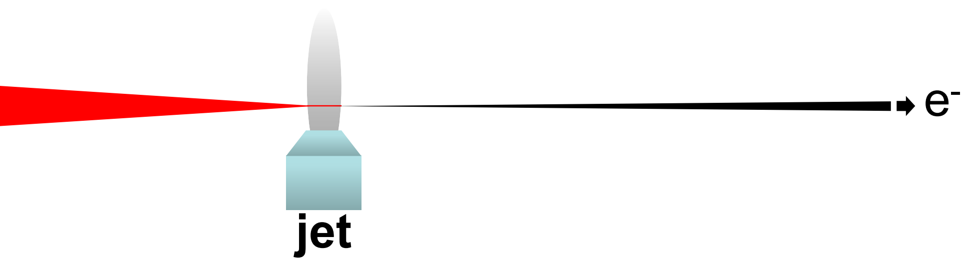

Integrated Thomson (inverse Compton) source

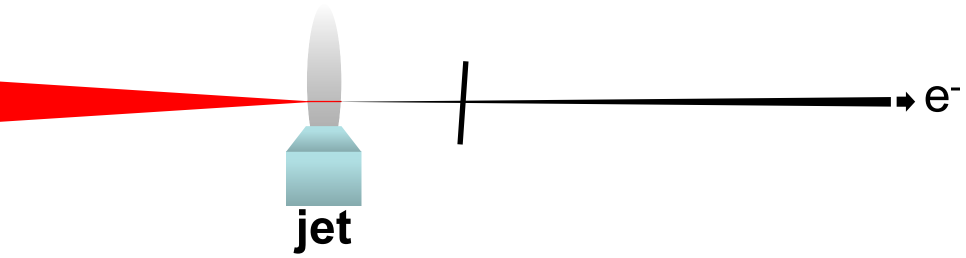

Integrated Thomson (inverse Compton) source

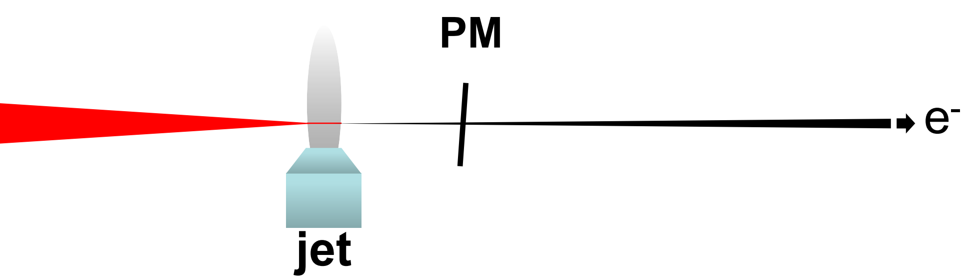

Integrated Thomson (inverse Compton) source

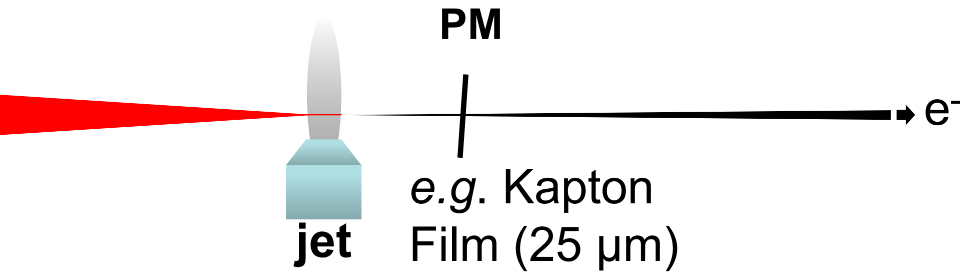

Integrated Thomson (inverse Compton) source

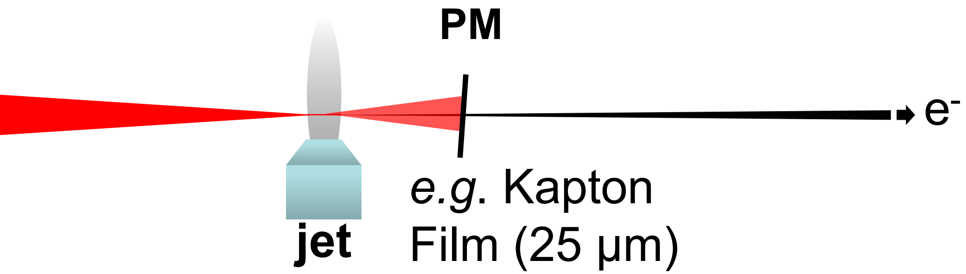

Integrated Thomson (inverse Compton) source

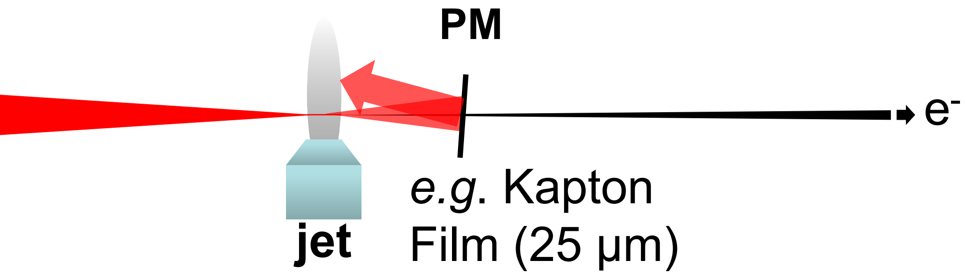

e.g. Kapton
Film (25 µm)

Integrated Thomson (inverse Compton) source

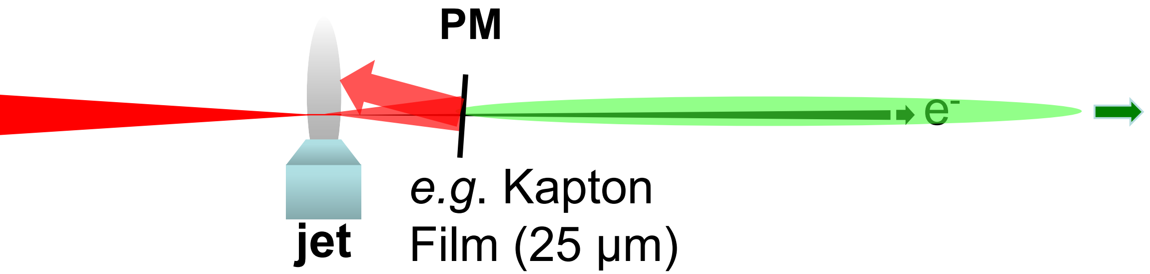

Integrated Thomson (inverse Compton) source

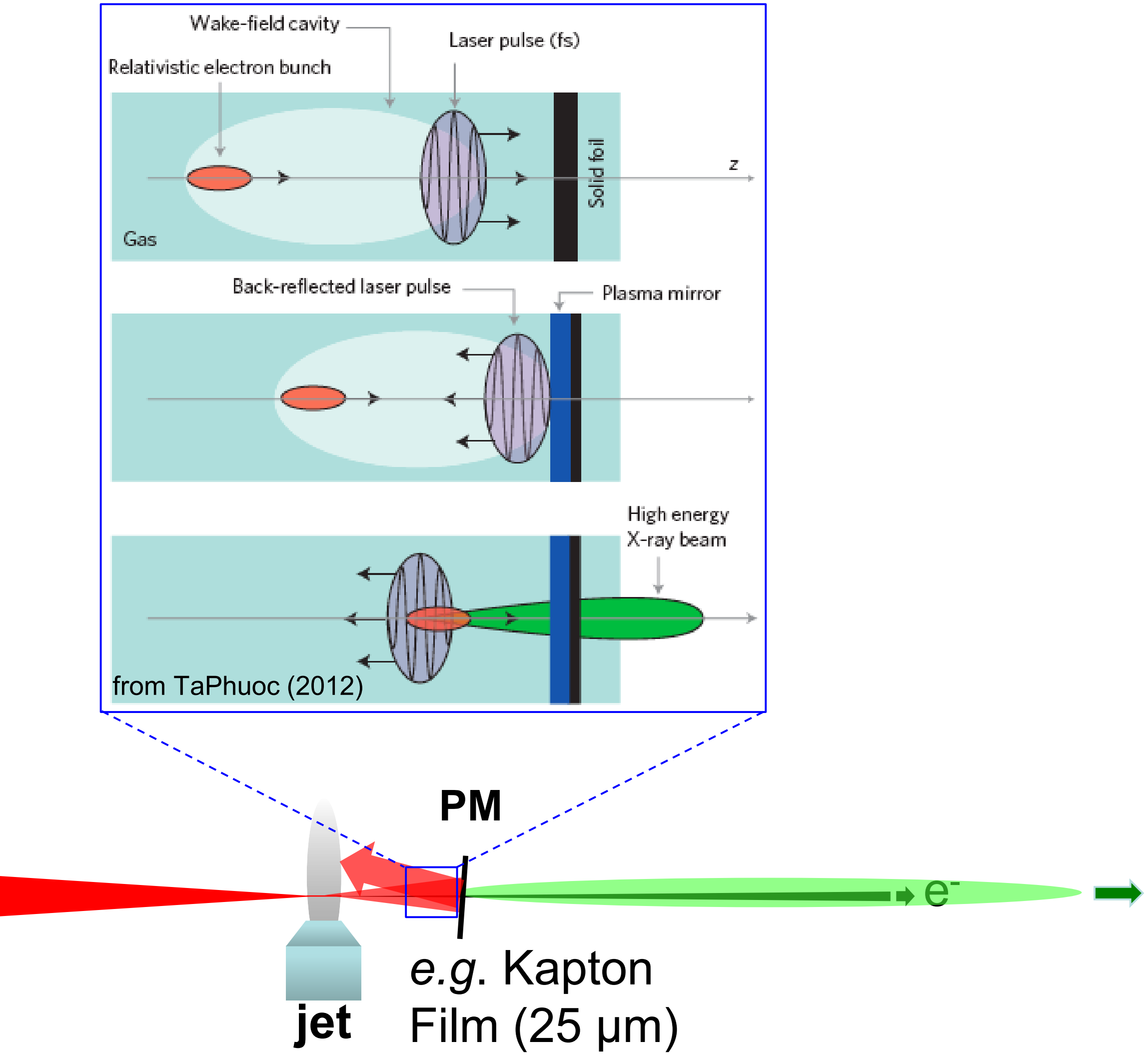

Integrated Thomson (inverse Compton) source

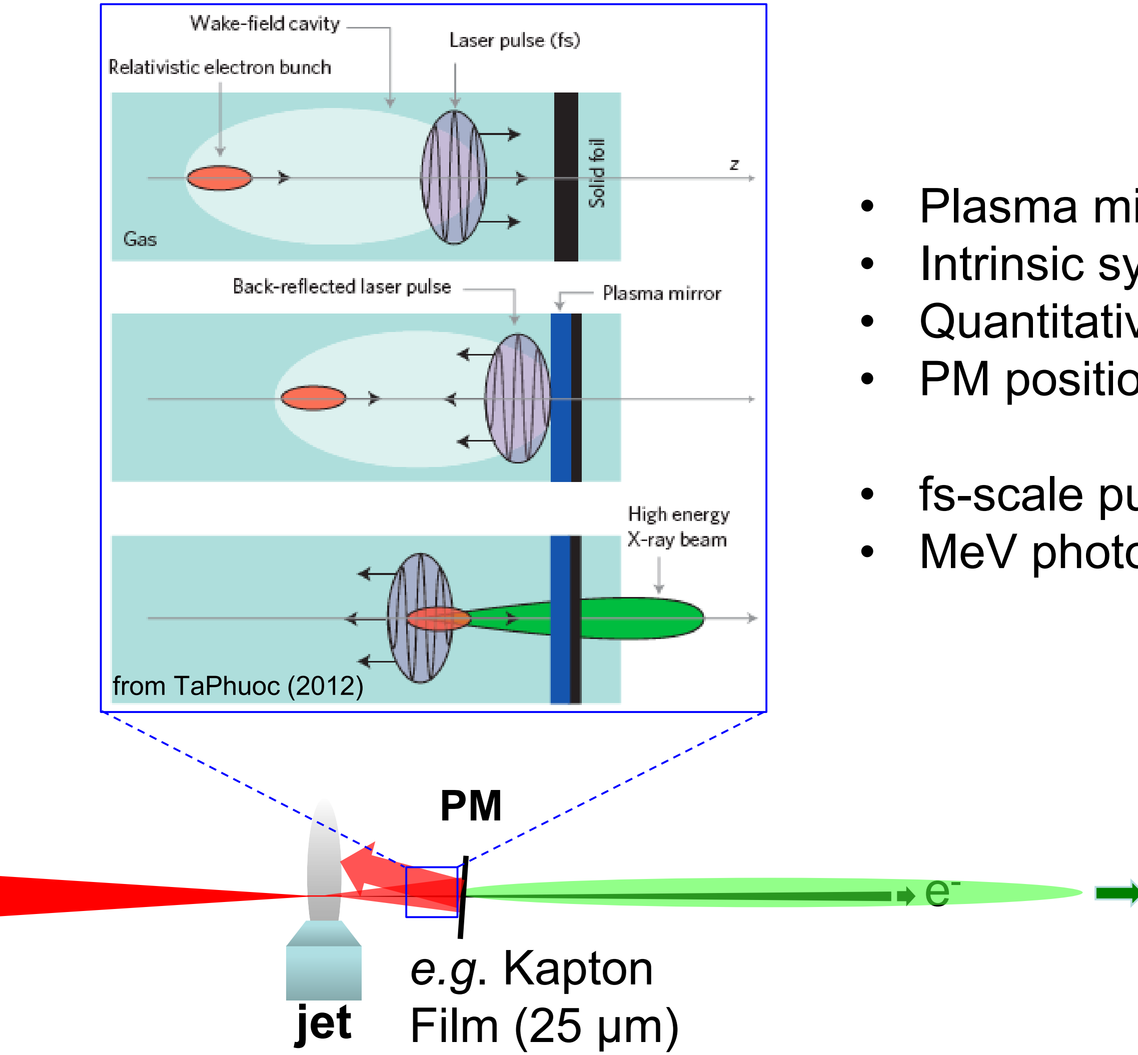

- Plasma mirror for recycling of the drive laser
- Intrinsic synchronization
- Quantitative control still difficult
- PM position controls oscillation strength

- fs-scale pulse duration
- MeV photon energies

Detection via spatially resolving calorimeter stack

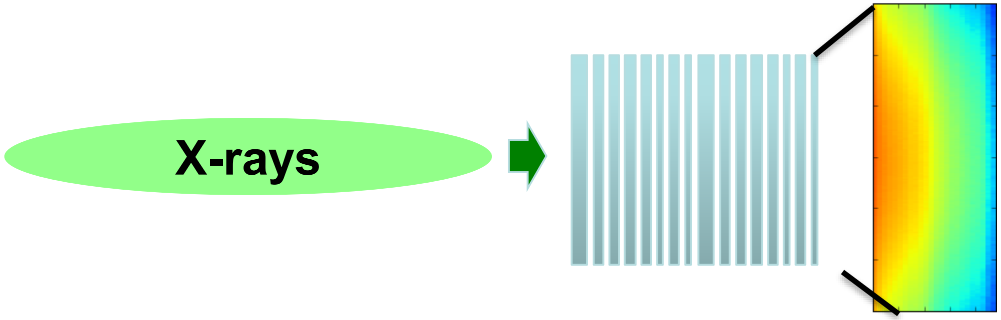

Calorimeter stack layers

- Varying material
- Image plates/scintillators

Detection via spatially resolving calorimeter stack

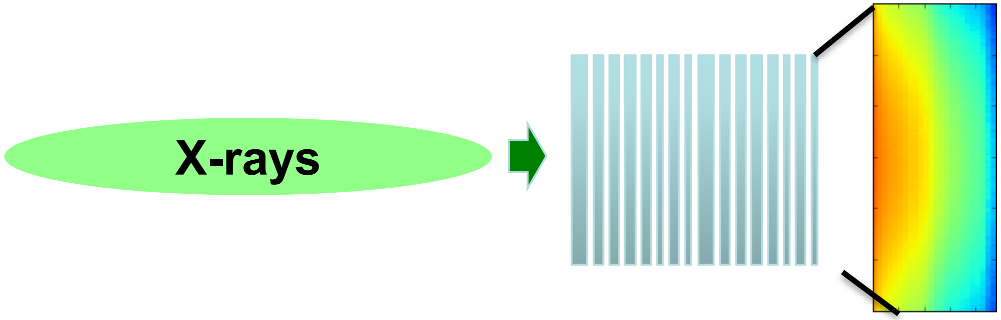

Calorimeter stack layers

- Varying material
- Image plates/scintillators

Increase in divergence and reduction in max. photon energy

Detection via spatially resolving calorimeter stack

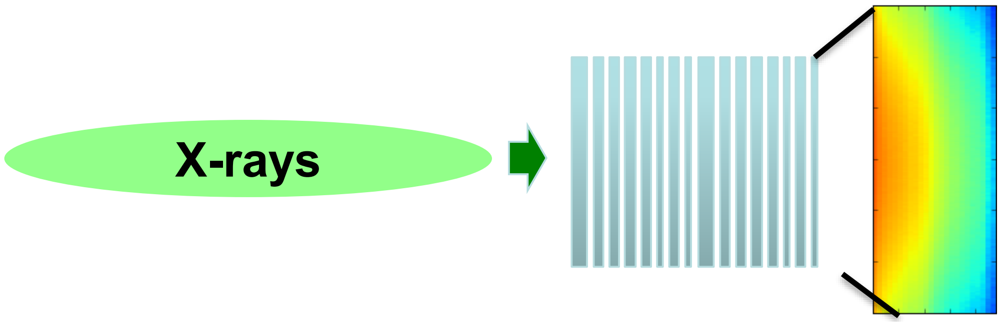

Calorimeter stack layers
- Varying material
- Image plates/scintillators

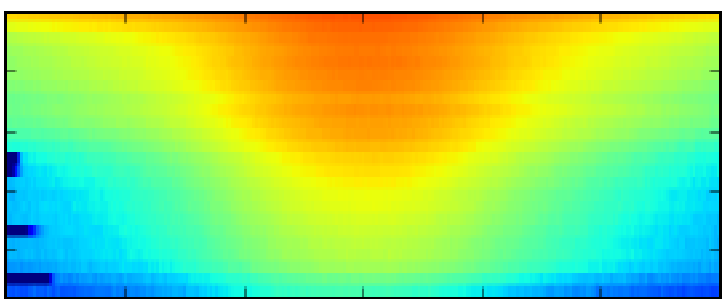

Increase in divergence and reduction in max. photon energy

Detection via spatially resolving calorimeter stack

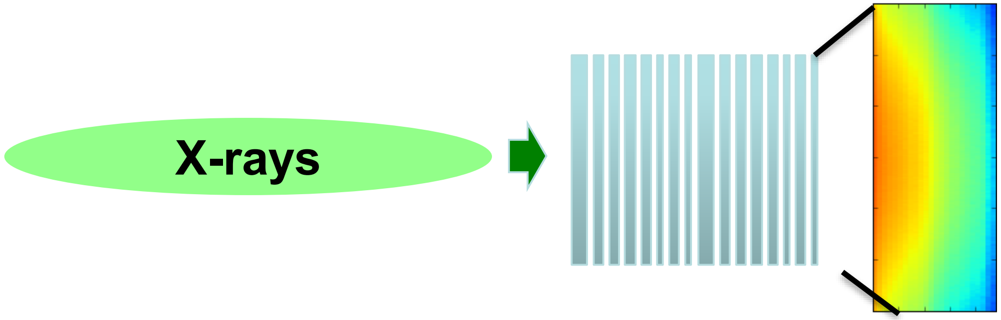

Calorimeter stack layers
- Varying material
- Image plates/scintillators

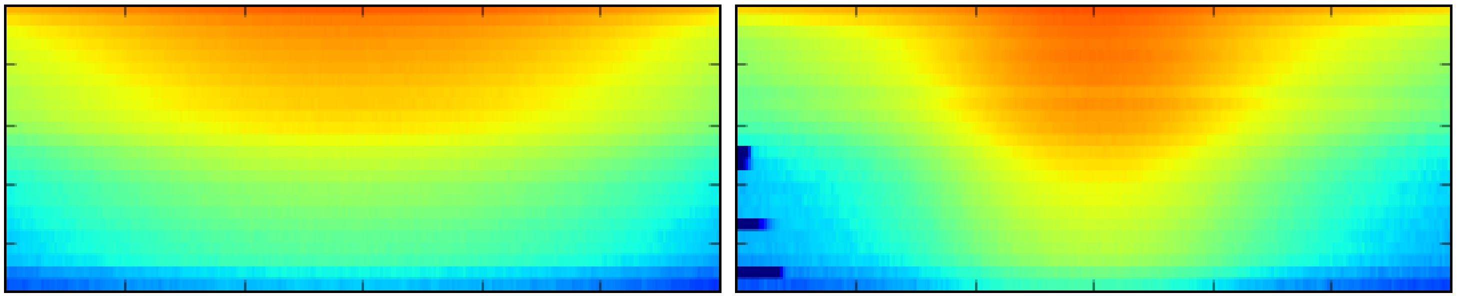

Increase in divergence and reduction in max. photon energy

Detection via spatially resolving calorimeter stack

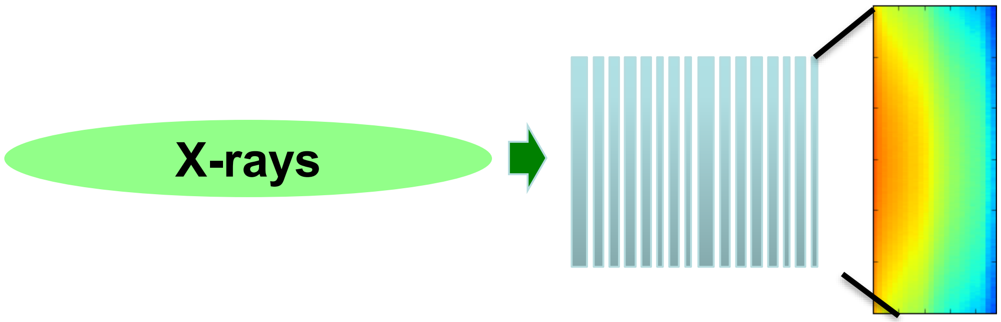

Calorimeter stack layers

- Varying material
- Image plates/scintillators

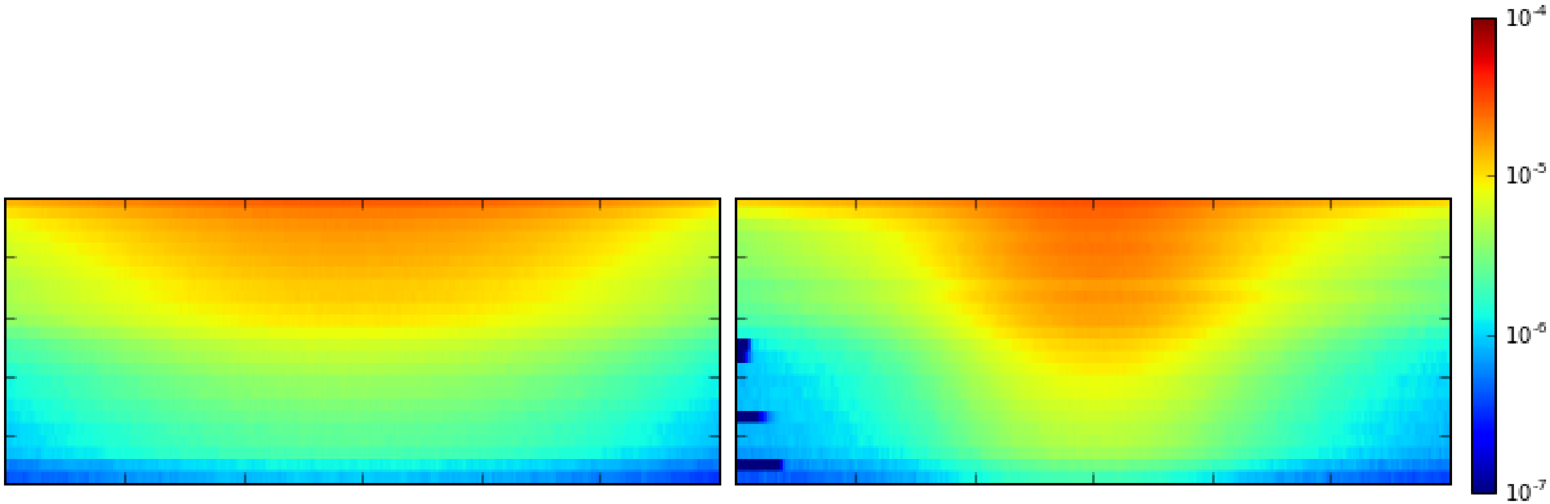

Increase in divergence and reduction in max. photon energy

Detection via spatially resolving calorimeter stack

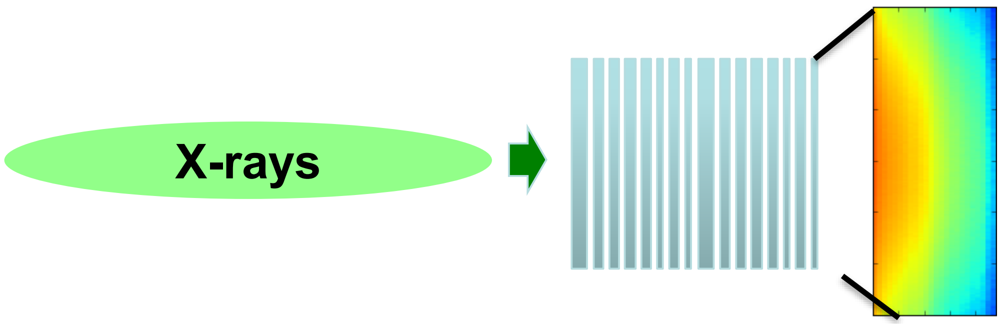

Calorimeter stack layers
- Varying material
- Image plates/scintillators

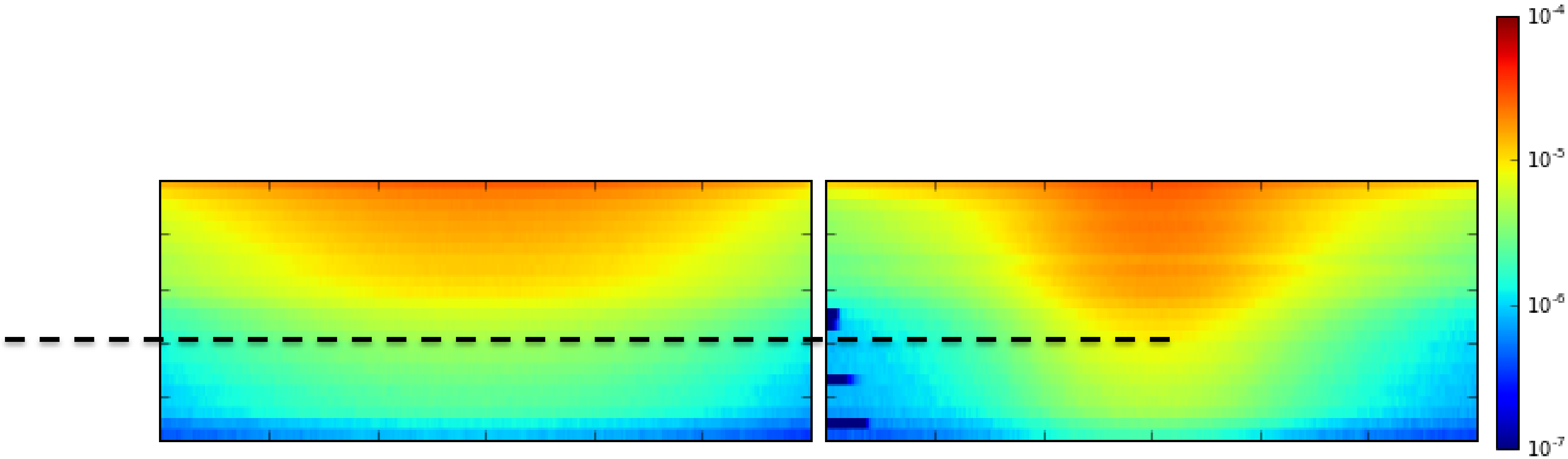

Increase in divergence and reduction in max. photon energy

Detection via spatially resolving calorimeter stack

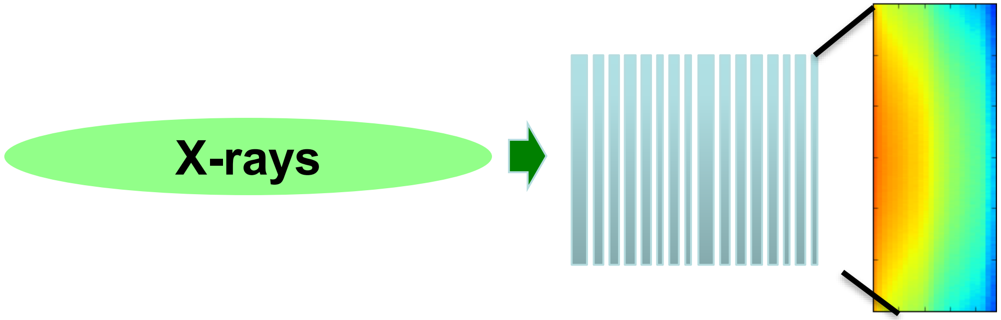

Calorimeter stack layers
- Varying material
- Image plates/scintillators

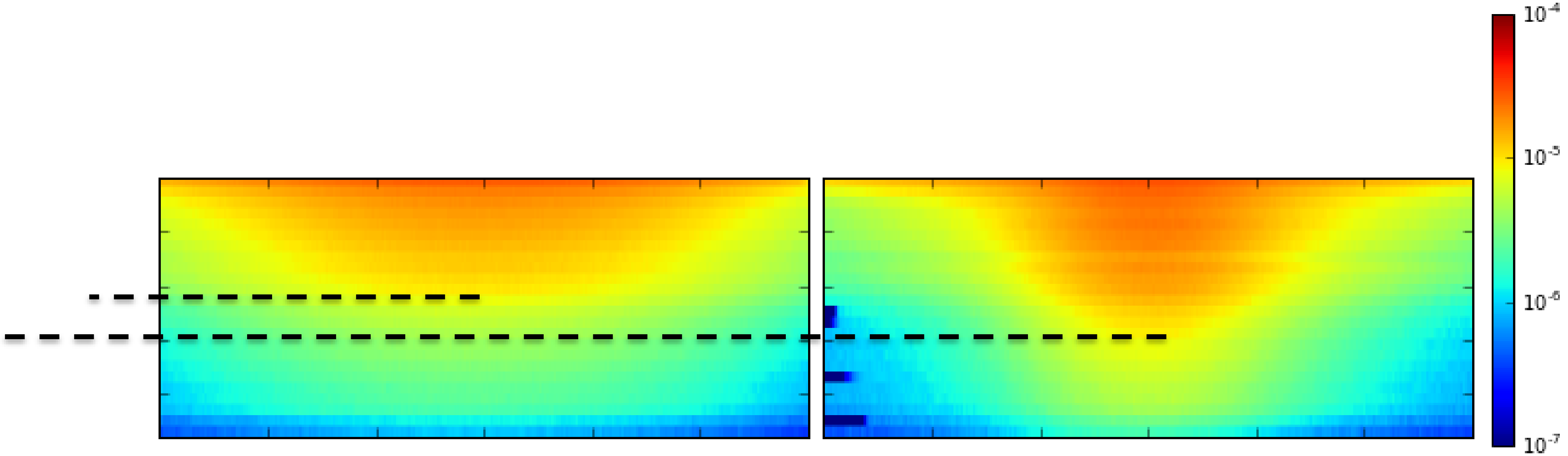

Increase in divergence and reduction in max. photon energy

Detection via spatially resolving calorimeter stack

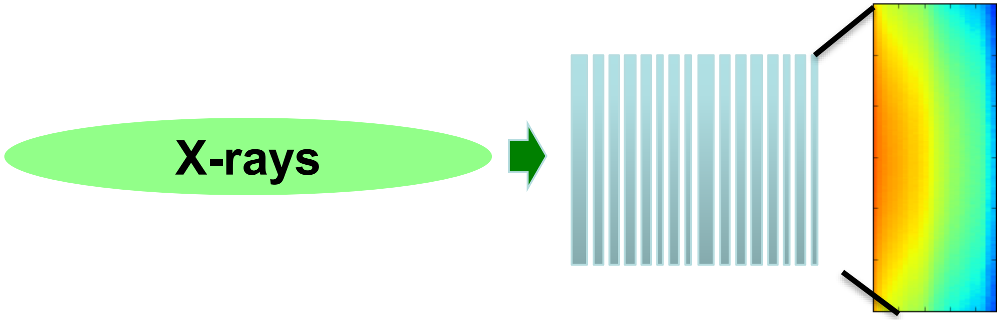

Calorimeter stack layers

- Varying material
- Image plates/scintillators

PM @ z = -200um
Highly non-linear

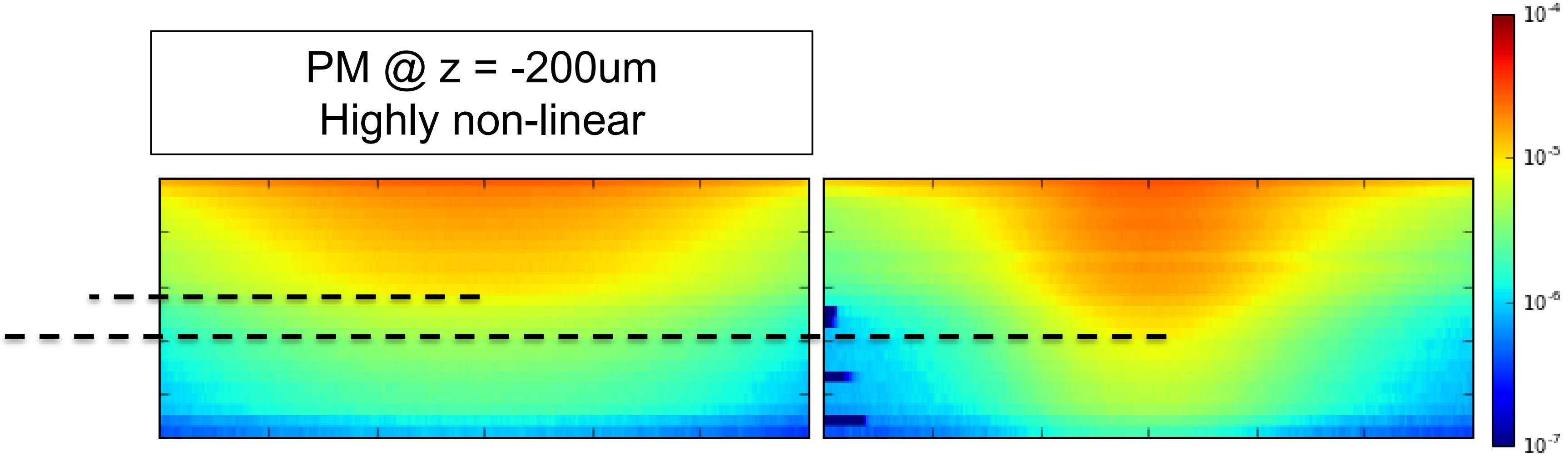

Increase in divergence and reduction in max. photon energy

Detection via spatially resolving calorimeter stack

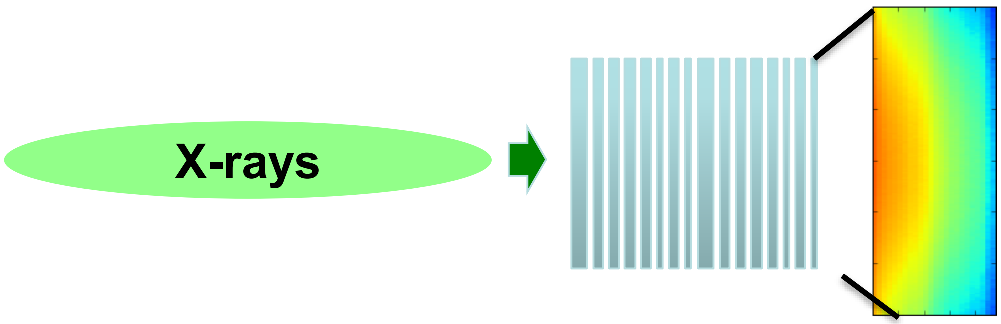

Calorimeter stack layers
- Varying material
- Image plates/scintillators

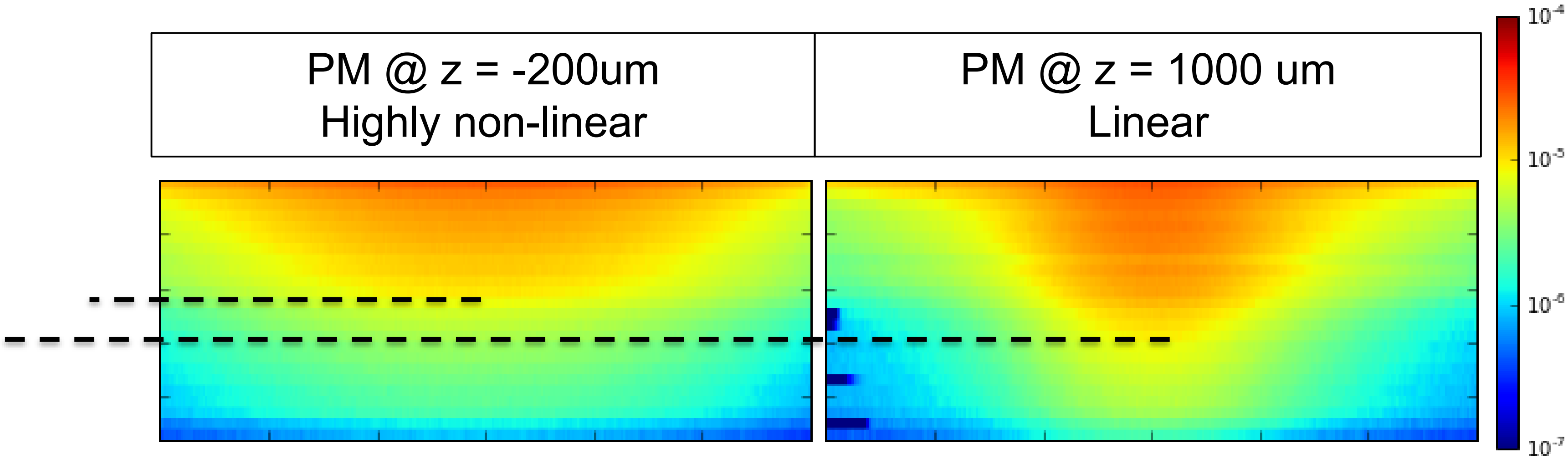

Increase in divergence and reduction in max. photon energy

HZDR

Detection via spatially resolving calorimeter stack

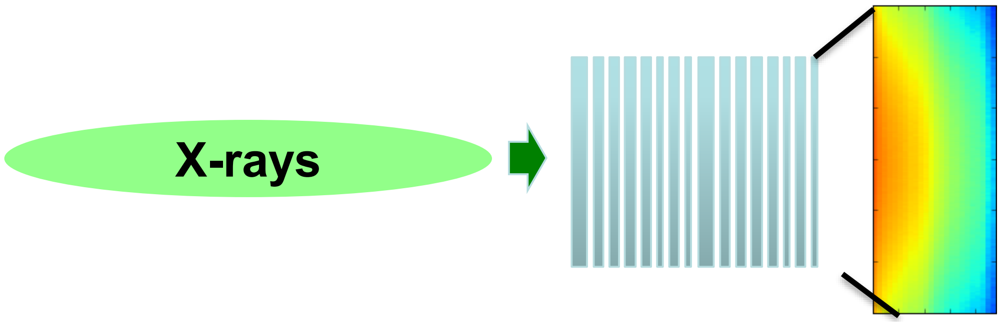

Calorimeter stack layers
- Varying material
- Image plates/scintillators

PM @ z = -200um Highly non-linear	PM @ z = 1000 um Linear

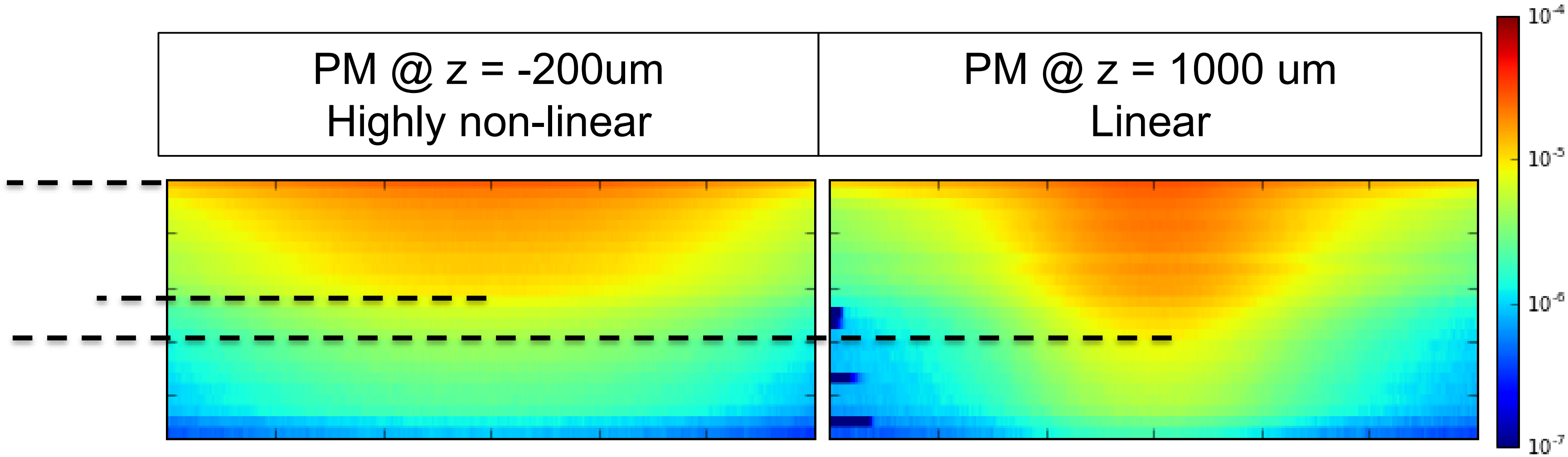

Increase in divergence and reduction in max. photon energy

Applications of laser wakefield acceleration

Detection via spatially resolving calorimeter stack

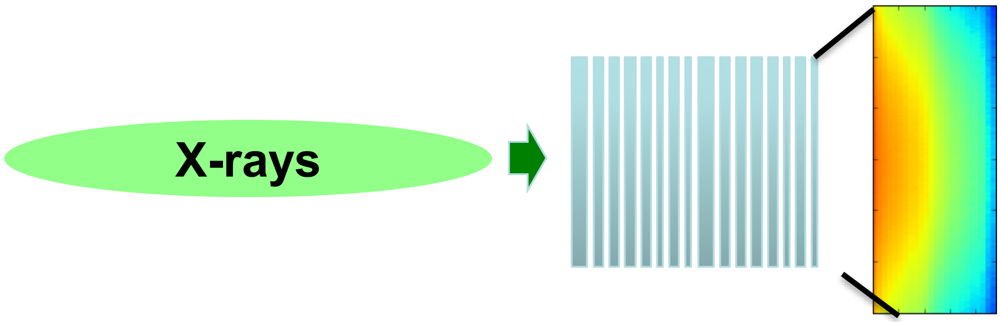

Calorimeter stack layers
- Varying material
- Image plates/scintillators

PM @ z = -200um Highly non-linear	PM @ z = 1000 um Linear

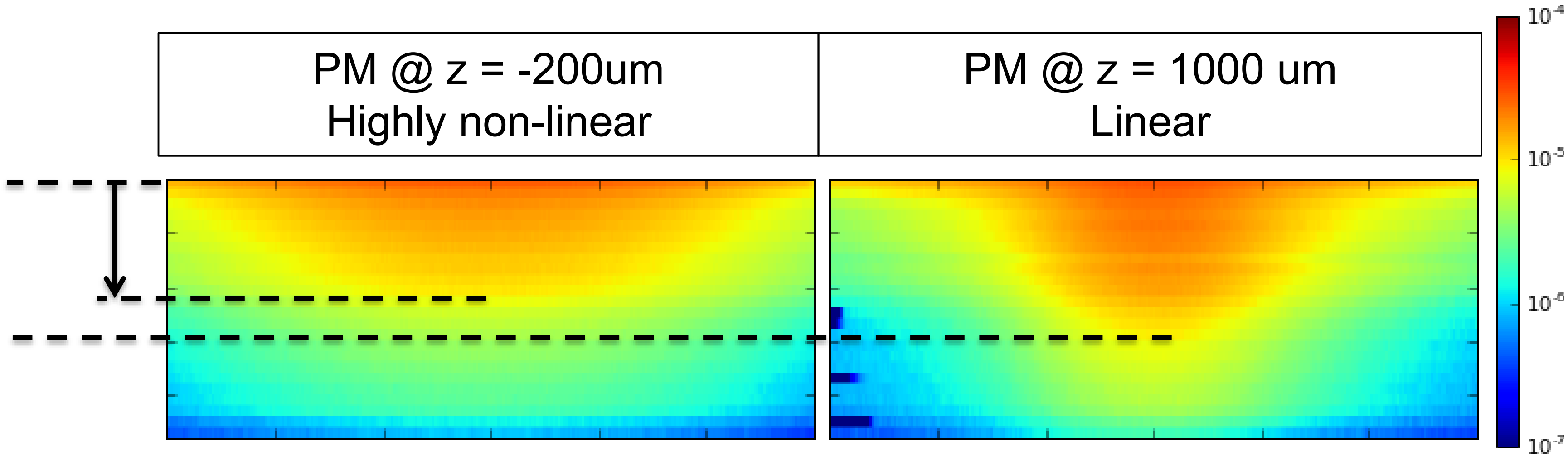

Increase in divergence and reduction in max. photon energy

Detection via spatially resolving calorimeter stack

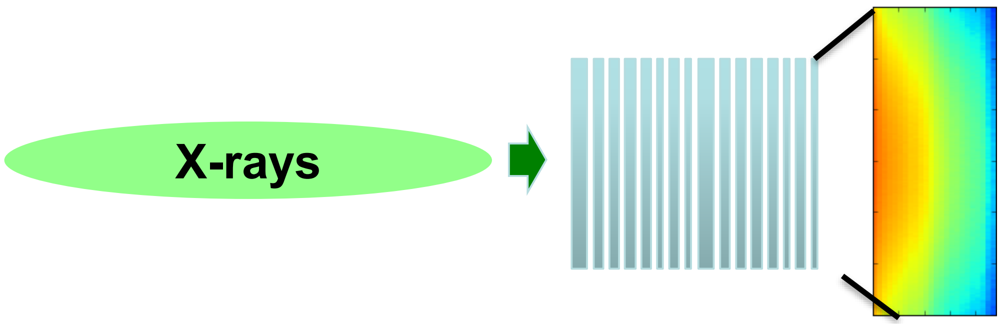

Calorimeter stack layers
- Varying material
- Image plates/scintillators

PM @ z = -200um Highly non-linear	PM @ z = 1000 um Linear

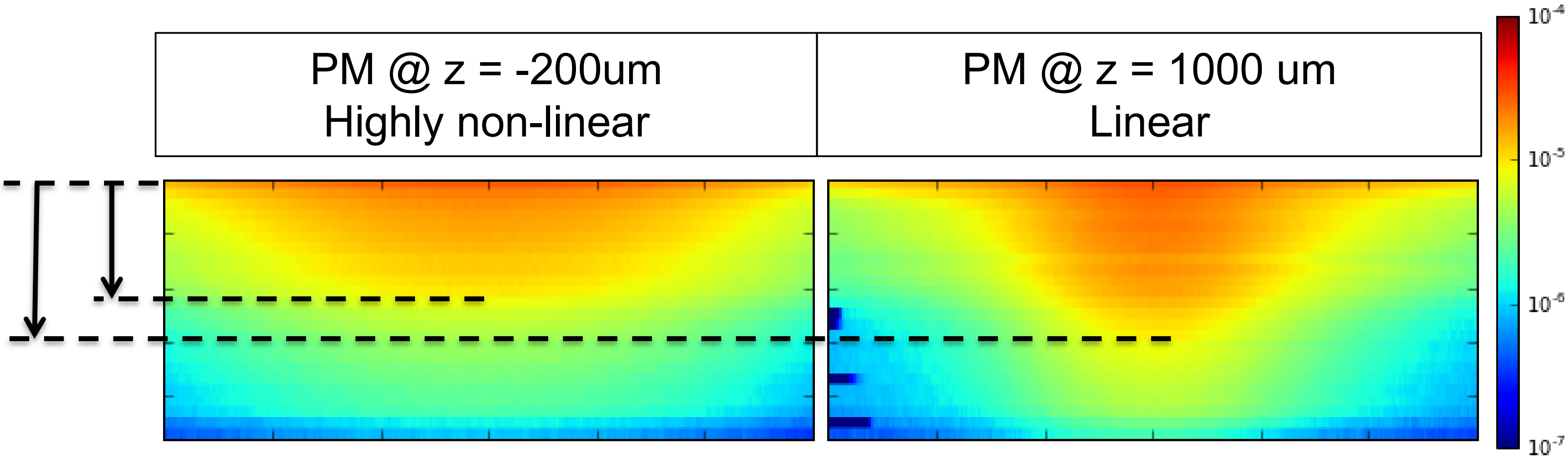

Increase in divergence and reduction in max. photon energy

Detection via spatially resolving calorimeter stack

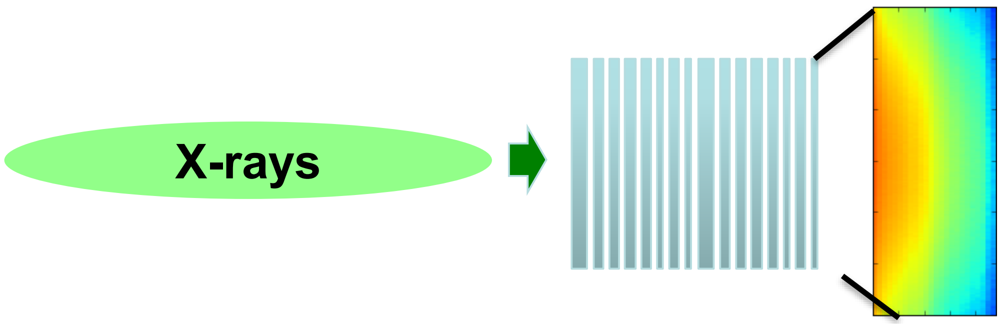

Calorimeter stack layers
- Varying material
- Image plates/scintillators

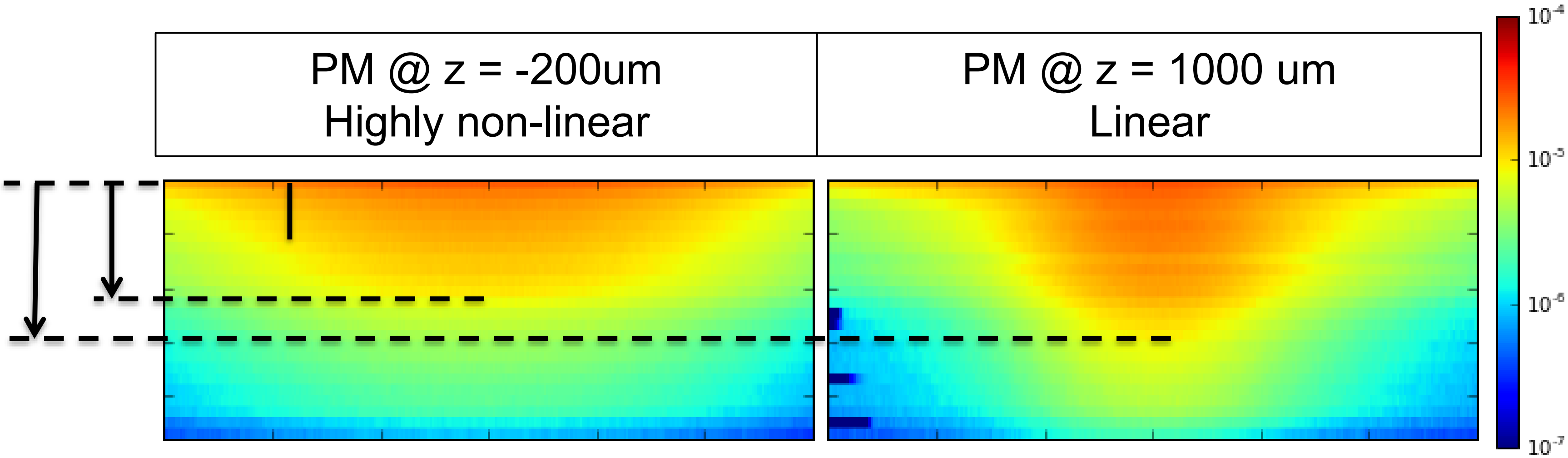

Increase in divergence and reduction in max. photon energy

Detection via spatially resolving calorimeter stack

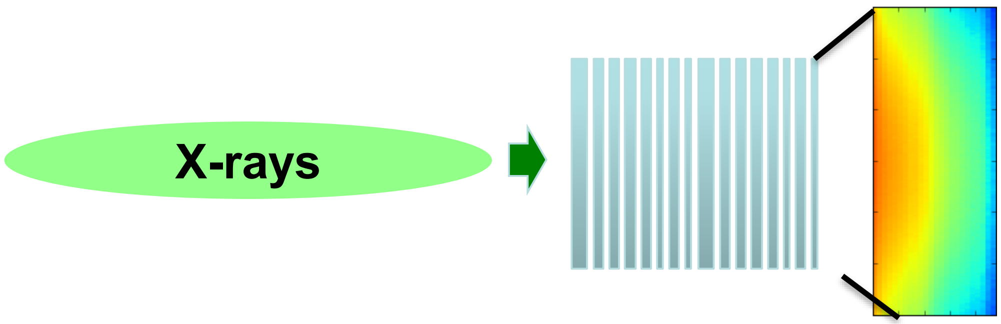

Calorimeter stack layers

- Varying material
- Image plates/scintillators

PM @ z = -200um Highly non-linear	PM @ z = 1000 um Linear

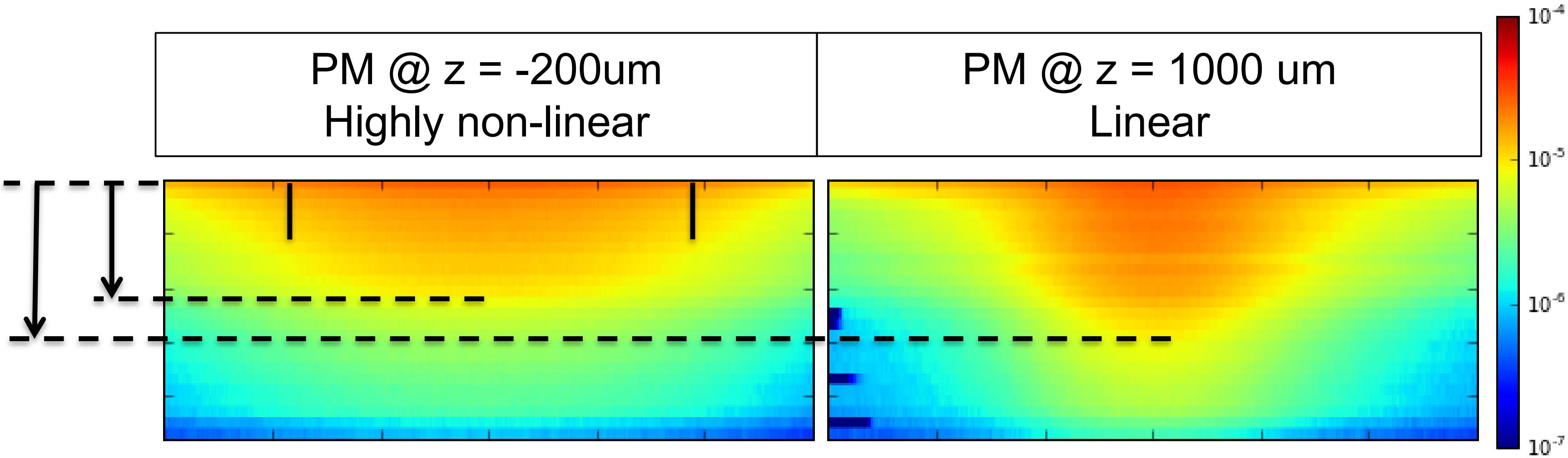

Increase in divergence and reduction in max. photon energy

HZDR

Detection via spatially resolving calorimeter stack

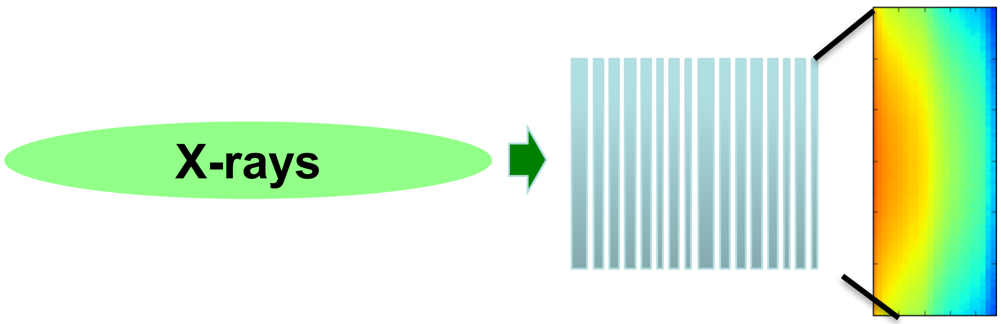

Calorimeter stack layers
- Varying material
- Image plates/scintillators

PM @ z = -200um Highly non-linear	PM @ z = 1000 um Linear

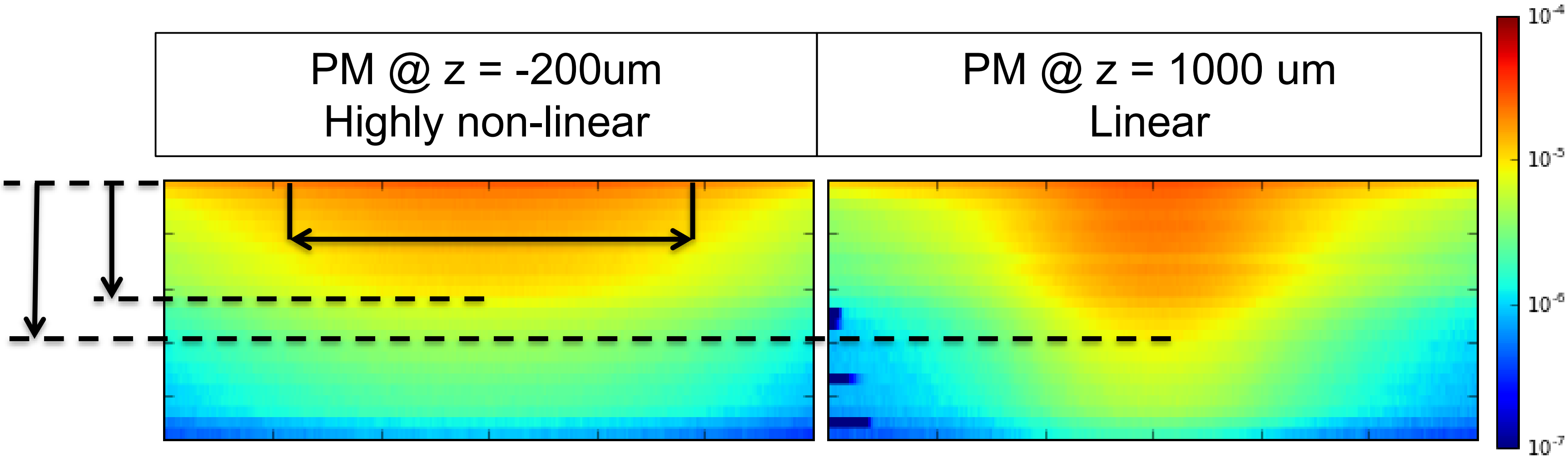

Increase in divergence and reduction in max. photon energy

Applications of laser wakefield acceleration

HZDR

Detection via spatially resolving calorimeter stack

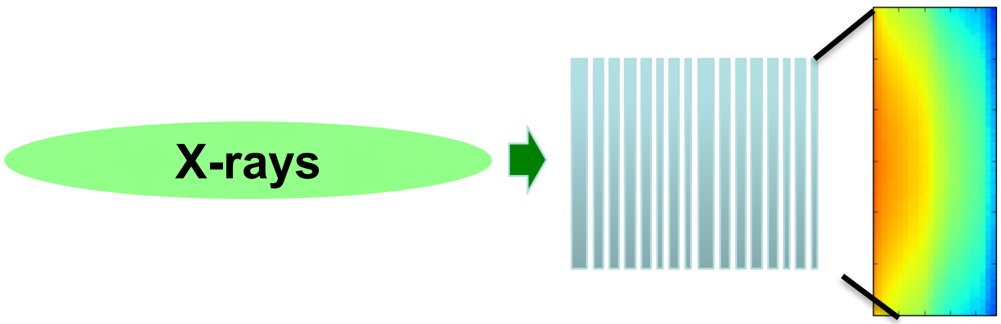

Calorimeter stack layers
- Varying material
- Image plates/scintillators

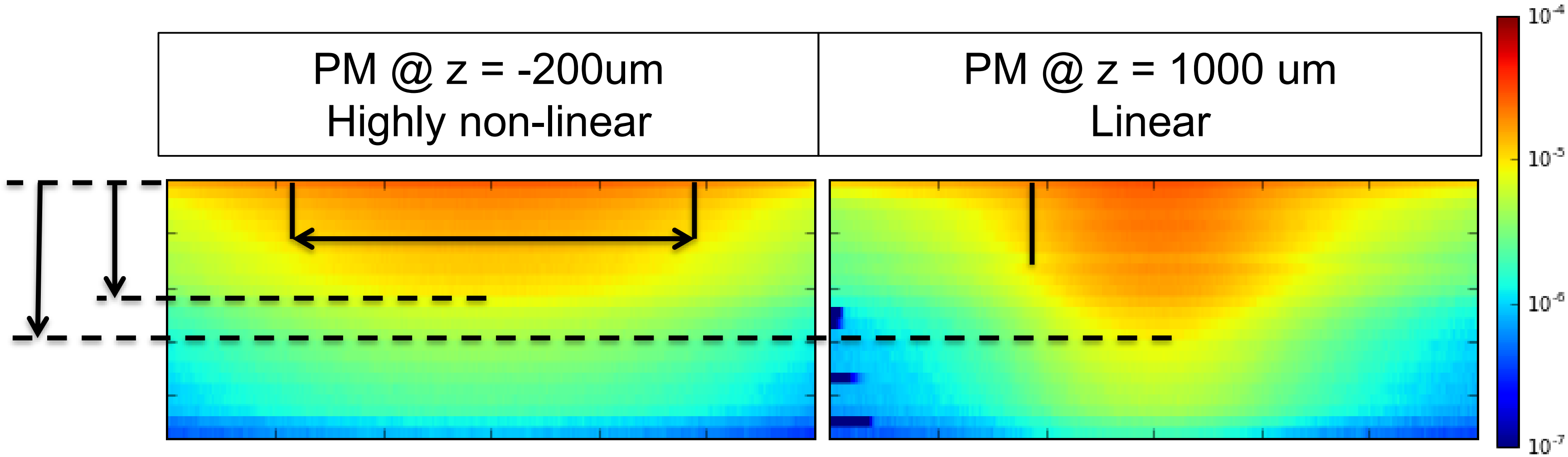

Increase in divergence and reduction in max. photon energy

Detection via spatially resolving calorimeter stack

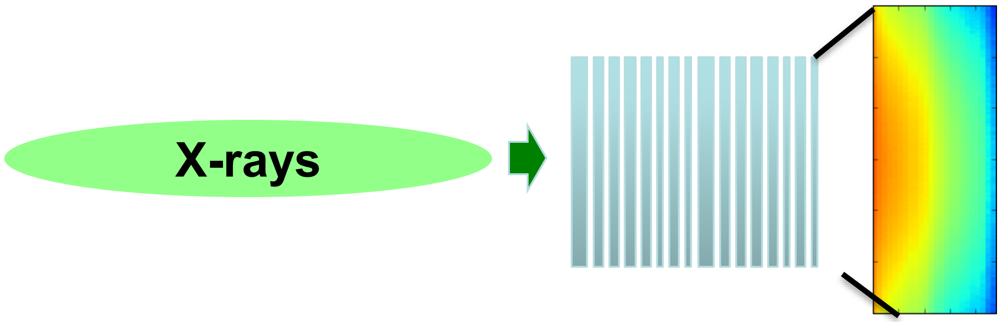

Calorimeter stack layers
- Varying material
- Image plates/scintillators

PM @ z = -200um Highly non-linear	PM @ z = 1000 um Linear

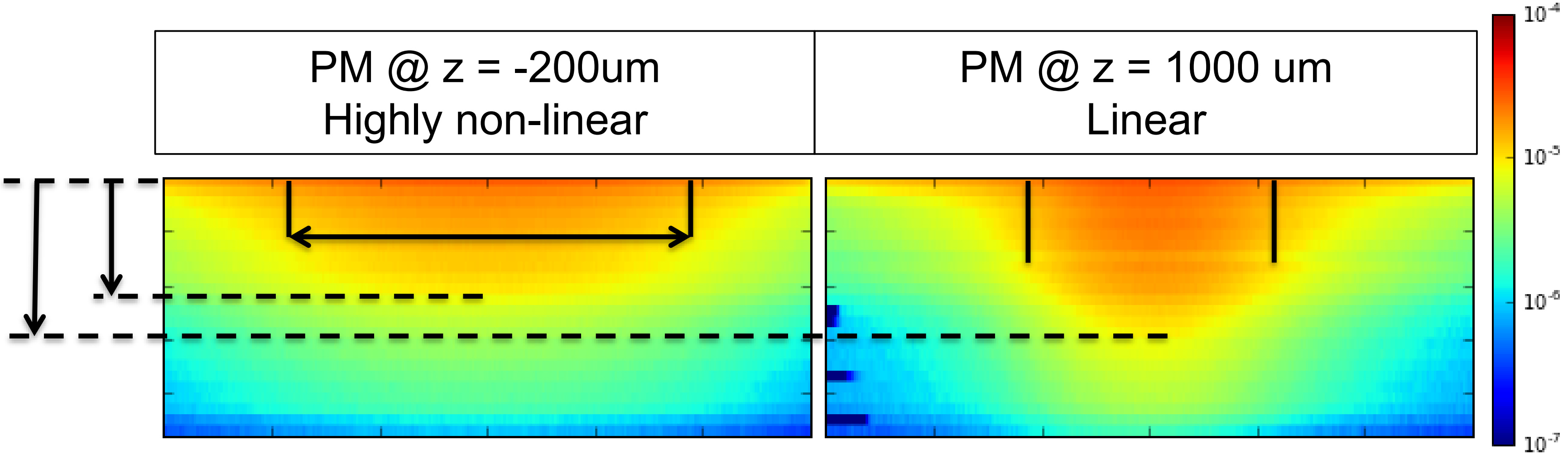

Increase in divergence and reduction in max. photon energy

Detection via spatially resolving calorimeter stack

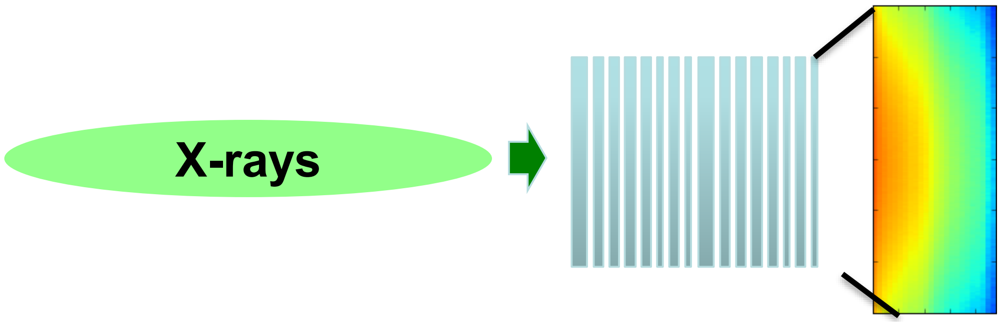

Calorimeter stack layers
- Varying material
- Image plates/scintillators

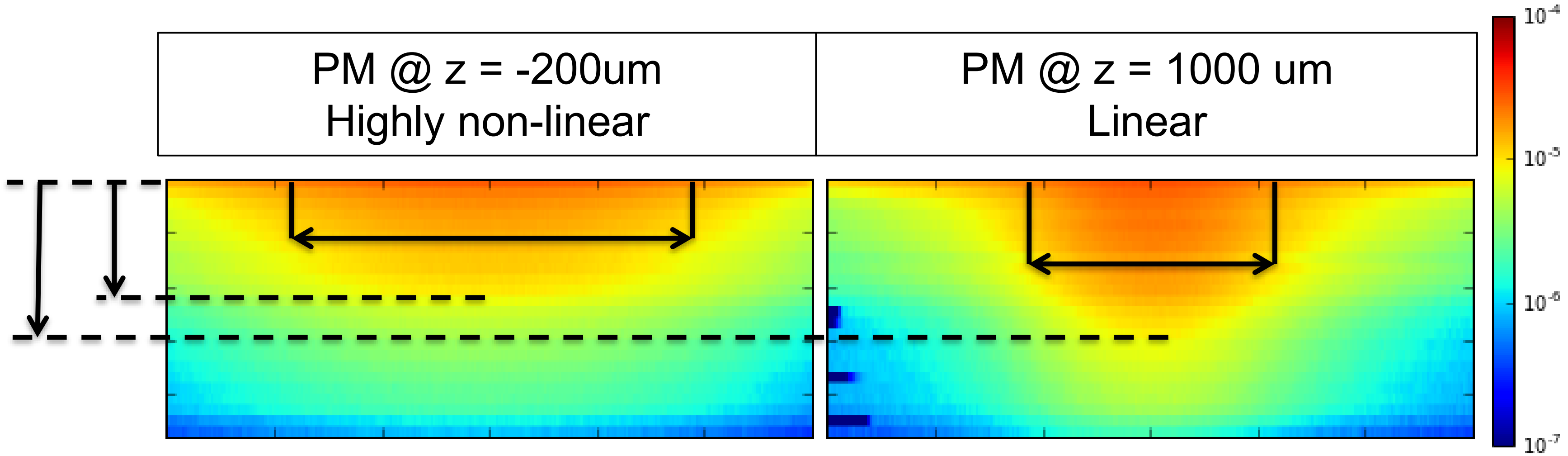

Increase in divergence and reduction in max. photon energy

Detection via spatially resolving calorimeter stack

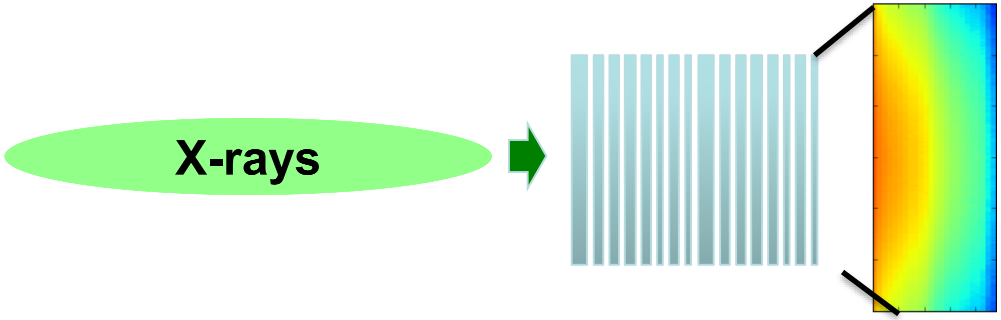

Calorimeter stack layers
- Varying material
- Image plates/scintillators

PM @ z = -200um Highly non-linear	PM @ z = 1000 um Linear

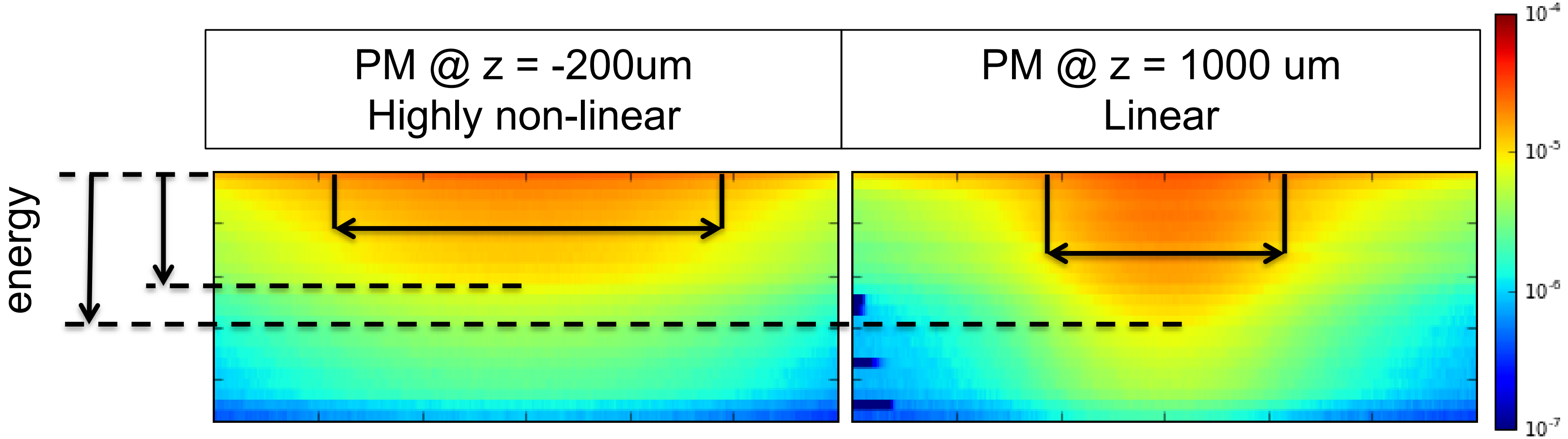

Increase in divergence and reduction in max. photon energy

- Controlled LWFA to >10kA peak currents with (only) 100 TW on target (~0.5nC in ~20fs @ 200-800 MeV, ~10%BW)

- Thomson scattering (internal / external) as source (30%BW) and diagnostics
- Betatron radiation as source (100%BW)
- Hybrid schemes for advanced accelerators

- **A. Irman, J. Couperus, J. Krämer**, A. Köhler, T. Kurz, O. Zarini, et al.
- **R. Zgadzaj, M. LaBerge, A. Hannasch**, M. Downer
- **A. Debus, R. Pausch, K. Steiniger**, A. Hübl, T. Kluge, M. Bussmann, et al.

- K. Zeil, J. Metzkes, F. Brack, S. Kraft, F. Kroll, L. Obst, M. Rehwald, H.P. Schlenvoigt, T. Ziegler, A. Laso-Garcia, et al.

- M. Siebold, D. Albach, S. Bock, R. Gebhardt, U. Helbig, M. Löser, T. Püschel, et al.

- U. Schramm, T. Cowan, R. Sauerbrey